UNIVERSITÀ DELLA CALABRIA

UNIVERSITA' DELLA CALABRIA

Dipartimento di Ingegneria Informatica, Modellistica, Elettronica e Sistemistica

Dottorato di Ricerca in

Information And Communication Technologies

CICLO

XXXI

TITOLO TESI

Analysis and Development of Physical and MAC Layer Protocols
in Mobile Ad Hoc Networks Involving Directional Antenna Communications

Settore Scientifico Disciplinare ING-INF/03

Coordinatore: Ch.mo Prof. Felice Crupi

Firma

Supervisore/Tutor: Ch.mo Prof. Floriano De Rango

Firma

Dottorando: Dott. V Dott. Vincenzo Inzillo

Firma _ Firma

UNIVERSITÀ DELLA CALABRIA

DOCTORAL THESIS

Analysis and Development of Physical and MAC Layer Protocols in Mobile Ad Hoc Networks Involving Directional Antenna Communications

---

Author:
Vincenzo INZILLO

Supervisor:
Prof. Floriano DE RANGO

A thesis submitted in fulfillment of the requirements for the degree of Doctor of Philosophy

in

Information and Communication Technologies
DIMES

May 24, 2019

Declaration of Authorship

I, Vincenzo INZILLO, declare that this thesis titled, "Analysis and Development of Physical and MAC Layer Protocols in Mobile Ad Hoc Networks Involving Directional Antenna Communications" and the work presented in it are my own. I confirm that:

- This work was done wholly or mainly while in candidature for a research degree at this University.
- Where any part of this thesis has previously been submitted for a degree or any other qualification at this University or any other institution, this has been clearly stated.
- Where I have consulted the published work of others, this is always clearly attributed.
- Where I have quoted from the work of others, the source is always given. With the exception of such quotations, this thesis is entirely my own work.
- I have acknowledged all main sources of help.
- Where the thesis is based on work done by myself jointly with others, I have made clear exactly what was done by others and what I have contributed myself.

Signed:

_____

Date:

_____

"Computers are incredibly fast, accurate and stupid. Human beings are incredibly slow, inaccurate, and brilliant. Together they are powerful beyond imagination."

Albert Einstein

Abstract

Most recent Studies and Researches in IT (Information Technology) are bringing to an increasing development of Pervasive Communication Environments Systems such as MANET and Sensor Networks that assumed great importance, since 802.1X development IEEE Standards, due to their features based on nodes mobility and power consumption that lead to the rise of several protocols which implements different designs about routing algorithms and QoS (Quality of Service) specifications. Conventionally, these kinds of network environments are equipped in their physical layer with Isotropic and Omnidirectional Antennas Systems, that lead to a radiation pattern with a constant gain in all TX/RX directions so it results in a non-directive behavior of nodes. In this context there are lots drawbacks that heavily affect and reduce protocols efficiency and SNR (Signal to Noise Ratio) such as: communication reliability, latency, scalability, power and energy consumption. For example, using an isotropic antenna in nodes, without position knowing mechanism, bring to a notable waste of consumption energy due to the non-directive behavior because the same power is transmitted/received in all directions. To overlapping this drawback are developed in last years the so called Smart Antenna Systems that usually consists of several directive radiation elements implementing adaptive algorithms for the estimation of DOA (Direction of Arrival) and SOI (Signal Of interest); for this purpose are employed beamforming techniques that are largely used in Radar Communication Systems and Phased Array Systems. The resulted radiation pattern generates a beam that should be electronically controlled, and the main beam should be pointed towards the direction of interest in communication transmission/reception. The beam is generated according an adaptive algorithm (i.e. Least Mean Square) that models the weight vector as Smart Antenna input System. Beamforming techniques take lots advantages in medium access control, effectively, employing of SDMA (Spatial Division Multiple Access) allows a great efficiency protocol growth. MANET performance can be enhanced if more efficient antenna systems such as Massive MIMO (Multiple Input Multiple Output) systems are employed; indeed, massive MIMO underlie the development of 5G Mobile Wireless Network environments. However, despite of their capability to improve network performance they introduce different kinds of issues especially in terms of energy consumption that should be addressed. The main purpose of this thesis is to limit most of the mentioned issues related to directional communications in MANET in order to improve the current state of art referring both to protocols and network performance. From

a protocol point of view, important to highlight that the most of the overall contribution of the present work aims to address energy efficiency, deafness problem and finally, mobility issues occurring at physical and MAC (Medium Access Layer) layer. The reminder of the thesis is the following:

- **Chapter 1**: introduces main concepts about network communications using directional and omnidirectional antennas in MANET and their common related issues.
- **Chapter 2**: gives basics and fundamentals theoretical notions about Smart Antenna Systems (SAS) and Massive MIMO with particular emphasis to beamforming algorithms.
- **Chapter 3**: essentially, this chapter is divided into two parts. The first one, illustrates basic features of the main instrument used for experimental analysis that is the Omnet++ network simulator. The second part exposes the most significant works produced to extend the default Omnet++ framework for enabling simulation scenarios supporting SAS and massivo MIMO systems.
- **Chapter 4**: provides a detailed discussion about deafness problem in MANET directional communications and subsequently illustrates the most significant proposals in this field with a special focus on designed Round-Robin based approaches.
- **Chapter 5**: describes main issues related to mobility and energy consumption of nodes in directional MANET with particular attention to handoff problem. Nevertheless, it illustrates novel proposed strategies aiming to mitigate energy consumption in very high gain beamforming communications employing SAS and massive MIMO systems.

All of the above chapters are organized in a similar way. More specifically, each chapter consists of three main parts:

- **Background**: gives a briefly theoretical explanation of the most important concepts mentioned in the chapter.
- **State of art**: illustrates the most significant works related to topics encountered in the chapter.
- **Personal contribution**: highlights the main contribution achieved (by author of this thesis) allowing to improve the current state of art related to a particular topic.

Acknowledgements

First of all, I would to thank my tutor Professor Floriano De Rango for the possibility he offered to me to accomplish a productive PhD path and for the invaluable support that he gave to me in these years. This experience, has enabled me to learn a lot of useful things about research world and to understand the importance to provide a personal contribution to the research, enhancing the existing state of art. At the same way, I would to give a very special grateful to Professor Alfonso Ariza Quintana for the extremely precious collaboration, especially in terms of code programming and modeling and simulation, resulting in a large number of publications. In addition, I want to thank professor Quintana for putting me up in the Telecommunications and Electrical Department, during my abroad study period at University of Malaga, Spain. Next, I would to thank my department colleagues Amilcare Santamaria, Mauro Tropea, Paolo Sciammarella, Pierfrancesco Raimondo and Prof. Domenico Luca Carnì, for the invaluable friendly support given in these years. Last but not least, I would like to extend my heartfelt thanks to my family that supported me in this very difficult path all the time.

Contents

List of Figures

List of Tables

Acronyms

ABT-RRMAC Adaptive Beamforming Time RR-MAC. 113

ACK Acknowledgement. 11

AoA Angle of Arrival. 11

AODV An On Demand Distance Vector. 14

BER Bit Error Rate. 58

CMA Constant Modulus Algorithm. 29

CTS Clear To Send. 6

DAODV Directional An On Demand Distance Vector. 15

DCF Distributed Coordinated Function. 5

DCTS Directional Clear To Seend. 6

DDSR Directional Dymanic Source Routing. 14

DMAC Directional Medium Access Control. 11

DNAV Directional Network Allocator Vector. 6

DOA Direction of Arrive. 70

DRTS Directional Request To Send. 6

DSP Digital Signal Processing. 22

DSR Dymanic Source Routing. 14

ESPAR Electrically Steerable Passive Array Radiator. 14

FIFO First In First Out. 8

IoT Internet Of Things. 45

IP Internet Protocol. 44

ISM Industrial Scientific and Medical. 46

LMS Least Mean Square. 28

MAC Medium Access Control. 14

MANET Mobile ad Hoc Networks. 2

MIMO Multiple Input Multiple Output. 17

MISO Multiple Input Single Output. 17

MSE Mean Square Error. 28

MSK Minimum Shift Keying. 29

NED Network Description Language. 45

NIC Network Interface Card. 51

Ns2 Network Simulator 2. 44

Ns3 Network Simulator 3. 44

OTcl Object Oriented TCL. 44

PDR Packet Delivery Ratio. 73

QAM Quadrature Amplitude Modulation. 58

QoS Quality of Service. 18

RF Radio Frequency. 22

RR Round Robin. 107

RR-MAC Round Robin MAC. 70

RREP Route Reply. 16

RREQ Route Request. 15

RTS Request To Send. 5

SAS Smart Antenna Systems. 17

SCFQ-MAC Self Clocked Queuing MAC. 85

SDMA Spatial Division Multiplexing. 17

SIMO Single Input Multiple Output. 17

SINR Signal Interference To Noise Ratio. 14

SNR Signal to Noise Ratio. 22

SOI Signal Of Interest. 24

TTL Time To Live. 16

UDP User Datagram Protocol. 47

VHT Very High Throughput. 57

WRR-MAC Weighted Round Robin MAC. 80

List of Symbols

QSF	Queue Size Factor (term referred to the queue size)
N	number of nodes
N_s	number of sectors
w_Q	queue weight
$\overline{W_Q}$	queue weight vector
S_i	i-th sector
T_i	i-th sector time
A_D	activity degree of nodes
M_L	misalignment level between a couple of nodes
N_{ACTIVE}	number of active nodes
N_{TOTAL}	total number of nodes in a sector
qs_i	i-th sector queue size
T	duration beamforming lowerbound of RR-MAC
w_s	weight related to the number of sectors
w_{A_D}	weight related to the activity degree
w_{M_L}	weight related to the misalignment level
$(DRTS/DCTS)_{ratio}$	Directional Request to Send/Clear to Send ratio
$\overline{W_{A_D}}$	activity degree weight vector
$\overline{W_{M_L}}$	misalignment level weight vector
$\overline{W_s}$	weight vector associated to $\overline{N_s}$
$\overline{N_s}$	number of sectors vector
λ	wavelength
s	seconds
m	meters
mps	meters per second
$Mbps$	Mega bit per seconds
J	joules
dBm	decibel-milliwatts
W	watt
MHz	Mega Hertz
GHz	Giga Hertz

Dedicated to my parents and my
sister Giulia representing the
source and the reason of my
life…

Chapter 1

Directional and Omnidirectional antennas in MANET

1.1 Introduction

Over the past few years, research into ad hoc networks has yielded considerable advances, notably in the areas of new routing and medium access techniques. Yet, significant shortcomings of ad hoc networks remain, especially when compared with wireline networks. Wireless networks suffer from fundamental capacity limitations [1]–[3], connectivity energy consumption and security problems, and are prone to jamming and eavesdropping. Attempts to overcome these problems at the medium access, network and transport layers by way of innovative and often ingenious protocols have yielded only incremental success. One of the most critical tasks in wireless network environments is to perform a set of communication between nodes correctly. Ideally, the goal is that, given a generic communication system consisting of a transmitter node T and a receiver node R, separated by a channel C, the node T perform a certain communication with node R by transmitting a signal that propagates in the channel and successfully should arrive or not to the receiver R depending on, for example, to the power of the transmitter signal, the sensitivity at the receiver, the condition of the channel etc. However, this signal is function of the medium by which it was generated, other than of the physical properties of nodes and the channel. The instrument used both for generating and receiving the signal related to a certain communication is the antenna. Basically, the antenna allows to convert an electrical signal into a wave that is able to drive in the radio medium [4], [5]. However, with regard to wireless network applications, in order to understand the behaviours experienced in different contexts, it is useful to investigate about different kinds of antennas employed by nodes. For this purpose the following subsections present an overview highlighting the most important differences and aspects between directional and omnidirectional antennas with reference to layer features and protocols which they are related.

1.2 Directional and Omnidirectional antennas features

In the study of wireless networks, the set of antenna models use by nodes can be grouped under omnidirectional and directional. Omnidirectional antennas, also known as isotropic antennas, radiate and receive equally well in all directions [6], [7]. Main advantages of omnidirectional antennas includes: ease of configuration and implementation, low designing cost, very and simple architecture (hardware-less). For instance, in cellular systems, they allow to amplify cell signals from multiple carriers with different cell towers in multiple locations [8]. Nevertheless, despite from this few benefits they introduce a considerable number of drawbacks such as: limited range and coverage (derived due low gain provided), high energy consumption, high interference probability (especially in dense networks), very high performance dependency on the environments in which they are employed (indoor or outdoor); nonetheless, omnidirectional antennas cannot exploit the benefits of cross-polarization because they are vertically polarized [9], [10]. More specifically, this last issue, contributes to increase the probability of interference between communicating nodes in the channel [11]. From a topological point of view, this approach implies that, the signal generated from the transmitter T, reach desired users with only a small percentage of the overall energy sent out into the environment. Due to this huge number of limitations, omnidirectional antennas may not be efficient due to interference caused by the transmission of packets in all directions (other than target direction) and limited range of communications [12]. Unfortunately, in Mobile ad Hoc Networks (MANET), omnidirectional antennas have been used to communicate with other nodes for transmission as well as for reception; this approach results in very limited performance relating to physical, link and routing layer statistics.

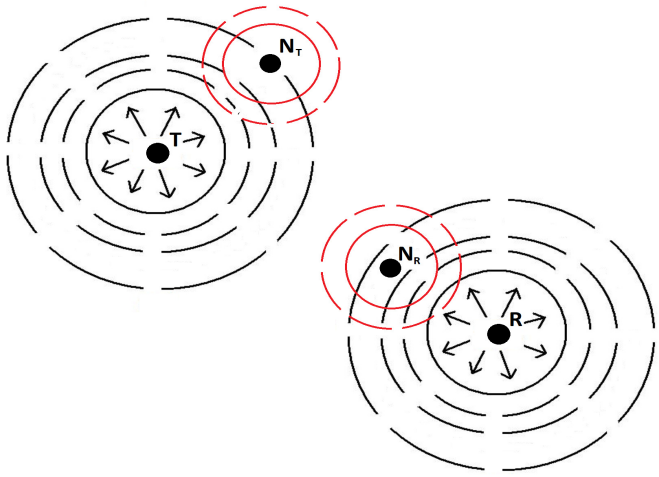

FIGURE 1.1: Interference caused by omnidirectional antennas.

The Figure 1.1 illustrates an wireless network scenario in which nodes use omnidirectional antennas to perform communications. In particular, the transmitter node T send to the receiver R a communication signal by using an omnidirectional antenna; R attempts to capture the signal with the same antenna model. Because

the transmitter signal is radiated in all directions with the same intensity, if there are such nodes in the neighboring of the transmitter/receiver is high likely that the radiated signal is captured by these nodes that, in turn, may attempt a communication at the same time. In this case, interferences and collisions can occur; these issues could enhance as the mobility of nodes increases [13]–[16]. Nevertheless, in this case, because nodes radiate in the same way toward all directions, a huge waste of the battery life of nodes is certainly achieved [17], [18]. The majority of these issues could be partially mitigated using directional antennas. Directional antennas may be useful to increase network efficiency by directing the transmitted power in the desired/intended direction. Directional antennas have a great number of advantages over omnidirectional antennas in ad hoc networking. By focusing energy only in the intended direction, directional antennas can increase the potential for spatial reuse and can provide longer transmission and reception ranges for the same amount of power. Increased spatial reuse and longer range translates into higher ad hoc network capacity (more simultaneous transmissions and fewer hops), and longer range also provides improved connectivity [19]–[21]. Different kinds of issues have to be investigated when directional communications occur with respect to the traditional omnidirectional case; problems such as the hidden terminal and the deafness problem [22]–[24] have to be properly handled as well as handoff issue implied by mobility of nodes [25].

1.2.1 Using directional antennas in Ad hoc networking: motivations

The use of directional antennas in MANET is motivated because the great number of benefits which they introduce with respect to omnidirectional antennas. Main adavantages can be summarized by: spatial reuse exploitation, coverage range improving, energy saving. In this subsection main features of cited advantages are summarized.

- **spatial reuse exploitation**: In wireless networks spatial reuse is defined as the capability to accommodate multiple concurrent communications in the same space resources. Although increasing the number of concurrent transmissions helps the network capacity, there is a counter effect to arbitrarily increasing this number. The wireless medium is essentially shared among nodes, and hence, signals that arrive at a receiver from other concurrent transmissions, even if attenuated, will be taken as interference by the receiver.

  Consider the scenario shown in Figure 1.2 where node T wants to communicate with node R and node T' with node R'. If omnidirectional antennas are used, then node T' cannot communicate with node R' when node T is sending packets to node R. This is due to the fact that communication of pair T'-R' may interfere with communication between T and R; this situation is illustrated in Figure 1.2(a), in which it also can be highlighted that all of nodes stay within

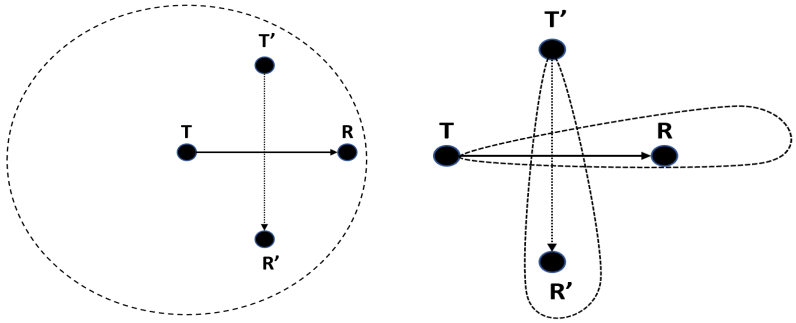

(a) Omnidirectional mode (b) Directional mode

FIGURE 1.2: Spatial reuse in omnidirectional and directional mode.

the communication range of node T; because more simultaneous communications are in the same range, it is very probably that a collision or interference occur. If the nodes use directional antennas, each transmitter will focus the beam towards its intended receiver. This features enables transmission between A-B and C-D to go on concurrently as shown in Figure 1.2(b). From the above example, it can be deduced that, if the nodes use directional antennas, neighboring nodes that are not in the direction of signal can go ahead with their transmissions. Multiple transmissions can now be initiated by different nodes instead of a single transmission in omni mode if they do not interfere with one another and thereby increasing spatial reuse factor.

- **coverage range improving** Given a couple of nodes (T,R) the coverage range is basically the capability of transmitter node T to perform a communication towards the receiver R using a certain signal. In particular, the intensity of the signal emitted by a node determines the maximum communication range which that node can cover. The intensity of the signal, in turn, is determined by physical features of the node such as the antenna power, that is very related to the antenna radiation pattern (and so to the antenna gain).

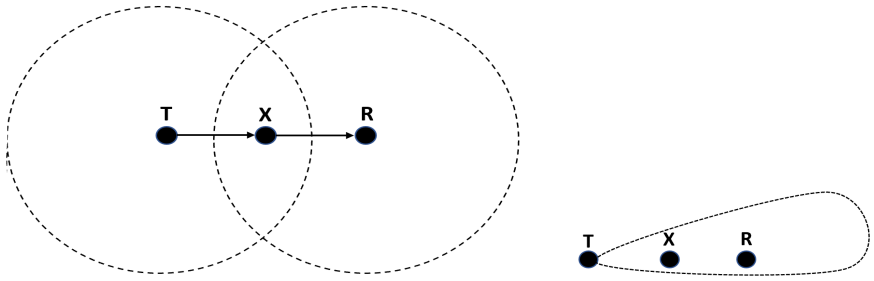

(a) Omnidirectional mode (b) Directional mode

FIGURE 1.3: Coverage range omnidirectional and directional mode.

In Figure 1.3(a) node T wants to communicate with node R. If omnidirectional communication is performed, T cannot reach R using a single hop because R is outside from the communication range formed by T. Hence, because T cannot

directly reach its intended receiver, for communicating with R it has to transmit towards node X that lies between ranges of T and R. In Figure 1.3(b) instead, a directional communication is performed by T; in this context, the gain provided by the transmitter antenna is higher than gain allowed by omnidirectional case, therefore T is able to reach node T in a single hop. The advantage of higher directional gain can be explained in two ways: firstly, because of the fact that focused beam can travel a larger distance than the unfocused omnidirectional signal, the sender can now reach a receiver which farther away resulting in a improvement of the transmission range. The greater reception gain helps the nodes to listen to a weaker signal if the signal is arriving at a direction in which the antenna is turned towards. Secondly, the radiation pattern formed by directional antenna is shaped such that the main beam concentrates the majority of the emitted power; this allows to radiate in the intended direction with the maximum gain resulting in higher coverage with respect to omnidirectional.

- **energy saving**. In MANET, energy consumption is an important issue as most mobile host operates on limited battery resources. A mobile node not only consumes its battery energy when it is actively sending or receiving packets, but it also consumes battery energy when idle and listening to the wireless medium for any possible communication requests from other nodes. Thus, energy efficient routing protocols are requested in order to minimize both the active communication energy which is required to transmit and receive data packets or the energy consumed during inactive periods [26], [27]. Generally proactive protocols consume more energy due to large routing overheads and reactive protocols suffer from route discovery latencies [28]. In pervasive distributed environments, a very common drawback related to the energy consumption issue is that, usually, mobile nodes are equipped with omnidirectional antennas. The employment of omnidirectional antennas as part as physical layer of a node often could bring to a considerable wasting of energy, especially in cases in which a network environment requires the establishment of a lot of communication links for traffic exchange. In this case, because of the properties of omnidirectional antennas, a node that is deeply involved in communications is subject to a remarkable energy consumption and consequently it could drain its battery life in a very short time, that could lead to the shutdown of the node.

1.3 Medium Access Control Layer and Directional Antennas

In the case of omnidirectional antennas, only those nodes within the radius of the transmitter can detect the carrier on the channel. This location-dependent carrier sensing results in the hidden terminal, exposed terminal and capture problems [29]. The application of IEEE 802.11 Distributed Coordinated Function (DCF) (Request To

Send (RTS)/Clear To Send (CTS)) scheme to wireless networks with directional antennas can induce new problems of location-dependent carrier sensing, such as new hidden terminal problem and the deafness problem that never happen with omnidirectional antennas [30]. In contexts in which directional communications are used, the carrier sensing have to be properly addressed. The use of Directional Request To Send (DRTS) and Directional Clear To Seend (DCTS) frames in association with a Directional Network Allocator Vector (DNAV) information, helps to decrease the large amount of collisions that usually occurs when using omnidirectional antennas [31].

1.3.1 MAC layer issues using directional antennas

Different kinds of issues have to be investigated when directional communications occur with respect to the traditional omnidirectional case; carrier sensing mechanisms employed in wireless networks involve undesired phenomena such as the hidden terminal and the deafness problem, that have to be properly handled in order to avoid a significant reduction of network performance. Below, we illustrate the main issues that usually occur in MANET at MAC layer using directional antennas.

- **Deafness**. Deafness is a very common problem in directional communications that arises when a transmitter fails to communicate to its intended receiver, because the receiver is beamformed towards a direction away from the transmitter. When an omnidirectional antenna is used, all neighbors are capable of listening to an ongoing transmission, however, when directional antennas are employed, there is a possibility that a certain node is turned in a particular direction while it is engaged in a communication related to another direction; in this case, that node is said to be *deaf* in all the other directions.

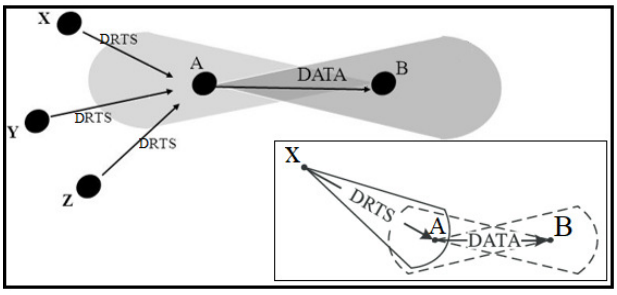

FIGURE 1.4: Deafness example.

Figure 1.4 illustrates an example of deafness problem in a directional scenario; Node A is beamformed by node B while a node X that is neighbored to A wants to communicate with node A. Node X does not know if Node A is busy so it keeps to send DRTS to A. Suppose that node B has a large amount of traffic to transmit toward node A, and for this reason it beamforms node A for a long time, is highly likely that a considerable number of frame collisions occurs in

the scenario; as result, the overall throughput will be significantly degraded and a large amount of DRTS/DCTS will be dropped.

- **Hidden Terminal Due to Asymmetry in Gain**. This problem occurs when hybrid directional basically due to the fact that the antenna gain in the omni-directional mode (G_o) is smaller than the gain when the antenna is beam-formed (G_d) [32]. If an idle node is listening to the medium omnidirectionally, it will be unaware of some ongoing transmissions that could be affected with its directional transmission.

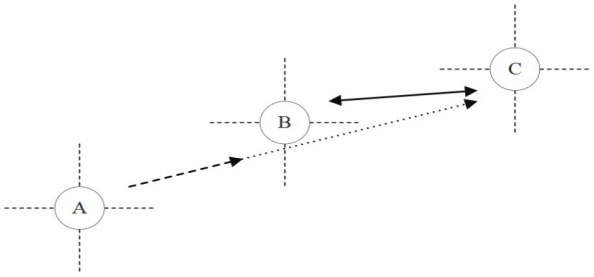

FIGURE 1.5: Hidden terminal due to asymmetry in gain example.

To explain this type of hidden terminal problem, we refer to the scenario in Figure 1.5. Assume that node A and node C are out of each other's range when one is transmitting directionally (with gain G_d) and the other is receiving omnidirectionally (with gain G_o). However, they are within each other's range only when both the transmission and reception are done directionally (both with gain G_d). First, node B transmits RTS directionally to node C, and node C responds back with a directional CTS. Node A is idle (still in omnidirectional mode) so it is unable to hear the CTS. Data transmission begins from node B to node C with both nodes pointing their transmission and reception beams towards each other. While this communication is in progress, node A has a packet to send to node B. Node A beamforms towards node B (which is the same direction of node C) and performs the carrier sensing. Since the channel is sensed idle, node A sends a directional RTS to node B. However, since node C is receiving data directionally using a beam pointed toward node B (and node A), the RTS from node A interferes with node B's data transmission at the receiver C causing collision.

- **Hidden Terminal Due to Unheard RTS/CTS**. This type of hidden terminal problem occurs as a result of the loss in the channel state information during beamforming. When a node is involved in a directional communication, it would appear deaf to all other directions and important control packets may be lost during that time. In contrast to the deafness problem in which the packet cannot be received by its intended receiver, this type of new hidden terminals occurs when a "neighboring node" fails to receive the channel reservation packets (RTS/CTS) exchanged by a transmitter-receiver pair. Hence,

it becomes unaware of the imminent communication between that particular transmitter- receiver pair and accordingly could later initiate a transmission that causes collision.

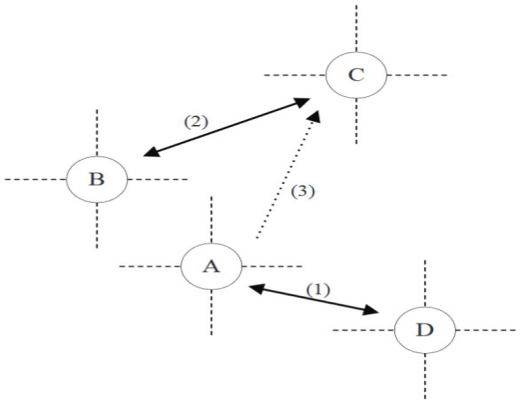

FIGURE 1.6: Hidden terminal due to unheard RTS/CTS example.

An illustrating example is shown in Figure 1.6. Suppose that node A is engaged in a directional communication with node D. While this communication is in progress, node B sends RTS to node C which in turns replies with CTS. Since node A is beamformed towards node D, it cannot hear CTS from node C. While the communication between node B and node C is in progress, node A finishes the communication with node D and now decides to transmit to node C. Since the DNAV at node A is not set in the direction of node C (due to the unheard CTS), node A transmits RTS to node C causing collision at node C.

- **Head of Line Blocking**. The Head-of-Line (HoL) blocking problem with directional MAC protocols was first identified in [33]. It occurs as a result of the typically used First In First Out (FIFO) queueing policy. This policy works fine in the presence of omnidirectional antennas since all outstanding packets use the same medium. If the medium is busy, no packets can be transmitted. However, in case of beamforming antennas, the medium is spatially divided and it may be available in some directions but not others.

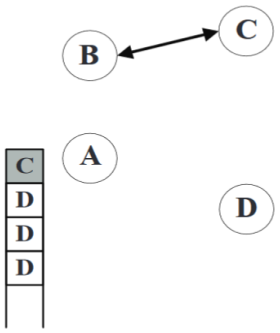

FIGURE 1.7: Head of Line Blocking example.

If the packet at the top of the queue is destined to a busy node/direction, it will block all the subsequent packets even though some of them can be transmitted as illustrated in Figure 1.7. Using the FIFO queueing policy, although node A has packets that can be transmitted to node D, theyare blocked by the packet destined to the busy node C. The HoL blocking problem is aggravated when the top packet goes into a round of failed retransmissions including their associated backoff periods as discussed in [34].

- **Exposed terminal problem**. The exposed node problem [35] occurs when a node is prevented from sending packets to other nodes due to a neighboring transmitter.

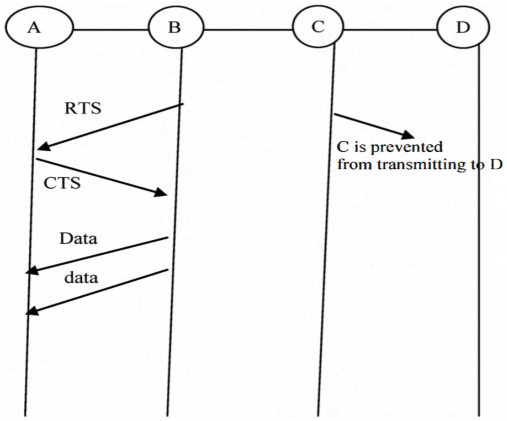

FIGURE 1.8: Exposed terminal problem example.

Consider the below figure 1.8, an example of nodes labeled A, B, C, and D, where the two receivers are out of range of each other, yet the two transmitters in the middle are in range of each other. Here, if a transmission between A and B is taking place, node C is prevented from transmitting to D as it concludes after carrier sense that it will interfere with the transmission by its neighbor node B. However note that node D could still receive the transmission of C without interference because it is out of range from B. Therefore, implementing directional antenna at a physical layer in each node could reduce the probability of signal interference with respect the case of use of omnidirectional antennas, because the signal is propagated in a narrow band but do not completely solve the problem.

- **Handoff problem**. The handoff problem is commonly implied by mobility of nodes in directional communication contexts. Considering a couple of nodes (T,R) involved in a communication, the handoff arises when the receiver node R moves out of the beam of the transmitter T. Moreover, in wireless systems, the channel can vary rapidly over time. Fig. 1.9 illustrates an example of handoff: the transmitter node T is communicating with a node R; during the communication R moves in the position R' and exit out of the transmitter beam and consequently the communication fails and the beams need to be re-pointed. In

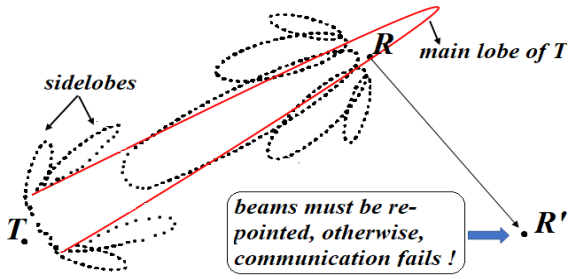

FIGURE 1.9: Handoff example.

this case, if the node in the position R' can still be reached by T through a beam switching, we can refer to this operation as inter-beam handover. This undesired phenomenon results in a dramatic decrease of throughput especially in moderate-high mobility environments where any mobility prediction model is employed.

1.3.2 Related MAC works in Directional Antennas

The MAC protocol for Directional Antennas in ad hoc network has received significant interest in recent years. There are many variations of MAC protocols that have been proposed for these antennas. The design of these protocols are influenced by the 802.11 MAC protocol. Many proposed protocols use the RTS-CTS mechanism used in the 802.11. The difference between them can be found in at least one of the following categories:

- **Directionality of frames**: All the protocols transmit the DATA frame directionally to use the advantages of directional antenna. The initial protocols considered using a mix of omni-directional and directional transmission for RTS and CTS.
- **Directional virtual carrier sensing**: Some protocols had the same virtual sensing mechanism as present in the 802.11. The more advanced protocols accounted for the channel state in each direction and proposed/used a new directional carrier sensing.
- **Directional range**: Initial protocols assumed that the range of the directional antenna is same as that of the directional antenna.
- **Number of channels**: Some of the protocols use more than a single channel.

One of the initial directional MAC protocol was proposed by Ko et al. [36]. In this work, they propose that by sending CTS in omni-directional mode, the ACK collision can be reduced. They advocate the use of omni-RTS when the complete channel is free and use directional-RTS otherwise. While using the directional-RTS in this case, there may be chances of deafness and hidden terminal problem which may result in packet collision. Overall this is a probabilistic model to reduce the

collisions. The virtual carrier sensing is not used in the MAC proposed by Ko et al. The Directional Medium Access Control (DMAC) that has been used in this study always uses D-RTS and D-CTS. Hence, it is vulnerable to collisions but because of virtual carrier sensing, this is less likely. The problem of routing layer discovering directional routes has not been addressed in this study. It assumes that each node knows its location and its neighbors' location. Nasipuri et al. [37] proposes a directional MAC protocol which uses omni-RTS and omni-CTS with a directional DATA and Acknowledgement (ACK) packets. The ability to measure the Angle of Arrival (AoA) of a packet can be recorded. Hence, after the omni-RTS and CTS, the source and receive will always know the direction of their counterpart. If the packet needs to be sent in omni mode, then the channel should be idle in all sectors around the node. This leads to a scenario which is similar to 802.11 where the packet transmission cannot be initiated even if the channel is idle in the direction of the receiver. If such a scheme was followed for the Head of line blocking described in the previous subsection then there would no benefit. This is one of the drawbacks of the protocol. It also assumes that the range of the directional transmission is same as that of the omnidirectional transmission. The higher gain of directional antenna is hence not used. Wang et al. [38] proposed another directional MAC which uses multiple channels. They assume three channels, one for data transfer and two more to send the busy tones. Sender sends the busy tone in sender-channel and the receiver in receiver-channel. The sender senses the receiver-channel before transmitting RTS and receiver senses the sender-channel before responding with CTS. This reduces the hidden terminal problem present. The use of multiple channels not only reduces increases the complexity in deployment but also reduces the bandwidth of the data channel. The DMAC that is used in this thesis is a single channel DMAC. The paper has not dealt with discovering the neighbors. It assumes that the direction to reach the neighbor is known by the node. The closest directional MAC protocol that was used for the study is the directional MAC protocol suggested by Roy Choudhury et al. in [39]. The virtual carrier sensing is done in a way similar to [40]. The RTS is always sent in directionally. The receiver will receive the RTS in omni-directional mode. The receiver sends the directional CTS to the sender. The reception of the DATA and the ACK packet are directional. This protocol does a good job to identify the transmission and reception modes can be both omni and directional. They also propose a method to shorten the hops by sending multi-hop RTS and send the DATA to hop which can be reachable by directional transmission but not by omni mode. The drawback of this protocol is that they assume that there is a existing neighbor discovery layer which knows the angles in which the beam has to be focused to reach the receiver. The overhead and errors due to routing layer during route discovery will hence be totally eliminated. The protocol that was used for study does not assume that the sending and receiving directions to neighboring nodes are known. The AoA cache explained in section 3.3.1 maintains the table with the node ID and angle if it has already heard a transmission from that node. If the direction

is unknown then omni-RTS will be sent to the intended receiver. The higher gain of directional antenna was tried to be used by Korakis et al. in their directional MAC protocol [41]. Since the omni transmissions cover lesser range, they proposed to use the circular RTS. Instead of sending a single omni-RTS, the protocol suggests to send a directional beam in all the sectors thus covering 360 degrees around the node. The drawback of such a protocol is the wait time to transmit omni beam. If a omni beam needs to be sent then the channel should be idle in all directions around the node. This eliminates the hidden terminal problem to some extent but will suppress the channel reuse factor. The protocol does not study the omni-directional transmission of broadcast packets. Hence, it does not resolve the issue of finding routes even though it proposes the method to know the direction of the neighbor after listening to its transmission. The virtual carrier sensing in directional antenna that was used by the study was introduced by Takai et al. in [40]. They basically cache the Angle of arrival into memory tables . Based on the state of the DNAV, transmissions are scheduled. If the sector in which the beam is to be transmitted is busy, then it will be marked in the DNAV. This information is made use before initiating the conversation. However the signal may be listened by side lobes too. This does not address the effect of side lobes while the antenna is locked in some other direction which may lead to incorrect updates of the AoA cache.

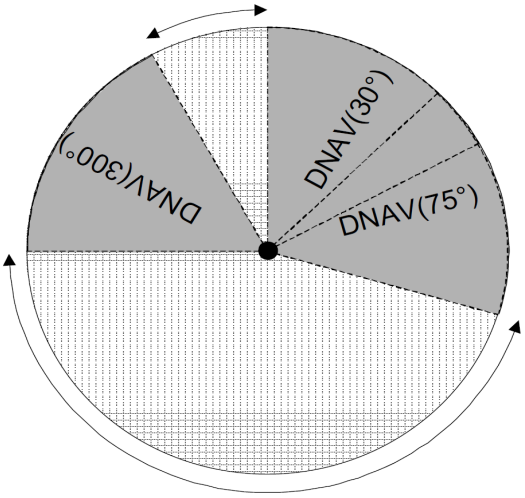

FIGURE 1.10: DNAV setting for virtual carrier sensing.

Figure 1.10 depicts an example of DNAV setting; three DNAVs are set up towards 30°, 75° and 300° with the 60° width. Until the expiration of these DNAVs, this node cannot transmit any signals whose direction is between 0° and 105° or between 270° and 330°, but is allowed to transmit signals towards 105° to 270° and 330° to 360°. Choudhury et al. attempt to mitigate deafness problem by proposing a novel method in [39]. Sinusoids are sent in a separate channel after the data transmission is over. If the sender or receiver was deaf to any RTS that could have arrived during that time, then the sender of the RTS will update its state after hearing to the sinusoid and will realize that the other node was deaf. It may attempt to re-contact

the node after listening to the sinusoid. However, the use of multiple channel to solve deafness is the deployment barrier. The DMAC studied in this thesis does not employ this method to detect deafness.

1.4 Routing and Directional Antennas

Although recent research activity has addressed some of the problems related to directional medium access, the impact of directional antennas on the performance of higher layer protocols has not been adequately explored. As evident from subsequent sections of the report, the impact of directional communication on the performance of an ad hoc network is often counter-intuitive. While fewer hop routes may be discovered due to the higher transmission range of directional antennas, performing a simple neighborhood broadcast may now require the antenna system to sweep its transmitting beam sequentially over multiple directions. As a result, neighbors of a node receive broadcast packets at different points of time (unlike with omnidirectional antennas). Also, sweeping incurs greater delay and can incur higher control overhead, partially negating the advantages derived from reducing the hop-count of discovered routes.

1.4.1 Directional Routing Related Works

Work on routing protocols using directional antennas is limited [42], [43]. In [42], Nasipuri et al. have utilized directional antennas for the purpose of on-demand routing. Their primary aim is to minimize routing overhead by intelligently using directional antenna elements for propagating routing information. Their results highlight the large routing overhead incurred by using omnidirectional antennas and show that it is possible to perform better using switched beam antenna systems. However, the authors have equalized the transmission range of directional and omnidirectional antennas, thereby under estimating the potential of directional beamforming. Put differently, the impact of discovering shorter routes using directional antennas has not been studied.

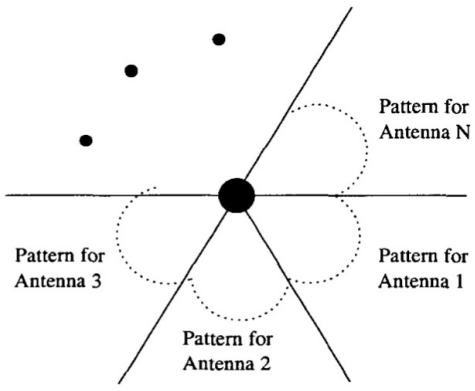

FIGURE 1.11: Nasipuri directional routing model.

In Figure 1.11 the mentioned directional routing model is illustrated. The radio transceiver of each mobile node is equipped with M directional antennas that are placed in order that their formed radiation beams do not overlap. Any node that wants to send a data packet have to establish a link with the desired destination (route discovery) through RTS and CTS packet exchange; the route discovery process provides that the transmitter node send a query with the same antenna used for latest communications. As a variant, protocol establishes that, at the end of the route discovery process, the transmitter records the directions of the antennas to be used on every hop of the newly discovered routes. In work [43] author propose a proactive routing protocol (originally proposed for omnidirectional antennas [44]) over Electrically Steerable Passive Array Radiator (ESPAR) antennas. The protocol provides that, when a transmitter node wants to communicate with a receiver, it sends omni-directional RTS to inform all of its neighbors about the current communication request also by specifying the intended receiver; it also specifies the approximate duration of communication. The target node (the transmitter) sends an omnidirectional CTS to grant the request and to inform the neighbors about the fact that the receiver is busied in a communication. In addition, all of the neighboring nodes of the transmitter are aware of the direction of the receiver engaged in the communication by using the Angle Signal Interference To Noise Ratio (SINR) Table (AST). The routing protocol performs well and gives reason to believe that directional antennas may be acceptable for ad hoc networking. However, the Medium Access Control (MAC) protocol is complex, requiring several exchanges of control packets before actual data can be transmitted. Most of the routing layer protocols like An On Demand Distance Vector (AODV) [45] and Dymanic Source Routing (DSR) [46], broadcasts the route request packets to find out the routes. All such requests use omnidirectional mode of transmission for broadcasting. Hence directional neighbors are not discovered by using omni-directional route discovery. This is a major hindrance which makes the directional neighbors invisible to the routing layer. Hence, the next hop for apacket will always be a omni-directional neighbor. Even though the packet may be transmitted directionally, it is transmitted to a node who can be reached by omnidirectional communication. This excludes the use of greater range of directionally focused signals. The idea of sending directional beams in all sectors instead of a single omnidirectional transmission was suggested by Korakis et al. in [33] which was used for sending RTS. Choudhury et al. [39] works on discovering the directional neighbors by sweeping the directional beam for all broadcast packets over each sector to transmit an omni-directional packet. This makes it possible to discover the directional neighbors. However, this approach introduces a large amount of overhead. A possible solution to this issue is proposed in works [47], [48], in which authors presents a Directional DSR protocol; The routing protocol should handle the upcalls from the MAC layer to utilize the upcalls. The Directional Dymanic Source Routing (DDSR) protocol maintains a table which is updated according to the upcall information. This table is called one-hop table. This table stores all

the nodes that can reached by one hop. Effectively, this contains the neighbors of the given node. When the upcall function is called by the MAC layer when a node was added, then the node was added to the one-hop table. If the upcall for purging of the node then the entry is purged from the one-hop table too. Since the DSR works on source routing, the packet contains the complete route which the packet needs to take. While the packet is to be forwarded, the source route is searched to select the next hop that is reachable from directional transmission and which is nearest to the source in the source route. The one-hop table will aid the search process by revealing if a given node in the source route is a directional neighbor. This makes it possible for the packet in DDSR to take a shorter route than the one specified in its source route if a directional neighbor can be reached in one hop instead of two hops.

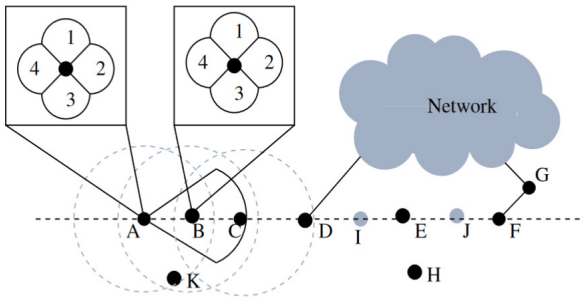

FIGURE 1.12: Directional DSR scenario example.

In Fig. 1.12 an example of application of DDSR is illustrated. If an Route Request (RREQ) is transmitted directionally by A, link A–C can be on the route. If the RREQ is transmitted omnidirectionally by node A in Fig. 1.12, then node C would not receive A's transmission, and link A–C cannot be on the chosen route. If the beam being used for transmission senses the channel idle, it transmits the RREQ. Antenna beams that sense the channel busy are marked during the first round of transmission. Once the round is completed, Directional MAC attempts to transmit the RREQ only over the marked beams (sequentially). If some of the marked beams now sense the channel idle, the RREQ is transmitted using them. For beams that still sense the channel busy, Directional MAC drops the RREQ. This entire procedure constitutes a single sweep. In [49] authors present a Directional AODV routing protocol based on hop count to a gateway. Directional An On Demand Distance Vector (DAODV) uses hop count, which is the number of hops from a gateway in order to limit the retransmissions of RREQ packets. Each node learns its number of hops from a gateway through gateway and hop count discovery. On receiving RREQ packets, a node compares the hop-count value on the RREQ packet with its hop count, then it broadcasts only RREQ packets with a higher hop-count value then itself. Before broadcasting a RREQ packet, each node tags its hop-count value on the RREQ packet. Thus, RREQ packets are directionally flooded toward the gateway. The AODV uses periodical HELLO messages to indicate the presence of a node to its neighbors. In the DAODV, these HELLO messages are also used for gateway and

hop-count discovery without any protocol overhead. HELLO packets have a Time To Live (TTL) of 1 and therefore, will not be forwarded to other nodes. Since they are derived from route reply packets they have a number of unused fields. The main effect of DAODV is the reduction the number of broadcasting route request (RREQ) packets through the use a restricted directional flooding technique.

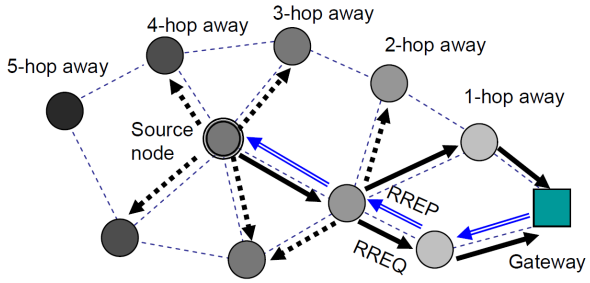

FIGURE 1.13: Route discovery in DAODV.

The Figure 1.13 illustrates the Route Discovery operation in DAODV. When a node receives the RREQ, it establishes a reverse route to the RREQ source in its routing table, and it either replies to the RREQ if it has an entry for the gateway or it forwards the RREQ. Eventually, the RREQ reaches the gateway and it unicasts a Route Reply (RREP). The node receiving a RREP sets up a forward route to the gateway and desirable routes can be discovered.

Chapter 2

Smart Antenna and Massive MIMO Systems

2.1 Introduction

Above years, designers and programmers of wireless communications systems have been attempting to get to overcome the problems facing the systems, co-channel interferences, multipath fading and inter symbol interference are deemed as main challenges that lead to the decrease in the quality of service and limit the numbers of customers served by system. In MANET environments, although the most of traditional systems employ omnidirectional antennas, it has largely demonstrated that these kinds of solutions are not adequate to the modern requirements for wireless systems as well as the need to decrease infrastructure and maintenance costs. The employment of Smart Antenna Systems (Smart Antenna Systems (SAS)) in wireless mobile environments allows a more efficient medium utilization with respect to the classical Omnidirectional approach [50]–[52]. For example, Spatial Division Multiple Access (Spatial Division Multiplexing (SDMA)) seeks to increase the capacity of a system. Generally, Smart Antennas fall into three major categories: Single Input Multiple Output (SIMO) ,Multiple Input Single Output (MISO) and Multiple Input Multiple Output (MIMO) Multiple Input, Multiple Output) [53]. In SIMO technology, one antenna is used at the source, and two or more antennas are used at the destination. In MISO technology, two or more antennas are used at the source, and one antenna is used at the destination. In MIMO technology, multiple antennas are employed at both the source and the destination. A Smart Antenna System combines generally an antenna array with a digital signal-processing capability to transmit and receive in an adaptive, spatially sensitive manner. In other words, such a system can automatically change the directionality of its radiation patterns in response to its signal environment. This can dramatically increase the performance characteristics (such as capacity) of a wireless system. SAS are able to outperform conventional omnidirectional systems in terms of spectral efficiency by achieving more capacity in order that a larger number of end-users can be served [54], [55]. In literature, many researches have been demonstrated how the use of directional antennas and the most recent SAS technology is capable of significantly allow high

Quality of Service (QoS) requirements in spite of the omnidirectional systems that foresee limited functionalities. However, these solutions are unlikely to fulfil the requirements for the the 5G next generation wireless communication systems technology [56]. For this purpose, the massive MIMO technology has been proposed as efficient solution for satisfying the requirements for 5G that certainly include very high antenna gain and very high data rate in order to achieve huge system performance [57]–[59]. In this chapter a deep overview about smart antenna and Massive MIMO systems is presented, with reference to the architectures employed in this field; the present chapter will highlight the most important benefits and drawbacks of this systems and its applications in communication field.

2.2 Antenna arrays background

Before introducing SAS concepts, because they represents a particular case of antenna array,it is necessary to focus on main antenna array mathematical aspects. Basically, an antenna array is a set of radiating elements that are spatially distributed at fixed locations [60], [61]. The object responsible to scan the radiation pattern in a certain direction/area called the *beamformer* electronically produces the beam and can also provide for placement of nulls in any direction by changing the phase and amplitude of the exciting currents in each of the antenna elements. Antenna elements are arranged according a geometric pattern that can usually be linear, circular or planar arrays.

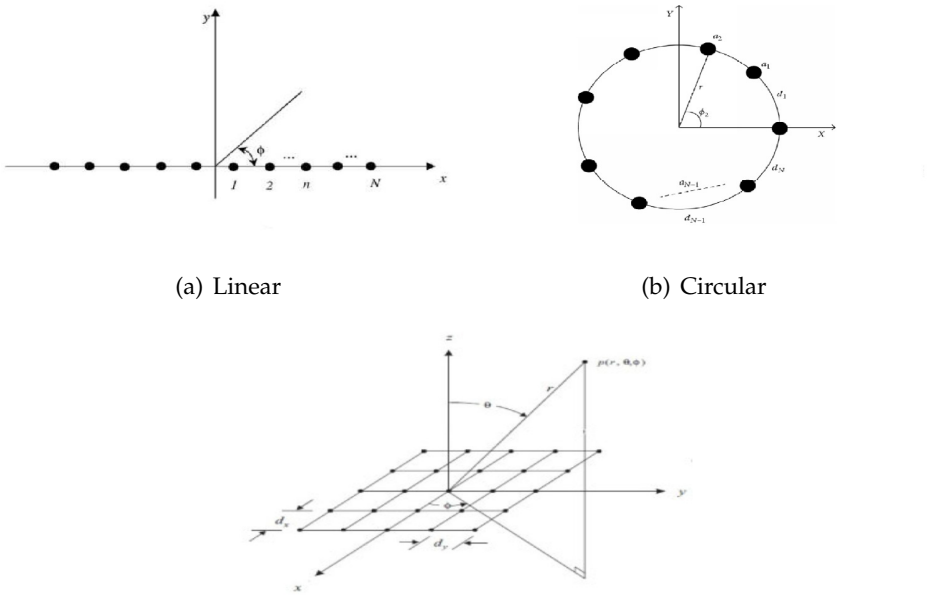

(a) Linear

(b) Circular

(c) Planar

FIGURE 2.1: Different kinds of geometry patterns for antenna arrays.

Linear arrays (Figure 2.1(a)) have their elements placed along a straight line, and are further called uniformly spaced linear array if the spacing between the array

elements is equal. Circular arrays (Figure 2.1(b)) have their elements placed on a circle while planar arrays (Figure 2.1(c)) present elements that are typically lying in a two-dimensional plane according a rectangular pattern. However, both linear arrays and circular arrays belong to the set termed planar array, with all their elements lying on a single plane. Arrays whose elements do not lie on a single plane but conform to a given nonplanar surface are categorized into conformal arrays [62]. The radiation pattern of an array is determined by the radiation pattern of the individual elements, their orientations and relative positions in space, as well as the amplitudes and phases of the feeding currents. If each element of the array is an isotropic point source, the radiation pattern of the array will depend solely on the geometry and feeding current of the array. Therefore the total field of an array is a vector superposition of the fields radiated by the individual elements [63]. In particular, the electrical field of the i-th array antenna element, assuming far-zone field condition, could be expressed as:

$$E_i = M_i E_{n_i}(\theta_i, \phi_i) \frac{e^{-j\left(kr_i \pm \frac{\beta}{2}\right)}}{r_1} \widehat{\rho_n} \tag{2.1}$$

Where M_i denotes the field magnitude of the i-th element, E_{n_i} is the normalized field pattern of the i-th element, r_n is the distance to the of the i-th element from the reference observation point, β represents the phase difference between feed of elements of the array and $\widehat{\rho_n}$ is the the polarization vector; electrical field is function of the spherical coordinates θ_i and ϕ_i. By making the following assumptions:

$$1.\ E_{n_1}(\theta, \phi) = E_{n_2}(\theta, \phi) = ... = E_n(\theta, \phi)$$

$$2.\ \widehat{\rho_1} = \widehat{\rho_2} = \widehat{\rho_n}$$

$$3.\ M_1 = M_2 = M_n$$

The total field can be expressed by $E = EF \times AF$ where terms:

$$EF = \widehat{\rho_n} M_n \frac{e^{-jkr}}{r} E_n(\theta, \phi) \tag{2.2}$$

$$AF = N \cos\left(\frac{kd\cos\theta + \beta}{2}\right) \tag{2.3}$$

Denote the element factor and the array factor respectively. Observe how the array factor AF depends on the total number of elements of the array N. The array factor is usually normalized with respect to N:

$$AF_n = \cos\left(\frac{kd\cos\theta + \beta}{2}\right) \tag{2.4}$$

Finally, the normalized field pattern of the array is given by:

$$f_n(\theta, \phi) = E_n(\theta, \phi) \times AF_n(\theta, \phi) \tag{2.5}$$

The Equation (2.5) expresses the pattern multiplication field rule establishing that the total radiation pattern of the array is the product by the radiation pattern of the single antenna element multiplied by the array factor. In the case of linear uniformly spaced array the normalized array factor can be expressed as:

$$AF_{LINEAR} = \frac{\sin(N\psi/2)}{N\sin(\psi/2)} \tag{2.6}$$

Where $\psi = kd\cos\theta + \beta$. It can be easy verified that $AF_{MAX} = N$. Antenna array systems usually falls in two categories:

- **Phased Arrays**. The phased array consists of several elements of radiation are arranged and linked in a certain way to give direction radiation model [64], [65]. This Array has wide applications in radar, communications, and at the present time in the microwave frequencies used in satellite communications, the main objective of this technique is to increase gain in the desired direction and suppression the radiation in the unwanted direction, by adjusting the phases of the signals that feed input elements in array. For illustration purposes it can be said that the total electromagnetic field of an array is obtained by vector addition of the fields emitted by the array elements, combined in both phase and amplitude.

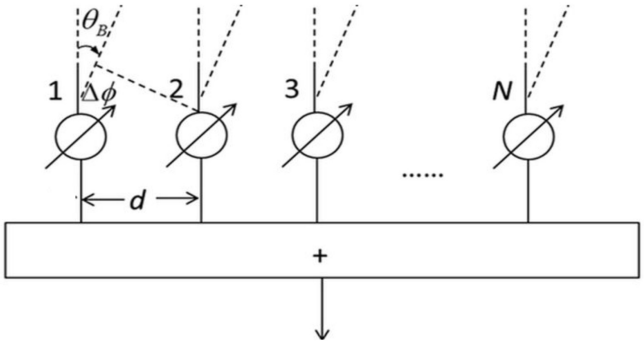

FIGURE 2.2: Phased Array example.

For phased array we have:

$$\psi = kd\cos\theta_0 + \beta \tag{2.7}$$

Where, the term θ_0 denotes the direction of the main beam (also known as steering angle) and β is the phase difference. The Figure (2.2) illustrates an example phased array. Each branch of the array is equipped with a phase shifter (the circle with an oblique arrow in the figure). The direction of the main beam is electronically controlled by the term β. The scanning is required to be continuous, while the feeding system is able to vary the progressive phase β between the elements; this last operation is accomplished by phase shifters.

- **Adaptive Arrays**. In communication the term adaptive array usually refers to the radiation properties of array which is characterized by the capability to change the radiation pattern according on changes and requirements of system; this array can be distinguished from traditional antennas due that it is able to operate with high performance in dynamic environments; these kinds of systems are suitable to adapt the beam based on desired or unwanted signals arriving from different directions and different levels of energy [66], [67]. In addition, the use of adaptive arrays in communication system increase reliability and translates into higher performance compared to the conventional systems; the efficiency of network performance is improved by reducing the level of side lobes in the direction of undesired signals and by reducing the interference while maximize the radiation pattern toward the desired user. The adaptive operation is mainly performed through signal processing units improving the performance by adapting the weights based on the received signal; the main goal of an adaptive array is to maximize reception in the desired direction and minimize the reception from undesired users.

2.2.1 Beamforming

Beamforming is the most significant process accomplished by an antenna array in order to perform the scanning of the overall signal toward a certain area/direction; it is the process that is referred to the generation of the radiation pattern from the output of array elements such that the energy either focuses or disseminates along a specific direction in space. Electronically scanning of the antenna array can be done using a power dividing beamforming matrix such as the Butler matrix [68], phase array approaches or optimal combining. By applying beamforming to an array of antenna elements, one can obtain directional antenna beams at low cost [69]. In addition, the beam patterns formed by an antenna array are very flexible. For simplicity, it is desirable to electronically scan the beam of an antenna by changing the phase of the output from the antenna elements. If only the phases are shifted with the amplitude unchanged when a beam is steered, the array is a phased array.

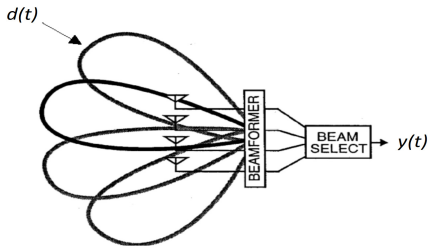

FIGURE 2.3: Beamforming operation.

As it can be observed in Figure 2.3, beamforming is generally accomplished by a beamformer that selects the beam, through a beam selector, based on desired signal $d(t)$ and returns the output signal $y(t)$ (if we assume to be in the time domain).

Beamforming can be achieved through either analog or digital methods. Commonly, when referring to analog beamforming devices such as power dividers, power combiners, and phase shifters are employed to perform this operation [70]. In particular, they are used to adjust the amplitudes and phases of the signals received from each antenna element in order to form the desired directional beam. However, beamforming can also be carried out digitally [71].

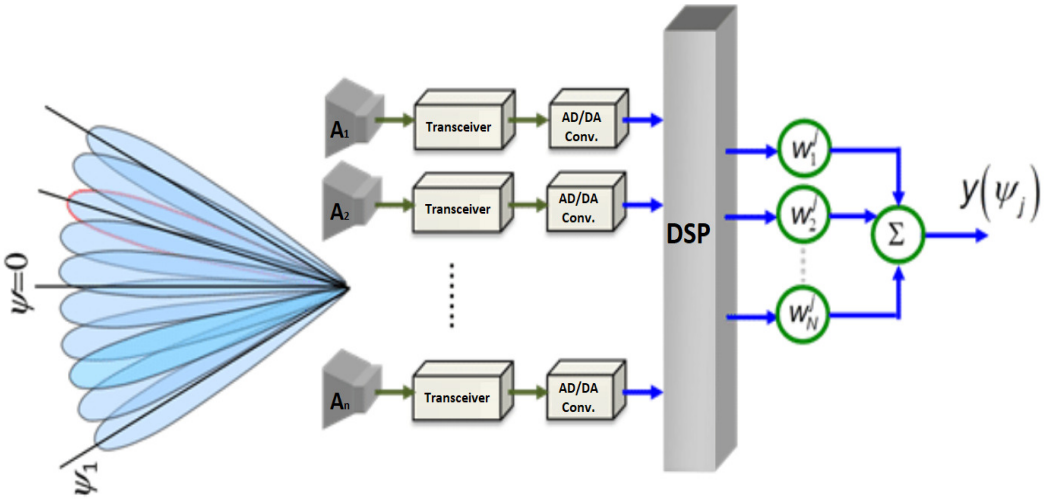

FIGURE 2.4: Digital beamforming example.

The Figure 2.4 illustrates an example of digital beamforming. The transceivers are required to perform frequency down-conversion and upconversion, filtering, and amplification. A/D and D/A converters transform signals in the digital domain into analog domain, and vice-versa. Various digital signal processing (Digital Signal Processing (DSP)) techniques can be used to form the desired beams. The major advantage of digital beamforming is the fact that Radio Frequency (RF) signals are captured in digital form, enabling a multitude of digital signal processing techniques and algorithms to be used for spatial processing. It also brings great flexibility without any degradation in Signal to Noise Ratio (SNR).

2.3 Smart Antenna Systems

Generally, Smart Antenna System (SAS) is defined as a combination of devices properly placed identifying a a software and an hardware part [72], [73]. The hardware section is represented by the antenna array, which, in turn consists of a certain number of antenna elements; the software part is usually represented by the digital signal processing unit that enable the overall system to be smart. In latest years researches tended to develop algorithms that allow to these kinds of systems to be ability to identify, locate and track user dynamically through the concept of DOA (Direction of Arrival); DOA is a parameter related to the direction of the arriving signal that can be estimated through appropriate algorithm; note that the direction of an incoming signal can often denoted with Angle of Arrival [74]. In order to improve

the efficiency and capabilities of a DSP, especially for Adaptive Array SAS, adaptive algorithms have been developed. More specifically, adaptive algorithm improves the accuracy in order as concerns the beamforming operation; in this regards it is advisable to direct the main beam towards the desired target and nulls in unwanted directions via beamforming algorithms; this would significantly reduce the noise and maximize the directivity of antenna. Indeed, as it will explained in next sections, adaptive algorithm are able to minimize error in the channel by improving the DOA estimation in order that the signal is powered toward the intended direction. In other words, SAS can be defined as a smart technology that can increase the gain of antenna array system which in turn reduces interferences, thus increases the quality of service and performance of the system, and the spectral efficiency is achieved. Based on the way in which beamforming is accomplished we could distinguish two main categories of SAS:

- **Switched Beam**: this kind of systems are able to form a finite number of fixed and predefined patterns without channel feedback.
- **Adaptive Array**: an infinite number of patterns that are adjusted in real time based on such parameters (for example channel noise conditions).

In the following sections, more details about different typologies of systems are illustrated.

2.3.1 Switched Beam SAS

A switched-beam system is the simplest smart antenna technique [75]. This system is based on the idea of cell-sectoring in dynamic manner, where it is characterized by fixed, predefined lobe-patterns as illustrated in Figure 2.5. This system is called switched-beam because it is able to switch between multiple fixed beams, that are formed by a phase adjustment process, according to direction and movement of the user, in order to increase the gain and enhance the reception. These systems are more able, with respect to sectorized antenna systems, to choose the appropriate beam and achieve the characteristic of directivity without the need for a fixed metallic physical design.

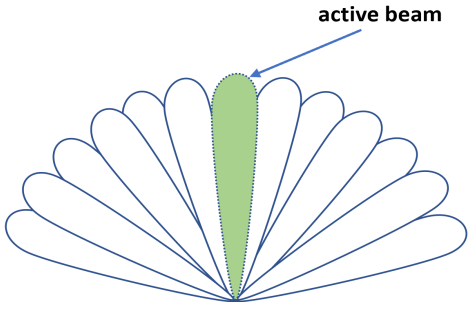

FIGURE 2.5: Fixed beams formed by Switched Beam SAS.

As it can be observed in Figure 2.5, beams produced by switched beam system are identical but shifted in phase. Only a beam at a time can be active; however, the system has the capability to switch electronically from a beam to another according to the intended direction of the user. Switched beam are the most simple SAS technology, however because in this case the DSP does not support any adaptive algorithm. Performance are limited with respect to Adaptive Array systems.

2.3.2 Adaptive Array SAS

Adaptive array systems is classified as the most intelligent in smart antenna systems [76], this classification is due to its ability to adapt the radiation pattern in real time this system exploits the spatial signal signature in order to estimate the desired user's location and then directs the radiation towards it as well as tracks the signal of interest Signal Of Interest (SOI) while places null in all unwanted direction, thus can reduce the effect of noise, multipath fading and interferences on the system. By signal processing unit,this technology can adjust the parameters of the system adaptively in order to optimize the performance. Adaptive Array systems, because of the use adaptive algorithm in DSP unit, are able of to effectively locate and track various types of signals in order to dynamically minimize interference and maximize the intended signal at the receiver. In this case, produced beam is variable and adapts itself depending on transmission channel conditions and a weight array that dynamically varies in time.

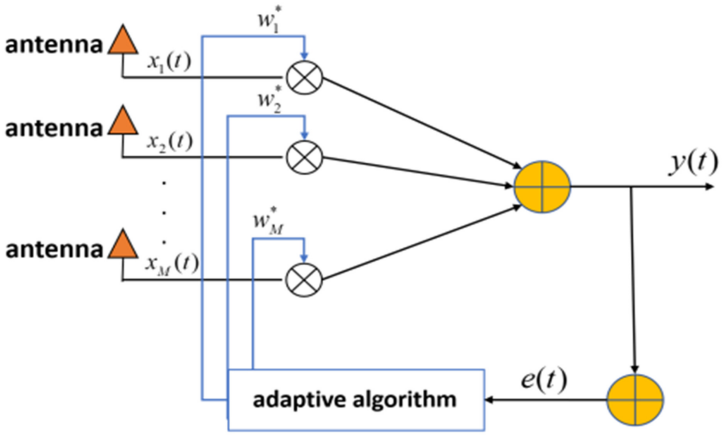

FIGURE 2.6: Adaptive array SAS structure.

In Figure 2.6 inputs $x_1(t), x_2(t), ..., x_M(t)$ are multiplied by elements of a weight vector $\overline{W} = [w_1, w_2, ..., w_M]$ that varies according to an adaptive algorithm; $y(t)$ is the output while $e(t)$ denotes the error; all terms are defined in functions of the discrete time t. Instead, when a switched beam approach is employed, because any adaptive algorithm is executed, the weight array can be considered missing or simply as a constant. Based on the kind of produced geometry pattern, SAS can be categorized into different ways. The most common categories include, rectangular, hexagonal and the circular arrays. However, in latest 5G technologies, the antenna

arrays should be adaptive and it is required that they have an adaptive capability to point the main beam toward the desired direction and steer the nulls toward the undesired interfering directions. The main difference between adaptive antenna and switched-beam antenna systems is the ability of the adaptive array system to form the main beam by controlling the angle and amplitude of radiation pattern in adaptive manner to achieve an optimal gain in desired direction and suppress other interferences, while the second system is unable to form a shape of a main beam, it is only able to selects the appropriate fixed beam and switch between the predefined beams depending on the movement of the user, that makes the switched-beam system less efficient in dealing with interference close to the desired signal and less ability to increase the capacitance compared with the adaptive system as well as the intra-cell handoff must be handled among beams other than the intra-cell hand of in other system.

2.4 Advantages and drawbacks of SAS

In the present section main advantages and drawbacks related to the use of SAS are synthesized:

- **Coverage improving**. Coverage area is commonly referred to the region where the communication between a user and the base station is available; due to the fact that smart antennas is more directive compared to conventional systems such as omnidirectional antennas or sectorized antennas, SAS can achieve better coverage [77], [78]. This feature is highly related to higher gain that is provided by the adaptive system. Moreover, it has been proved that this smart systems achieve coverage greater by M than conventional systems, while the number of required base station has decreased by $1/M$ by using smart antenna system with M antenna elements. However, the high-directivity of smart antenna system impacts on mobile devices through minimizing the required level of power and thus extending battery life of nodes.

- **Bit Rate increasing**. According to the spatial variation of the signals, SAS DSP unit allows to perform transmission/reception with a data rate that is generally one order higher with respect to conventional antenna systems [79]. Higher data rates means higher noise in the channel, but efficient adaptive algorithms there exist in order to limit channel interferences.

- **Security**. Security feature is considered a necessary issue in the field of communications to avoid intruding on users network data, the solution provided by the SAS is determined by the fact that they are able to radiate in adaptive manner with high gain; thus, the transmission of signals is not in all directions and thereby reducing the probability of spying on data and increase security whereas the hacker must be in the same location of the users [80].

- **Complexity**. The operations performed by the system on the receiving signals in order to optimize the service quality affect on the system and make it more complicated, especially in terms of the separation of incoming signals and synchronize them with real-time. In addition to the base station requirements to high-resolution powerful processors and controllers, this makes the system more complicated because of the need for complex mathematical operations in digital signal processing part.

- **Size**. The need to increase the number of elements in antenna array to provide better performance in addition to the fact that the separation distance between them restricted on condition and is depending on the operator frequency, lead to an increase in antenna array size, for example, the antenna array size would be approximately 1.2 meters wide at a frequency of 900 MHz and 60 cm at 2 GHz.

- **Cost**. The number of radiation elements, relating to SAS, because it is not excessive and limited (compared for example to Massive MIMO systems) does not affect the design cost; however, high accuracy in computation involves high cost; indeed, the higher is the complexity of the DSP unit the higher is the cost to implement such software.

2.5 SAS beamforming algorithms

Adaptive Smart antenna structure has by the capability to form and object the radiation of the main beam in the direction of the desired user while minimizing the undesired signals and noise. This feature is used to increase the performance during the transmission and reception of communication signal. This technique, which constitute the array beam pattern is referred as the beamforming. According to whether a training signal is used or not, most of the adaptive beamforming algorithms can be classified into Non-Blind Adaptive algorithm and Blind Adaptive algorithm [81]–[83]. Non-blind adaptive algorithms uses reference signal to modify the array weights repetitively, so that at the end of each every iteration the output of the weights is compared to the reference signal and the generated error signal is used in the algorithms to modify the weights. The examples are Least Mean Square Algorithm (LMS), Recursive Least Square algorithm (RLS), Sample Matrix Inversion (SMI) and Conjugate Gradient (CG). Blind adaptive algorithms do not make use of the reference signal and hence no array weight adjustment is required. The examples are Constant Modulus algorithm (CMA) and Least Square Constant Modulus (LS-CMA). By adaptively changing the antenna array pattern, nulls are formed in the angular locations of the interference sources so that Adaptive beamforming technique is able to operate in an interference environment. The digital signal processor is the heart of adaptive beam forming, which interprets the incoming data, determines the complicated weights (amplification and phase info) and multiplies

the weights to each element output and corrects the array pattern. The array thus minimizes the effect of noise and interference and produces maximum gain in the desired direction. Thus the SAS efficiency and performance is dependent on the adaptive algorithms used for digital beamforming. The present section provides for a brief overview of main beamfoming algorithms for SAS.

2.5.1 Adaptive Beamforming

Before illustrating main beamforming algorithms for SAS, because the meaning of beamforming for antenna arrays has already been introduced, it is possible to extend this concept referring to the so called adaptive beamforming. The term adaptive refers to the capability to update and adjust the weights continuously with the changing angles of arrived signals with time, while previous methods find the optimal weight without having to the re-calculations and that because the angles of arrived signals remain constant and do not change with the times [72], [84]. Unlike fixed beam systems, not only the steering directions but also the entire beam patterns are automatically formed during the adaptation process. In order to maximize the output signal power in desired direction and minimize the power in the unwanted direction, various powerful algorithms are used to adjust the weights of the smart antenna array adaptively, so that the output beam pattern is optimized for enhancing the system.

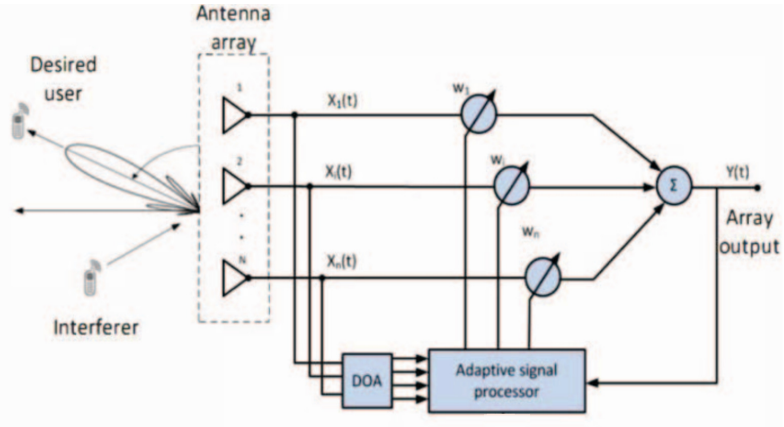

FIGURE 2.7: Adaptive beamforming principle.

The Figure 2.7 illustrates the adaptive beamforming principle. SAS are able to adapt the beam in function of the direction of the user; this is done through the DOA estimator that cooperates with an adaptive signal processor within which it is implemented the adaptive algorithm. In reception part of smart antenna system, the beam former implements the signal data of the training to establish the optimal vector of weights during the training time, data is then passed and the beam former investigates the computed weight vector to analyze any received signal. However, as mentioned, beamforming algorithms can be classified as blind algorithms and Non blind algorithms; the main difference between these algorithms is the fact that

blind algorithms tend to use, in its computation, the information of the desired signal more than non blind algorithms. In poor terms, blind algorithms usually does not need for a training sequence while non blind algorithms have to be trained.

2.5.2 The Least Mean Square algorithm

The Least Mean Square (LMS) algorithm was developed by Wirodw and Hoff in 1960 [85]–[87]. This algorithm is classified as a non-blind adaptive algorithm because it requires training sequence. By gradient method this algorithm can adjust the weights based on Mean Square Error (MSE) which is calculated from the difference between the input signal and desired signal, this ability to update the weights is based on the availability of information about desired signal and input vector, furthermore it does not need to correlation function or matrix inversion computation that makes this method simple and a reasonable choice for many applications. Least Mean Square (LMS) incorporates an iterative procedure that makes successive corrections to the weight vector in the direction of the negative of the gradient vector which eventually leads to the minimum mean square error.

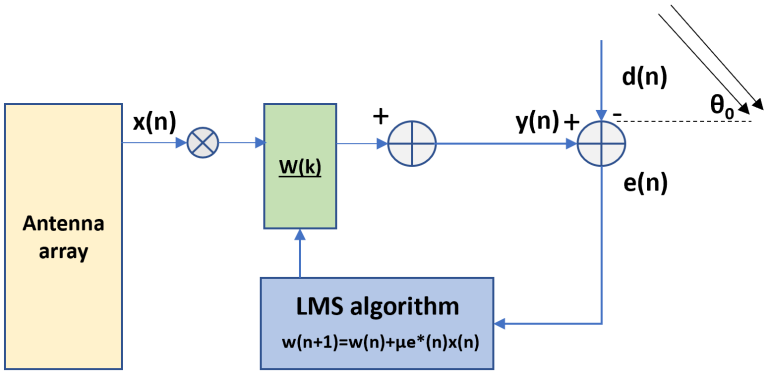

FIGURE 2.8: LMS operation.

The figure 2.8 represents a generic functional schema of an Adaptive Array SAS, in which $d(n)$ denotes the desired signal arriving with a certain desired angle θ_0 and $y(n)$ denotes the output of the Array System. The inputs are multiplied by weight of a weight vector $w(k)$ that dynamically varies according to the Adaptive Algorithm used. Finally, e(n) represents the error estimated by the system. All parameters depend on the length of the sequence n. LMS basic operation consists in the updating of weights of the systems; weight update operation can be synthetized by following few lines of pseudo-code:

Where the parameter μ denotes the step size and H represents the Hermitian operator. Stability and convergence rate of LMS algorithm is controlled by the step size that should be chosen in a range where convergence is insured; Typically, this range is $0 \leq \mu \leq (\lambda_{MAX})^{-1}$, where λ_{MAX} is the largest eigenvalue of the correlation matrix R. The main ad-vantage of LMS is its low computational complexity and disadvantage is slow convergence rate [9] [15]. In particular, if the step size is chosen in

Algorithm 1 LMS operation

1: **procedure** UPDATEWEIGHTS
2: **for each** n **do**
3: $e(n) = d(n) - W^H(n)x(n)$
4: $w(n+1) = w(n) + \mu e^*(n)x(n)$
5: **end for**
6: **end procedure**

the convergence range and is small the algorithm converges slowly with respect to higher step size values.

2.5.3 The Constant Modulus Algorithm

The Constant Modulus Algorithm (CMA) is classified as blind algorithm because the desired signal is not available. Constant Modulus Algorithm (CMA) is a gradient-based algorithm that works on the theory that the existence of interference causes changes in the amplitude of the transmitted signal, which otherwise has a constant envelope (modulus) [88], [89]. The Minimum Shift Keying (MSK) signal, for example, is a signal that has the property of a constant modulus. The algorithm is performed through the use of three distinct steps in each turn. In the first step, the computation of the processed signal with the actual weights is performed. In the second step, an error is generated from the computed signal. Finally, the weights are adapted with new error data in the third step. The CMA operation can be synthetized by the following instructions:

Algorithm 2 CMA operation

1: **procedure** UPDATEWEIGHTS
2: **for each** n **do**
3: $y(n) = W^H(n)x(n)$
4: $e(n) = \frac{y(n)}{|y(n)|} - y(n)$
5: $w(n+1) = w(n) + \mu e^*(n)x(n)$
6: **end for**
7: **end procedure**

Where $|\ y(n)$ is the absolute value of the output sequence that depends on the length of the sequence. We can say that the term $\frac{y(n)}{|y(n)|}$ in CMA plays the same role as the desired signal d(n) in the LMS algorithm. One severe disadvantage of the CMA is the slow convergence time. This drawback limits the usefulness of the algorithm in dynamic environment where the signal must be captured quickly. This also limits the usefulness of CMA when channel conditions are rapidly changing. CMA does not require a pilot signal but it has a major drawback of slow convergence. In summary, advantages of CMA are, slickness of implementation, adaptive tracking of sources, error estimation accuracy, therefore, the most common drawbacks are: slow

convergence, strong dependence on the step size (that should be small for having a good convergence) and sometimes, possible misconvergence to local minimum.

2.5.4 The Recursive Least Square algorithm

The Recursive Least Square algorithm (RLS) is one of the most popular adaptive beam-forming algorithms based on recursive least square. This algorithm requires no matrix inversion because correlation matrix is found directly. It uses the sum of squared errors for the inputs to update the complex weights instead of using the mean square error minimization [90], [91]. The first adaptation of this algorithm was derived from KALMAN filter for multi tap transversal filtering where samples are taken over variable time frame. However, this algorithm is applicable for other systems where the inputs are extracted from different sources. The algorithm uses desired signal and correlation matrix in the adaptation. The basic operations of the RLS can be summarized by the following code:

Algorithm 3 CMA operation

```
1: procedure UPDATEWEIGHTS
2:     for each n do
3:         g(n) = R_xx^{-1} x(n)
4:         w(n) = w(n-1) + g(n)(d(n) - x(n)w(n-1))
5:     end for
6: end procedure
```

In this case the step size is replace by the gain vector $\overline{g(k)}$, so $g(n)$ is the n-th element of the gain vector; while R_{xx}^{-1} is the reverse of the correlation matrix R_{xx} that is defined as:

$$R_{xx} = \sum_{i=1}^{k} x(i)x^H(i) \tag{2.8}$$

2.5.5 SAS beamforming algorithms state of art

Substantially, beamforming algorithms proposed in literature are derived from LMS, CMA and RLS and aim to partially solve drawbacks introduced by these algorithms. In the present section, the most important proposals in this context are illustrated. Several researches that attempt to analyze the slow convergence problem of the most common adaptive algorithms proposing new solutions for partially resolving this issue. In [92] authors proposed a Normalized version of LMS (NLMS) that solves the problem of input scaling usually present in LMS such as referred in [90], normalizing the power values in weight vector computation but the time convergence problem still persists. In [93] a Kernel Least Mean Square algorithm (KLMS) is proposed to overcome the short comings (like MSE) of existing algorithms for a smart antenna systems; the mechanism implemented allows an improving of the convergence time in terms of number of iterations. The authors in [94] propose a new Time-Varying LMS approach based on a time varying convergence parameter with general power

for LMS algorithm. This work represents an evolution of the idea proposed in [95]. The basic idea of NTVLMS algorithm is to adapt the step size during simulations in order to obtain acceptable convergence rate results even when the step size is small. Results show that the convergence parameter should be small for a better accuracy. There also exist some studies that try to enhance CMA algorithm; for example, Angular CMA [96] modifies the cost function of CMA to the form of real and imaginary parts allowing an enhancement in terms of computation accuracy. The authors in [97] proposes a new modified version of LMS and NLMS that present a variable step size in which, the new variable step size is computed using a ratio of the sums of the weighted energy of the output error with two different exponential factors. Simulations have been demonstrated that the proposed VS-LMS and VS-NLMS algorithms provide better performances in the implementations of the adaptive channel equalization and system identification compared to other existing algorithms. Although the evaluation of the adapted step size requires a lot of computations, the convergence time problem results weakened with respect to the original version of LMS and NLMS. A similar approach is used by author in [98] in which a new algorithm with variable step size is proposed using gradient vector's features to achieve an acceptable convergence time. Another resource adaptive approach is presented in [99]; in this work, authors provide a well-rounded mechanism to enhance the overall bandwidth management in wireless networks. More specific works such as [100] and [101] propose efficient models to overcome the issues related to interfering signals when an adaptation process has to be performed in high mobility environments such as in Vehicular Ad hoc Networks (VANET).

2.5.6 The Variable Metric Algorithm

As we have seen in the previous subsections the convergence of LMS and CMA algorithms closely depends on the value of the step size and on the error estimator used. In particular, LMS uses, as error estimator metric the MSE criterion, that does not allow a rapid convergence of the algorithm:

$$MSE := \left\{ [d(n) - y(n)]^2 \right\} = d(n) - w^H(n)x(n) \tag{2.9}$$

The complexity in this case is quadratic in term of number of computations. So, when the number of operations is large, this property could significantly limit the speed convergence of the algorithm. To reduce the impact of this drawback and accelerate the convergence we could use one or more error metric estimators that are "lighter" than MSE criterion, but maintaining the same accuracy in the error estimation process. For this purpose, a Variable Metric Algorithm (VMA) [102] has been designed. VMA presents a variable error metric estimator depending on the current error value measured after a certain number of iterations. As error metric estimator alternative Mean Absolute Error (MAE) and Mean Absolute Difference (MAD) [103] have been used. We can define MAE as the quantity used to measure

how close forecasts or predictions are to the eventual outcomes. MAD is defined as the average or mean (formally the expected value) of the absolute difference of two random variables X and Y independently and identically distributed with the same distribution.

$$MAE := \frac{1}{n}\left[\sum_n f_i - y_i\right] \qquad MAD := [X - Y] \tag{2.10}$$

Where f_i is the prediction value and y_i the true value. These two metrics have a $O(n)$ complexity (with the only difference that MAE requires a number of operations higher than MAD) and could be used as alternative of MSE to accelerate the estimation of the error during weight calculation operation. We propose two versions of VMA: the first one, beginning from the normal MSE criterion estimation, switches to a different metric when the bit error is higher than a threshold value (MAD has been preferred because from simulations has been verified be faster than MAE); the second version only uses MAD metric without using MSE. In both cases, it is possible to obtain a better error estimation at each iteration, improving the convergence speed of the algorithm. In our case, having a lower difference between the desired output and the system output at each iteration it means having a faster algorithm in terms of error computation. We can synthetize both versions of our algorithm with the following pseudo-code:

Algorithm 4 VMA-V1 operation

```
while !desiredAngleChange() do
    double avgError; double threshold=0.75;
    collectReceptions();
    int nrec=getNumReceptions();
    for each nrec do
        avgError=evaluateAvgError();
    end for
    if avgError >= threshold then
        use MAD;
    else
        use MSE;
    end if
end while
```

Algorithm 5 VMA-V2 operation

```
while !desiredAngleChange() do
    double avgError; double threshold=0.75;
    collectReceptions();
    int nrec=getNumReceptions();
    for each nrec do
        avgError=evaluateAvgError();
    end for
    use MAD;
end while
```

As the code illustrates, (*Receptions*), until the *desiredAngle* does not change during the simulation. Each Reception is associated to a desired sequence d(n) that could be represented by a binary string. For the Receptions collected, the function *evaluateAvgError* evaluates the average error on bit comparing (using a simple Hamming Distance metric) the desired sequence that is known a priori by the receiver and the output sequence $y(n)$. In particular, the average error is given by:

$$\text{avgError} := \frac{1}{n}\left[\frac{\sum_{k=1}^{N} e_k(n)}{N}\right] \tag{2.11}$$

Where $e_k(n)$ denotes the error measured related to the k^{th} sequence that is function of the length of the sequence n, while N is the number of sequences collected until a certain desired angle does not change (this parameter varies according to the traffic pattern set in the simulation). Acceptable convergence time results have been obtained with threshold values between 0.7 and 0.8, for this reason has been decided to set this value to 0.75. Output sequence is affected by the error introduced by the noise sequence $u(n)$ that corresponds to each interfering signal. If this error is higher than the threshold value, VMA-V1 switches to MAD else continue to use the MSE metric; VMAV2 instead, uses only MAD without using MSE. For example, suppose that we have a desired sequence of $n = 8$ bits 11001110 and three consecutive $y(n)$ sequences $(N = 3)$ having the same length of $d(n)$: $10001100, 01110001, 10001000$; the average error is given by: $[(2+7+3)/3]/8 = 4/8$; if this value is higher than the threshold the algorithm changes metric. VMA algorithm has been tested by using *PhasedArray* SAS Omnet++ module that we designed in [102]; The following table synthesizes main simulations parameters of the run configuration executed:

TABLE 2.1: VMA Main simulation parameter set.

Parameter	Value
SAS Array Elements Spacing	0.5 λ
Network standard	IEEE80211.g
Antenna Frequency	1 MHz
Message Length	512 *Byte*
Mobility model	Random Waypoint
Routing Protocol	AODV
Network Load	50 %
Simulation Area Size	500 x 500 m
Simulation Time	300 s
Number of samples	1000

The analysis has been accomplished in function of nodes mobility speed, increasing this value from $2m/s$ to $10m/s$; in particular 3 different configurations of node mobility speed have been considered: $2m/s, 6m/s, 10m/s$; for validating the model 20 different simulation runs have been performed, each one marked by a different seed for all configuration cases. Furthermore, after several simulations, because

LMS and CMS algorithm are closely dependent on the step size value, two different configurations (each one having a different value of step size) have been created : $\mu = 0.1$ (high step size) and $\mu = 0.01$ (small step size).

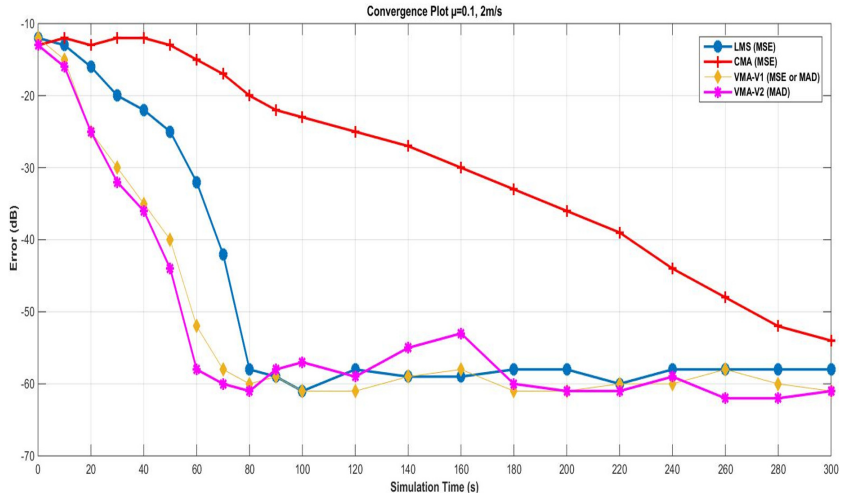

(a) $\mu = 0.1$

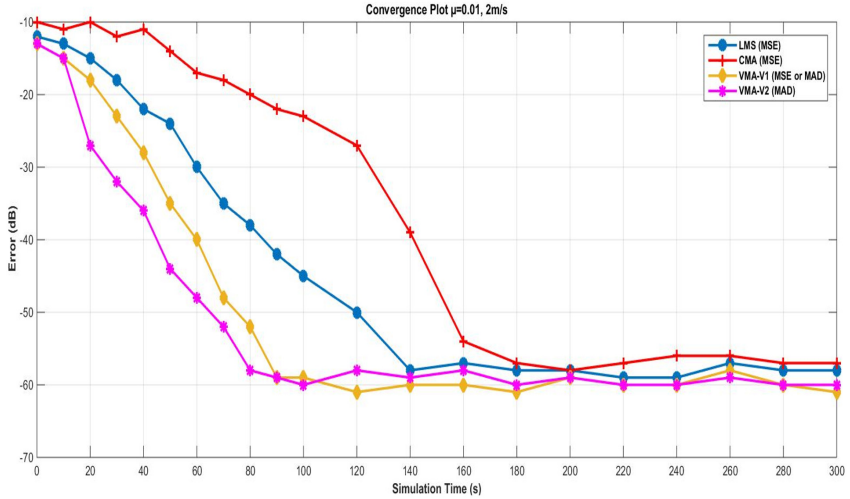

(b) $\mu = 0.01$

FIGURE 2.9: Convergence plots $2m/s$.

From Fig. 2.9(a) it can be observed that, LMS begins to converge after 80 s while CMA convergence is very slow with respect to LMS as it could be expected. In particular CMA measured error remains about constant until 60 s and begins to linearly decrease after 100 s CMA begins to converge after 280 s VMA-V1 curve begins to linearly decrease after 20 s and begins to converge after 70 s; VMA-V2 instead, converges slightly faster than VMA-V1 but as we can find especially from peaks to 140 and 160 s is not very stable in the interval between 80 and 200 s; In Fig. 2.9(b) we note that, as we can expect, because the step size decreases, LMS increases its convergence time that in this case is about 150 s CMA, instead, decreases its convergence time from 280 to 190 s VMA-V2 is faster than VMA-V1 and unlike previous case we have a linear trend during all simulation interval. However, in this case both

versions of VMA are faster than CMA and LMS but are slower with respect to the previous step size configuration. So, as the step size decreases, the convergence time increases slightly but remains acceptable.

TABLE 2.2: Algorithms performance comparison.

Algorithm	Avg. Speed Enh.	μ dep.	Cost
KLMS	52,32%	very high	low
NTVLMS	51,03%	medium	medium
ACMA	38,8%	very high	medium
VS-LMS	55,94%	low	high
NVS-NLMS	47,13%	very low	high
VMA-V1	55,58%	low	low

From Tab. 2.2 it can be noticed that, our VMA algorithm, provides similar performance in terms of convergence speed enhancement with respect to the VS-LMS algorithm that proposes a variable step size without modifying the error metric evaluation of the original LMS algorithm. Based on these results, we can conclude that, our proposed algorithm, should represent a good trade-off for obtaining a considerable speedup improvement and, at the same time, a little dependence degree from the step size parameter; VMA could be considered as a valid alternative to the most efficient algorithms that propose a dynamic step size to overcome the slow convergence problem in which, however, the updating process of the step size could be expensive in terms of computational cost.

2.6 Massive MIMO systems

Massive MIMO is a rising technology, that considerably enhances the basic MIMO features. The term massive MIMO, is referred to the whole of systems that use antenna arrays with at least few hundred antennas, simultaneously serving multiple terminals in the same time frequency resource [59], [104], [105]. Generally, a system can be called massive MIMO if a large number of antennas are deployed at one or both ends of the communication link. The number of antennas and communication schemes vary in different systems and applications. Two main categories of Massive MIMO exist, Single User (SU) MIMO and Multi User (MU) MIMO [106]; in the first case, only a user a time can access to Massive MIMO resources both in uplink and in downlink. However, MU-MIMO are are most commonly used with respect to SU - MIMO because they can exploit SDMA (Spatial Division Multiple Access) very efficiently; for this reason, in the present thesis we will refer to Massive MIMO considering a Multi User system. MU-MIMO technology in cellular systems, where a base station is equipped with tens to hundreds of antennas, and communicates with many users simultaneously through spatial multiplexing. Massive MIMO "problems" can be considered according the kind of transmissions that are involved; transmission can be downlink or uplink transmissions, for a single cell. MIMO with

a large number of antennas, however, should not be limited to multi-user scenarios. It can also be used in single-user scenarios, e.g., backhaul links between base stations in millimeter-wave communications.

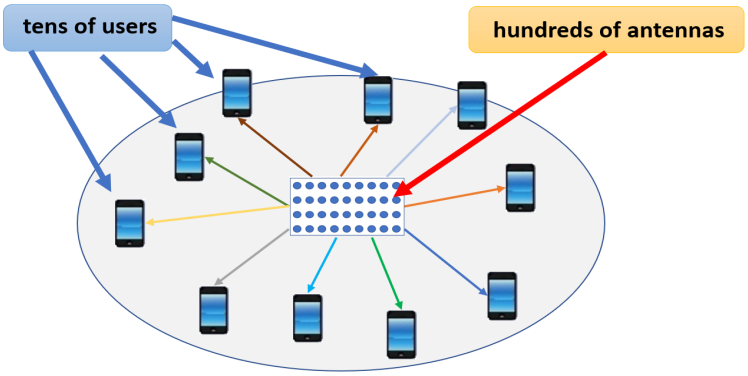

FIGURE 2.10: MU-Massive MIMO operation principle.

Figure 2.10 illustrates the basic operation principle of a massive MIMO; few users are served from a macro-device (for example a rectangular array) having a large number of base stations (antennas). Generally, massive MIMO is an instrument that allows to enable the development of future broadband (fixed and mobile) networks which will satisfy special requirements in terms of energy efficiency, security, and robustness. Structurally, a massive MIMO system consists of a group of small (relatively) antennas, supplied from an optical or electric digital bus that operates simultaneously related to a certain task. Massive MIMO, as well as the SAS systems are able to well exploit the SDMA (Spatial Division Multiple Access) allowing for an efficient resource channel utilization, both on the uplink and the downlink [107], [108]. In conventional MIMO systems, like the LTE (Long Term Evolution), the base station transmits waveforms depending on terminals channel response estimation, then, these responses are quantized by some processing units and sent out back to the base station. Fundamentally, this is not possible in massive MIMO systems, especially concerning high-mobility environments [109], because optimal downlink pilots should be mutually orthogonal between the antennas. However, the employment of these systems entails a series of issues that should be properly considered, for example, the interferences between terminals increase as the data rate increases. Other issue is the fact that terminals consume a lot of energy during the communication process in spite of the well SDMA exploitation. Finally, the difficulty of designing a system of limited size improves proportionally with the increasing of the number of antennas in the system. For this reason it is necessary to find a trade-off between the number of elements and the requirements. Therefore in spite of the difficult hardware and designing implementation, these systems are becoming increasingly prevalent in the modern applications due to the great benefits that could introduce:

- Massive MIMO can increase the wireless channel capacity up to 10 times with respect to the traditional LTE systems [110]. This means very high coverage.
- Massive MIMO can improve the radiated energy-efficiency up to 100 times with respect to the traditional LTE systems [111]. This translates into higher gains and higher performance.
- With large number of antennas, the energy can be focused with extreme sharpness into small regions in space [112]. This feature encourages a better energy system resource exploitation.
- Limited designing costs, if low power components are used [113].

However, the employement of these systems entails a series of issues that should be properly considered:

- Interferences between terminals increase as the data rate increases. However, techniques as the ZF (Zero Forcing) could be used to suppress such interferences [114].
- The terminals consume a lot of energy during the communication process in spite of the well SDMA exploitation [115].
- The difficult for designing a system of limited size grows up with the number of antennas [116]. For this reason it is necessary to find a trade-off between the number of elements and the requirements.

2.6.1 Planar Massive MIMO

Although there exist several kinds of massive MIMO systems depending on the geometry pattern, in this chapter only the planar massive MIMO technology is exposed. We use the term planar to indicate that the array can scan the beam along the elevation plane θ and the azimuth plane ϕ as opposed to the linear arrays that scan the main beam only along θ or ϕ. Planar arrays offer more gain and lower sidelobes than linear arrays, at the expense of using more elements . From an architectural point of view, a massive MIMO is structured depending on the geometry pattern that is able to form. There exist several design configurations that usually are function of the kind of application to which these systems are destined. Anyway, in this thesis, we consider three different types of planar antenna arrays: the URPA (Uniform Rectangular Linear Array), the UHPA (Uniform Hexagonal Linear Array), and the UCPA (Uniform Circular Linear Array). The following subsections synthesize the main feature of the mentioned configurations.

Massive MIMO URPA

The Uniform Rectangular Planar Array technology, is the most simple planar massive MIMO configuration [117]. The geometry pattern in this case is consist of a simple matrix within which the antenna elements are placed.

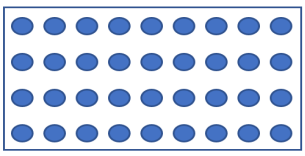

FIGURE 2.11: Massive MIMO URPA example.

The Fig. 2.11 illustrates an example of massive MIMO URPA configuration. Basically, a URPA is a two-dimensional matrix filled with a certain number of antenna elements (the circles in the figure) both along the x and the y axis; these antenna elements are equally spaced between each one and this spacing is usually expressed in wavelengths. If we denote the number of elements placed on the x axis with M (the rows of the matrix) and with N the number of antennas lying in the y axis (the columns of the matrix), the total number of elements of the URPA is given by:

$$NumElements = M \times N \tag{2.12}$$

Where M and N are arbitrary integers typically higher than 1. In the first versions of the URPA, M and N were identical and limited to 8; in the modern application M and N are commonly different and chosen between 8 and 12. In general, the radiation field formed by the antenna elements (known also with the term *element factor*) is given by:

$$E_m(r,\theta,\phi) = A \times f(\theta,\phi)\frac{e^{-jkr}}{r} \tag{2.13}$$

In the eq.2, A is the nominal field amplitude, $f(\theta,\phi)$ is the radiation field pattern , and r is the radial distance between the element and the reference point, that highlights the decrease of the field in function of the distance. According to the pattern multiplication principle, the antenna array total electrical field can be expressed as:

$$E_{TOT} = E_m \times AF(\theta,\phi) \tag{2.14}$$

The term $AF(\theta,\phi)$ is also known as *array factor* and it depends on the geometry structure of the array. In the case of URPA, the array factor equation is very similar to the Uniform Linear Array (ULA) with the only difference that is designed by considering two dimensions:

$$AF_{URPA}(\theta,\phi) = \left[\frac{\sin\left(\frac{M\psi_M}{2}\right)}{\sin\left(\frac{\psi_M}{2}\right)}\right]\left[\frac{\sin\left(\frac{N\psi_N}{2}\right)}{\sin\left(\frac{\psi_N}{2}\right)}\right] \tag{2.15}$$

With:

$$\psi_M = kd \sin\theta \cos\phi + \beta_M, \quad \psi_N = kd \sin\theta \sin\phi + \beta_N \tag{2.16}$$

$$\beta_M = -kd \sin\theta_0 \cos\phi_0, \quad \beta_N = -kd \sin\theta_0 \sin\phi_0 \tag{2.17}$$

The terms ψ_M and ψ_N indicate the array phase along the x and the y axis respectively while the terms β_M and β_N denote the scanning steering factors along x and y in function of the steering angle θ_0; finally, ϕ_0 is the azimuthal elevation steering angle term. Observe that the array factor expression related to eq. 4 is not normalized with respect to M and N. The overall gain of the URPA is expressed by the following:

$$G(\theta,\phi) = \frac{4\pi \left| f(\theta,\phi)\, AF(\theta,\phi)) \right|^2}{\int_{\phi=0}^{2\pi} \int_{\theta=0}^{\pi} \left| f(\theta,\phi)\, AF(\theta,\phi)) \right|^2 \sin\theta \, d\theta d\phi} \tag{2.18}$$

The eq. 7 is the generic expression of the gain valid for all antenna types and is function of the element factor and the array factor. If the antenna elements are isotropic we have $f(\theta,\phi) = 1$ and the gain becomes :

$$G(\theta,\phi) = D(\theta,\phi) = \frac{4\pi \left| AF(\theta,\phi)) \right|^2}{\int_{\phi=0}^{2\pi} \int_{\theta=0}^{\pi} \left| AF(\theta,\phi)) \right|^2 \sin\theta \, d\theta d\phi} \tag{2.19}$$

The eq. 8 also expresses the directivity of the antenna; thus, from antenna array theory it is possible to obtain the expression which correspond the maximum gain in case of isotropic antenna elements:

$$G_{MAX}(\theta,\phi) = \frac{4\pi \times NumElements^2}{\int_{\phi=0}^{2\pi} \int_{\theta=0}^{\pi} \left| AF(\theta,\phi)) \right|^2 \sin\theta \, d\theta d\phi} \tag{2.20}$$

Indeed, the maximum gain is the value corresponding to the maximum value of the array factor that in the case of the URPA is:

$$AF_{MAX}(URPA) = AF_{MAX}(ULA) = NumElements \tag{2.21}$$

Note that the maximum value of the array factor for URPA is the same for the ULA and it is equal to the total number of elements of the system. However, from theory, it is known that in the eq. 9 it is not possible to approximate the term $AF(\theta,\phi))$ to *NumElements* because is function of θ and ϕ which in turn determine the dependency parameters of the double integral.

Massive MIMO UHPA

A UHPA configuration (known as HPA) [118], usually, consists of M hexagonal rings, each one having a total number of $6m$ where m is the *m-th* ring of the system; the antenna elements are uniformly distributed in the hexagonal side. The typical structure of an UHPA is shown as follows:

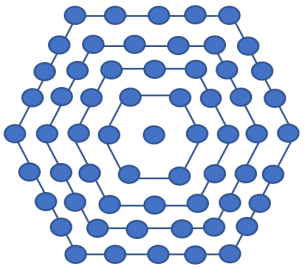

FIGURE 2.12: Massive MIMO UHPA example.

In case of isotropic elements, because the excitation amplitude is set to 1, the array factor can be expressed as the following expression:

$$AF_{UHPA} = \sum_{m=-M}^{M} e^{j\pi\left[mv_y - \frac{N}{2}v_x - \frac{m}{2}v_x\right]} \sum_{n=0}^{N} e^{j\pi n v_x} \tag{2.22}$$

Where:

$$N = 2M - |m| \; ; \; v_x = \sin\theta\cos\phi; \; v_x = \sin\theta\sin\phi \tag{2.23}$$

Note that in eq. 11 the dependence on θ and ϕ is omitted and furthermore the steering factor for beam scanning is not considered, while v_x and v_y denote the planar vectorial components along the x and the y axis respectively. The maximum theoretical gain is the same of the URPA case, except from the array factor term.

Massive MIMO UCPA

The geometry structure of a Uniform Circular Planar Array (also denoted as UCA) is very similar to a UHPA, except from the fact that the hexagonal ring is replace by a circular ring [119]. As assumed for the UHPA we can consider the widespread configuration having *6m* antenna elements uniformly placed around the circular edge of the *m-th* radius.

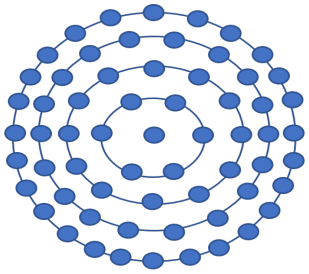

FIGURE 2.13: Massive MIMO UCPA example.

The Fig. 2.13 illustrates the UCPA configuration that consists of a certain number of circular rings having same center but different radius with the antenna elements placed on the circumference of each ring. Because an UCPA is a particular case of the hexagonal structure, the array factor equation is quite similar to the UHPA

expression. In case of isotropic elements the array factor could be expressed by the following:

$$AF_{UCPA} = 1 + \sum_{m=1}^{M} \sum_{n=1}^{6m} e^{-j(\pi m \sin\theta \cos(\phi - \phi_n) + \beta_M)} \tag{2.24}$$

Where:

$$\begin{aligned} \beta_M &= \sin\theta_0 \cos(\phi_0 - \phi_n) \\ \phi_n &= \frac{2\pi n}{6m} = \frac{\pi n}{3m} \end{aligned} \tag{2.25}$$

The eq. 13 (the dependence on θ and ϕ is omitted) considers the possibility to scan the beam through the use of the term β_M which is function of the steering elevation ϕ_0. The M and θ_0 are already defined in the previous subsection. From theory is also known that the steering vector and the array factor are closely related to the number of antenna elements, the array configuration and the antenna elements excitation (which in this case is unitary in amplitude). It is easy to conclude that the maximum achievable gain is the same of the UHPA and URPA case. However, as verified for the UHPA, the total number of elements is usually an odd number and depends on the number of circular ring in the structure.

Chapter 3

Extending Omnet++ Simulator with SAS and Massive MIMO modules

3.1 Introduction

The most recent antenna array technologies such as Smart Antenna Systems (SAS) and Massive MIMO (Multiple Input Multiple Output) systems are giving a strong increasing impact relative to 5G wireless communication systems due to benefits that they could introduce in terms of performance improvements with respect to omnidirectional antennas. Although a considerable number of theoretical proposals already exist in this field, the most common used network simulators do not implement the latest wireless network standards and, consequently, they do not offer the possibility to emulate scenarios in which SAS or Massive MIMO systems are employed. Indeed, unfortunately, the most of the network simulators does not offer a support for asymmetrical and directional communications [120], [121]. This aspect heavily affects the quality of the network performance analysis with regard to the next generation wireless communication systems that it can be translated in a huge limit from the point of view of the experimental study of these kinds of technologies. To overcome this issue, it is possible, for example, to extend the default features offered by one of the most used network simulators such as the Omnet++ Network Simulator [122], [123] which provides for a very complete suite of network protocols and patterns that can be adapted, in order to support the most modern antenna systems. The main goal of the present chapter is to illustrate the improvements accomplished in this field allowing to enhance the basic functionalities of the Omnet++ simulator by implementing the most modern antenna array technologies. In order to understand modifications carried out for designing new directional antenna modules, a brief summary about main feature of the Omnet++ simulator it will presented.

3.2 Network Simulators Overview And Omnet++

There are several network simulators [8] that could be used for creating a network mobile scenario containing nodes that are equipped with a particular kind of antenna system; some of the most used software are: Ns2, Ns3, Opnet, Omnet++.

- **Ns2**. It is open source, discreet event simulators for computer networks [124]. Network Simulator 2 (Ns2) code comprises of Object Oriented TCL (OTcl) and C++. OTcl is an interpreter used to execute the commands. NS2 follows two levels of hierarchy namely C++ Hierarchy and the interpreted OTcL, which is one to one correspondence. Two languages are linked because to achieve efficiency. C++ Hierarchy allows faster execution and to achieve efficiency. This gives detailed description, definition and operation of protocols, packets and processing time. On the other hand OTcL enables user to define network topology, protocols, applications that user tend to simulate. OTcL can make use compiled C++ Object through an OTcL linkage .OTcL Linkage creates a matching between OTcL and C++ Objects. Whenever you run a tcl file it will produce two outputs or two files namely trace file and namfile. Trace file differs for both wired and wireless scenario. It defines the event discrete simulators. It records the data for each millisecond and gives an output regarding packets send, received, dropped, initial energy of nodes, consumption of energy for transmitting, receiving, idle power, sleep power. It denotes the traffic model, simulation packets, packet size, and mac address. Nam file is a visual graphical window which shows the node movements, radio range, and packet transfer including time. Trace file can be given input to a new scenario file called NS VISUAL TRACE ANALYZER.

- **Ns3**. Network Simulator 3 (Ns3) is a discrete-event simulators primarily targeted for research and educational purposes. It was started in 2006 [125] and NS-3 is not an extension of ns2. NS3 is a new simulator. The similarity between ns2 and ns3 are both written in C++ Codes but ns3 does not support ns2 API. In ns3 simulators is written in C++ and python. The new modules ns3 has when compared with ns2 are: NS 3 can handle multiple interfaces or nodes correctly; Use of Internet Protocol (IP) Addressing and more alignment with Internet protocols and more detailed 802.11 models; Ns2 can be ported to ns3. The initialization and termination in ns3 is done by using run() and stop() commands. To free memory Destroy() method is used.

- **Opnet**. OPNET [126] is another network simulator, which again a best User Interface. It can be downloaded in IT Guru website. Test technology design in realistic conditions and evaluate enhancement to standard based protocols,develop new protocols and technologies. OPNET supports four simulation technologies as Discreet Event Simulator, flow analysis, ACE quick predict, hybrid simulations. Discreet event simulators provide models that

explicitly simulate protocols and simulate messages. It executes in same way as production environment. Flow analysis provides analytical techniques and algorithms to model Stead state network behaviour. ACE Quick Predict uses an analytical technique for studying the impact on application response time of changing network parameters (e.g., bandwidth, latency, utilization, packet loss) this technique is supported within the OPNET Application Characterization Environment (ACE). OPNET is a high level event based network level simulation tool .Simulation operates at "packet-level".originally built for the simulation of fixed networks. OPNET contains a huge library of accurate models of commercially available fixed network hardware and protocols.

- **Omnet++**. Omnet++ is a discrete event simulation environment. Its primary application area is the simulation of Communication networks, but because of its generic and flexible architecture, it is successfully used in other areas like the simulation of complex IT systems, queuing networks or hardware architectures as well. Omnet++ provides component architecture for models. Components (modules) are programmed in C++, and then assembled into larger components and models using a high-level language (Network Description Language (NED)). Reusability of models comes for free. Logical behavior of modules is generally written in .cc and .h files containing all logical functions. Because its simply features, and because this simulator enhanced and improved during years with some users contribution, therefore considering that it is extremely intuitive from user interface use Omnet++ simulator has been chosen for test simulations. In particular, Inet framework has been employed. Inet is a full-project folder that provides a very complete modules and protocols suite especially for Mobile Networks. Unfortunately, by default, Omnet++ does not support asymmetrical communication between nodes.

3.3 Inet and InetManet frameworks background

Because the extended features for Omnet++ are related to Inet framework modules, the present section provides for a complete background of Inet framework in order to understand the modification accomplished for implementing new antenna modules. An area of research in networking that has been the focus of a special attention in the latest years is MANET. With the emergence of the concept of Internet Of Things (IoT) the protocols that had been developed for MANET networks have returned to be an object of interest. A characteristic of this type of networks is the capability of auto-configuration. The nodes of this type of networks can discover the topology of the network, adapting autonomously to the possible changes in the topology, and creating a mesh network with the capacity of to send data from a node to other using intermediate nodes like routers, being able to reach nodes that are outside of the coverage area. At the time, several simulation tools have offered solutions to support the modelling and simulation of this type of networks.

However, all have in common several aspects, namely support for MANET routing protocols, the inclusion of wireless technologies that could work in Ad-Hoc mode and in the Industrial Scientific and Medical (ISM) bands, wireless propagation models and mobility models, which allow simulating the movement of the nodes. Some of these simulators also include energy models, which allow simulating the battery consumption of the nodes, and obstacles models, which allows studying the performance of a network in presence of obstacles that attenuate the radio signal strength. The first version of INET framework [1] had serious limitations in the simulation of MANET networks. It included only a basic support of some of these modules. It only offered some mobility models and the support of the standard IEEE 802.11b-1999. Keeping in mind this, InetManet framework emerges [127] initially as a fork from INET framework focused on the simulation of MANET wireless networks with the inclusion of several MANET routing protocols. Initially, it modified INET framework including an adaptation of the protocol AODV and overcoming some of the INET framework limitations. A significant limitation in the simulation of realistic MANET networks was the link layer protocol and the lack of routing protocols. Inet overcomes this limitation by introducing more advances 802.11 protocols, in this case, it included 802.11a/g/e and 802.15.4, which allowed simulating more realistic scenarios and complex networks. Later, it included the propagation models developed for MIXIM [2], allowing a comparison with the simulation results obtained with NS2 (even if the interference model in Ns2 is very basic). Other limitations that the INET framework had in its initial versions, was the lack of an energy model. With the objective of solving this problem, InetManet adapted the code of MIXIM, thus allowing simulating the consumption in wireless networks. With the objective of using some of the tools developed for Ns2, the module `Ns2MotionFile` was included, thus allowing the usage of several tools that can generate mobility patterns for Ns2. Another aspect to be solved, was the necessity of a source of traffic with the capacity of generating complex patterns. To solve this InetManet included the mode UDPBasicBurst that allows generating different patterns of traffic with the objective to test the performance of the MANET networks. Many of the code that was originally developed for InetManet has been included in INET framework. However, InetManet continues to have differences with INET framework. The differences are centered in:

- Routing protocols.
- Mobility models.
- Applications model.
- Routing and forwarding in the link layer.
- Antenna models.

[1] https://inet.omnetpp.org/
[2] https://github.com/omnetpp/mixim

- Miscellaneous tools.

Despite the differences, InetManet if fully compatible with inet-framework, any code, and model developed for the INET framework works without modification in InetManet.

3.3.1 Routing layer models

The initial fork of InetManet had the objective to include several MANET routing protocols, which at that moment inet-framework did not have. Later, the INET framework incorporated several routing protocols, but InetManet continues supporting routing protocols implementations that are not present in the main framework. The routing protocols implementations present in InetManet that are not available in inet-framework are:

- Aodv-UU.
- OLSR-UM.
- SAORS.
- DYMO-UM.
- DSR-UU.
- PASER.
- DYMO-FAU.
- BATMAN.
- DSDV.

Most of these routing protocols are defined in their respective RFC as programs that run in the user space and use the User Datagram Protocol (UDP) transport protocol RFC3561 RFC4728 dymoDrad DSDV. However, InetManet has a peculiar implementation of the MANET routing protocol as they are directly connected to the IP network layer module. Nevertheless, the MANET protocols encapsulate packets into UDP datagrams to ensure realistic overhead simulation. The main difference is that the identifier of the protocol type in the IP header is set to 254. The MANET routing protocol is directly connected to the network layer module. To activate the routing protocol it is enough to set in the configuration file the option routingProtocol. For example, to select the DSR protocol RFC4728 it is enough to include in the configuration (file omnetpp.ini) the option shown in the dsrSelect. The list of available protocols for this option is presented in Table 3.1.

Depending on the version of inet version used, routing protocols are usually contained in manetrouting package belonging to networkLayer namespace; however, latest inet release includes some of these protocols in the inetmanet folder. A complete overview of routing layer modules hierarchy is shown in the following figure:

From Figure 3.1 it can be observed how the most of routing layer protocols inherit ManetRoutingBase class; however, all modules also derive the cSimpleModule class that is the class responsible to pass the NED parameters to a generic instance of a object. Note that not all of Omnet++ class are associated with a NED file; this means that there exist special classes that can be defined as "passive classes" or "auxiliar classes" because they do not participate actively to the simulation process due that they are not related to a NED file. Anyway, typically, a class extending the

TABLE 3.1: List of MANET routing protocols and the option that must be selected in the configuration file

Option	Protocol
DSR	DSR-UU
AODVUU	AODV-UU
DSDV_2	DSDV
OLSR	OLSR
OLSR_ETX	OLSR with ETX implementation
DYMOUM	DYMO-UM
DYMO	DYMO-FAU
BATMAN	BATMAN
SaorsManager	SAORS
PASER	PASER

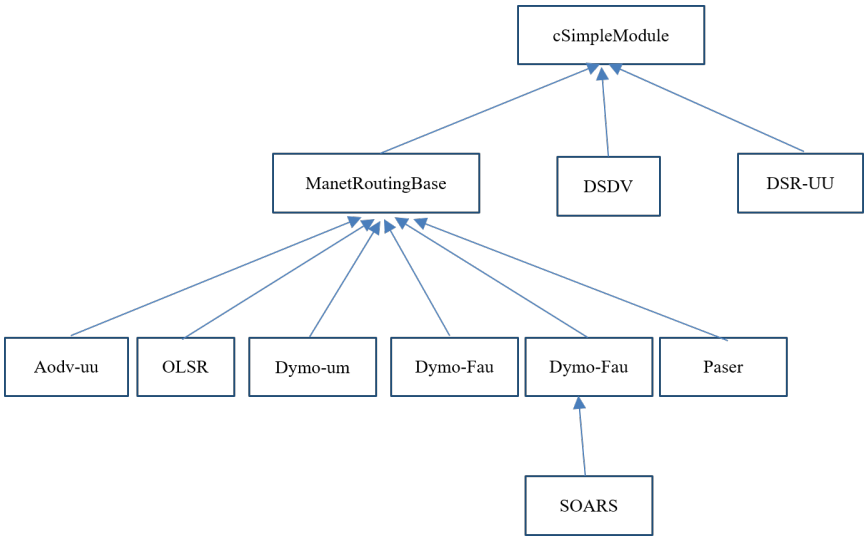

FIGURE 3.1: Inheritance of the MANET routing protocols implemented in InetManet

cSimpleModule interface has a NED file associated to itself, whereby is not a passive class. As shown in Fig. 3.1, most of the routing protocols are derived from the ManetRoutingBase class. This class offers an abstraction interface to other modules in INET framework (like access to the information of the routing or interfaces tables) that facilitates the adaptation of code. This class simplifies the port of code from other simulators like Ns2 or Ns3. Another advantage of this class is that it facilitates the adaptation of routing protocols to work in different layers. The routing protocols can work in the network layer, but also, can work in the link layer, making possible the routing and forwarding in the link layer, like is proposed in the standard 802.11s. The basic services that this class offers to the derived classes are:

- Signal processing
- Timer triggering functions

- The position of the node in the simulation area (similar to a GPS based device).
- Access to the ICMP protocol.
- Access to the IP routing table
- Access to the interface table. It is also possible to access to the interfaces of the node.
- Discover the wireless interfaces.
- UDP Encapsulation
- A transparent interface that allows the same code to be executed using the IP layer, or directly, in the link layer without the network layer.

3.3.2 Physical layer models

The Inet framework provides for several modules which allow the emulation of the most common node features and operations related to the physical layer including channel propagation models, modulations, energy consumption models and channel error models.

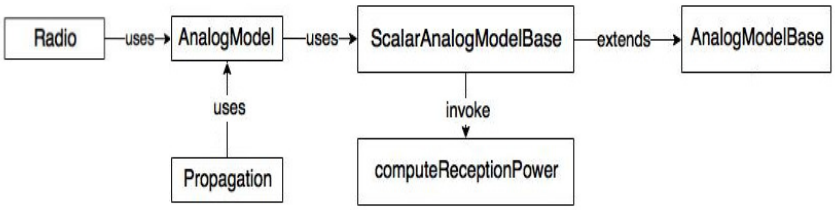

FIGURE 3.2: Physical layer logical block diagram

Figure 3.2 illustrates the hierarchical logical block diagram of the main modules involved in the physical layer operation. The radio model describes the physical device and implements transmission/reception node functionalities. The Radio module serves a certain analogical model that is responsible among other things for supporting the wireless channel propagation model. The Radio.ned module contains the following main parameters:

LISTING 3.1: Radio.ned main parameters

```
1 module Radio like IRadio {
2 parameters:
3 string antennaType; // the antenna model
4 string transmitterType; // transmitter model
5 string receiverType; //receiver model
6 string energyConsumerType = default(""); // energy consumer model
7 string radioMediumModule = default("radioMedium"); // path of the medium module
8 string energySourceModel = default(""); // path of the energy source module
```

The `antennaType` parameter points to the .ned of the used antenna module; the `transmitterType` and `receiverType` indicate respectively, the kind of transmitter

and receiver module that is equipped in the mobile node; please note that either the **antennaType** and either the `transmitterType` and **receiverType** parameters are strongly related to the kind of **radioMediumModule** set in the .ini configuration file. More specifically, the INET framework provides for several **radioMediumModule**; the most significant are:

- `IdealRadioMedium`: provides for the most simple channel propagation model, including a path loss free space model and a constant speed propagation model; in this regard, the transmitter and the receiver nodes are equipped with isotropic antennas

LISTING 3.2: IdealRadioMedium.ned file

```
module IdealRadioMedium extends RadioMedium {
parameters:
propagationType = default("ConstantSpeedPropagation");
pathLossType = default ("FreeSpacePathLoss");
analogModelType = default("IdealAnalogModel");
```

- *ScalarRadioMedium*: this radio medium model uses scalar transmission power in the analog representation; it is possible to choose between the different propagation models offered by INET framework and to equip the nodes with one of the different antenna models provided by INET framework.

LISTING 3.3: Ieee80211ScalarRadioMedium.ned file

```
    module Ieee80211ScalarRadioMedium extends Ieee80211RadioMedium {
        parameters:
            analogModelType = default("IdealAnalogModel");
            backgroundNoiseType = default("IdealAnalogModel");
```

  The Listing 3.3 depicts the features of one of the most relevant `ScalarRadioMedium` module, the `Ieee80211ScalarRadioMedium`. It should be noted that also the analog model provided by this class is scalar while the type of noise is almost "ideal"; this module is usually used in cooperation with a `ScalarTransmitter` and a `ScalarReceiver` that perform their operations depending on the power value that is set in the configuration file, in spite of the `IdealTransmitter` which operates according to the `maxCommunicationRange` parameter that determines the coverage radio of the communication related to a certain mobile node.

Features of physical layer related to nodes are defined in the `StandardHost` module and are function of the kind of RadioMedium model set in the simulation:

Figure 3.3 represents an example of the inner structure of a node: the module `StandardHost`. It can be noted that the overall structure is designed according to the TCP/IP stack principle. The layered architecture shown in Figure 3.3 is related to a mobile node, in fact, the third level (from bottom to top) that is the network layer, executes a routing protocol for Mobile ad Hoc Networks, the AODV protocol;

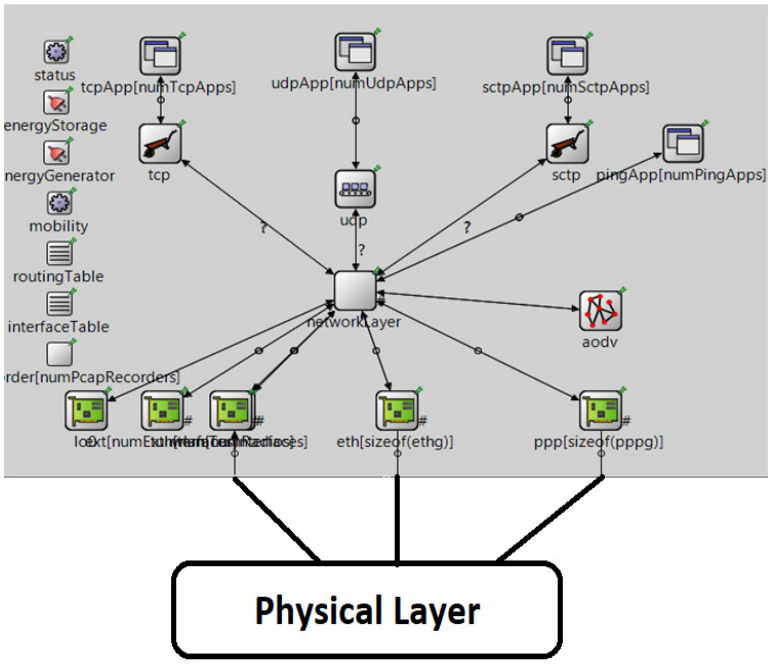

FIGURE 3.3: StandardHost module

however the analysis of the routing protocols modules is beyond the scope of this section. The physical layer communicates with the data link layer, which, in this case consists of a set of Network Interface Card (NIC) interfaces either in wired and either in wireless mode. It is important to highlight that all the physical layer functionalities and modules are not mapped in the default StandardHost architecture, consequently the communication process with the data link layer is indirect.

3.3.3 Antenna models

The package inet.physicalLayer.antenna contains all the antenna modules of inet. Actually, the default available modules are the following:

- **ConstantGainAntenna**: a simple antenna having a unique basic parameter, the gain. As suggested by the name the gain set in the configuration file remains constant while a simulation is executed. This module is useful when informations such as the orientation and the direction of the signal does not need to be considered.

- **CosineAntenna**: is the cosine pattern antenna designed in [128]; this model results very usefully for W-CDMA systems where the handover issue could become a critical task. Basically, this antenna is a combination of a directional high capacity antenna and a sectorized antenna. This combination allows to achieve some intra-cell benefits such as the insolation of interferences and user signals.

- **DipoleAntenna**: the well-known dipole antenna consisting of two identical conductive elements, which are bilaterally symmetrical; it is possible to set in the configuration file the length of the dipole (in meters).
- **InterpolatingAntenna**: this antenna model computes the gain in function of the direction of the signal, using linear interpolation. More specifically the antenna gain is computed based on the direction of the signal using linear interpolation extracting direction informations expressed in eulerAngles. This antenna module results useful when a fast-scanning and approximated antenna pattern is required if particular constraints about time-consuming applications need to be satisfied.
- **IsotropicAntenna**: is the classical omnidirectional/isotropic antenna; it provides for unity gain by radiating the signal at the same way towards all directions.
- **ParabolicAntenna**: this model is based on a parabolic approximation of the main lobe radiation pattern. Gain is function of the `maxGain` and the `minGain` together with the 3db beamwidth. This module result very useful to be employed in environments in which path loss issues have to be addressed. In particular, thorugh the functionalities of this antenna it is possible to avoid problems such as inter-cell intereference that usually occurs when antenna with poor orientation is used. Indeed, the resulted main beam in this case is very directive.

Observe that, originally, the only antenna modules provided for inetmanet were the **IsotropicAntenna** and the **DipoleAntenna**; other modules have been developed from customers later and then added to inetmanet. In order to understand the logical structure of a generic antenna module, the following listings illustrate an example code of the most simple antenna module offered by InetManet, the IsotropicAntenna module:

LISTING 3.4: IsotropicAntenna.h main parameters

```
1 class INET_API IsotropicAntenna : public AntennaBase {
2   public:
3     IsotropicAntenna();
4     virtual std::ostream& printToStream(std::ostream& stream, int level) const override;
5     virtual double getMaxGain() const override { return 1; }
6     virtual double computeGain(const EulerAngles direction) const override { return 1; }};
```

LISTING 3.5: AntennaBase.h main parameters

```
1 class INET_API AntennaBase : public IAntenna, public cModule {
2   protected:
3     IMobility *mobility;
4     int numAntennas;
5   protected:
6     virtual void initialize(int stage) override;
7   public:
```

```
8     AntennaBase();
9     virtual std::ostream& printToStream(std::ostream& stream, int level) const override;
10    virtual IMobility *getMobility() const override { return mobility; }
11    virtual int getNumAntennas() const override { return numAntennas; }
12 };
```

The Listing 3.4 highlights the main `IsotropicAntenna.h` file parameters; the main functions of this file are `computeGain()` and `getMaxGain()`; the first one implements the gain computation expression and returns the gain value; obviously, the gain expression depends on the kind of the used antenna; with regards to the isotropic antenna, for example, the gain is unitary and consequently the `getMaxGain()` function returns 1. It is important to note that the `IsotropicAntenna` class inherits all functions and variables of the `AntennaBase` class whose features are exposed in Listing 3.5. Observe that, in the `AntennaBase` class is possible to set the number of antennas used by the node to create an antenna array; this parameter is an integer and is denoted by `numAntennas`. The `mobility` interface points to the mobility pattern .ned file associated with the node; the utility function `getNumAntennas()` simply returns the number of antennas related to a certain node.

3.4 SAS design and implementation on Omnet++

There are several reasons for using Omnet++ for implementing a SAS or a Massive MIMO. Firstly, it is an open source instrument allowing the reusability of models for free. Yet, it provides a very full set of features and protocols expecially relating to wireless network, hence, the end user developer can create new modules or extending the default models quite comfortably. Nevertheless, it provides for an extremely intuitive user interface both in developping and simulations. Unfortunately, by default, Omnet++ does not support asymmetrical communication between nodes. For enabling the simulator to support directional communications and so the SAS, some modifications on the original source code are required. Let us suppose that we aim to implement the most simple SAS technology, that is the switched beam, the first needed step is to design the module. For example, a phased array system could be implemented. To do this, a new directive antenna model and the relative module denoted as PhasedArray has been designed [129]. The latter, implements all features of a phased array systems. The main definition of the class could be synthetized as follows:

The function initialize initializes the module in the simulation setup. Basically, the function computeGain as the name suggests computes the antenna gain; in the omnidirectional case this function simply returns 1. This function has been modified by implementing the expressions of gain for SAS:

$$G(\theta,\phi)_{TOT} = G(\theta,\phi)_{EF} * G(\theta,\phi)_{AF} \tag{3.1}$$

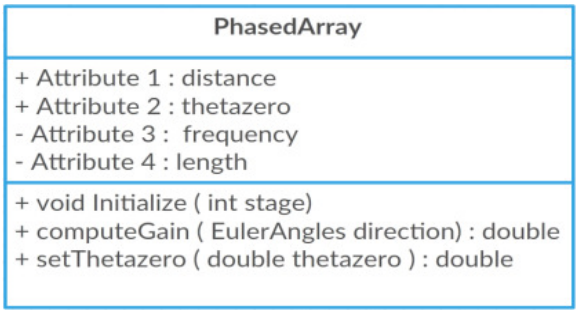

FIGURE 3.4: PhasedArray main parameters class definition

$$AF = \left| \frac{\sin\left(\frac{N\psi}{2}\right)}{N \sin\left(\frac{\psi}{2}\right)} \right| \tag{3.2}$$

$$\psi = kd\left(\cos\phi - \cos\phi_0\right) \tag{3.3}$$

Where, in the equation (3.1) the total gain $G(\theta,\phi)_{TOT}$ is expressed in function of the element factor gain$G(\theta,\phi)_{EF}$ and the array factor gain $G(\theta,\phi)_{AF}$: AF is the array factor while ψ is a term that depends on the steering angle. Please note that the equation (3.2) is normalized with respect to the number of antenna elements N. The second step concerns the modifications related to the mobile node module used in Omnet, that is the StandardHost module. Now, let us refer to Figure 3.3 representing the structure of StandardHost module; The physical layer defines the functions relating to channel model propagation, power management and modulation. More specifically, the ScalarAnalogModelBase class implements the channel propagation model that provides for a static power assignment by default, for example, in the case of isotropic antenna, both the transmission and the reception power are set to 1. This issue can be fixed by inserting a simple Power Algorithm for node power management in order to create a dynamic power quantity assignment based on transmission direction and angular position of each node.

Algorithm 6 Power-Algoritm procedure

```
int offset = getOffset();
double transmissionDirection = computeTransmissionDirection();
double transmissionPower;
if −0.5 ∗ offset ≤ transmissionDirection ≤ 0.5 ∗ offset then
    transmissionPower = scalarSignalAnalogModel.getPower();
else if −offset ≤ transmissionDirection ≤ offset then
    transmissionPower = 0.75 ∗ scalarSignalAnalogModel.getPower();
else if −2 ∗ offset ≤ transmissionDirection ≤ 2 ∗ offset then
    transmissionPower = 0.5 ∗ scalarSignalAnalogModel.getPower();
else if −3 ∗ offset ≤ transmissionDirection ≤ 3 ∗ offset then
    transmissionPower = 0.05 ∗ scalarSignalAnalogModel.getPower();
elsetransmissionPower = 0;
end if
```

The offset term is function of two parameters: the mainLobeAngle and the spreading factor. The first term, as already mentioned, represents the angle of maximum

radiation; the second term can vary from -1.5 to 2 according to the number of radiating elements of the array. In particular, the larger is the number of elements, the greater is the spreading factor value. This feature allows to take into account of the spreading effect that affects the overall pattern varying the number of elements. In Algorithm 1 it can be observed that, based on the transmissionDirection value, the power is fractioned opportunely. If the transmissionDirection value is not related to any sidelobe level, the power is reduced to 0. Therefore, if we want to implement an adaptive array system, the main problem is to individuate the best way for executing the adaptive algorithm into the simulation. A possible efficient solution could be to provide for a co-simulation. The co-simulation, for instance, can be performed using any combination of network simulators and Matlab. Matlab enhances the working of network, simulating tool and increases the speed of testing and processing by using different toolboxes. In this case, it is possible to divide the overall task, that is the simulation, into two sub-tasks [130]. The first sub-task is handled by Omnet++ that provides for the network scenario, while the second sub-task is managed by Matlab that performs the adaptive algorithm operations.

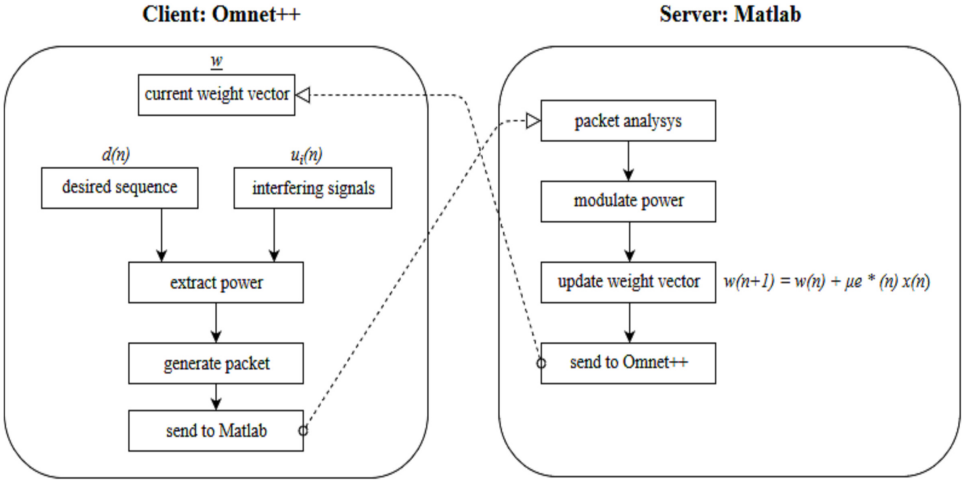

FIGURE 3.5: Co-simulation for SAS adaptive array

Figure 3.5 represents the communication process block between the two parts based on a client-server paradigm. Omnet++ executes the simulation and dynamically sends the physical parameters (the power and the noise in this case) related to a certain communication between couple of nodes to Matlab; Matlab executes the adaptive algorithm (the Least Mean Algorithm in this case) based on the data received in input, computes the updated weighted vector and sends backwards the data to Omnet++. The communication between the two parts can be easily realized by using TCP sockets.

3.5 Massive MIMO design and implementation on Omnet++

The latest release of the Omnet++ simulator (the 5.3 version), does not offer a support to asymmetrical communications and does not implement the latest IEEE802.11ac standard. More specifically, Omnet++ offers a complete support for 802.11b/g and the most recent 802.11n standard, but does not support the specifications related to the 802.11ac standard. Furthermore, these features are not sufficient for emulating the latest massive MIMO technologies in the simulator. In fact, the maximum data rate supported in the radio module used in the current latest version of Omnet++ is 54 Mbps, along with a 64-QAM modulation, according to the 802.11n specifications. In view of these issues, it is possible to extend the Omnet++ features both by providing a full 802.11ac radio environment and a new massive MIMO antenna module suitable for 5G wireless network environments operating according to the IEEE802.11ac [131].

3.5.1 IEEE802.11ac implementation

The first step consists in the implementation of the 802.11ac standard in the physical modules of Omnet++. Basically, this process involves modifications as regards two micro-layers: the error model and the modulation. The error model determines the computation of the BER (Bit Error Rate) curves and the error probability in function of the data rate. Obviously, as already stated, the current error models are determined by considering the maximum data rate of 54 Mbps. For this reason, this aspect should be fixed in order to design a support of data rates in the order of the Gbps. The modulation is the feature that offers the possibility to achieve the data rate values specified for VHT (Very High Throughput) and in the current latest version Omnet++ is limited to 64-QAM; this aspect determines the data rate upper-bound in the simulations. The family of modules related to the error model and modulation are contained in the physicallayer package.

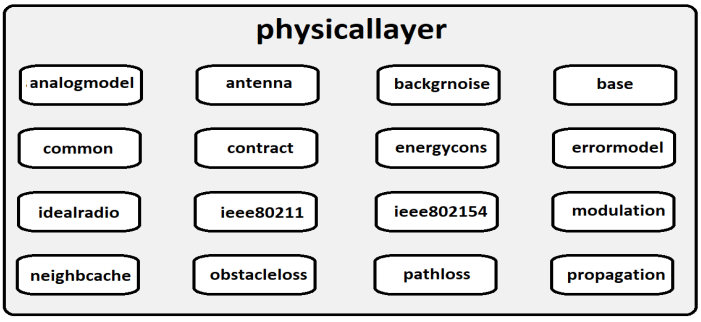

FIGURE 3.6: Physicallayer Omnet++ package structure.

Figure 3.6 illustrates the structure of the physicallayer package. The package consists of a remarkable number of subpackages each one determining a feature for the physical layer. Observe that the error model and the modulation micro-layers are contained in this package along with main modelling channel attributes, such

as the propagation and the pathloss management. Thus, in order to understand updates introduced for implementing the IEEE802.11ac standard, the following figures show a block diagram including the main Omnet++ classes (known also as modules) involved in the modification process.

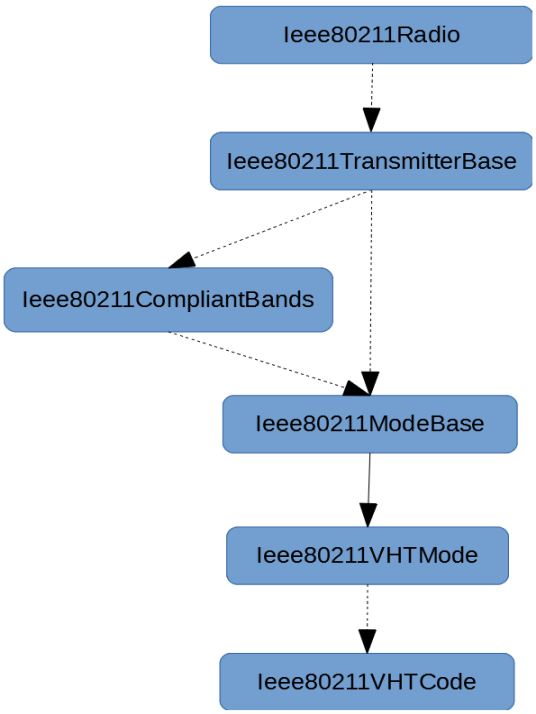

FIGURE 3.7: VHT implementation in the transmitter.

Figure 3.7 represents the module block diagram related to the implementation of the Very High Throughput (VHT) features for the transmitter at physical layer. Each class/module is represented by a rectangle while the dashed-line arrows and the continued-line arrows indicate the use and the inheritance relationship respectively. The Ieee80211Radio module uses the Ieee80211TransmitterBase module that is defined by the following NED (Network Description Language) code lines:

LISTING 3.6: Ieee80211TransmitterBase.ned definition

```
module Ieee80211TransmitterBase ... {
parameters:
string opMode @enum("a", "b", "g(erp)", "g(mixed)", "n(mixed-2.4Ghz)", "p", "ac");
string bandName @enum("2.4 GHz", "5 GHz","5 GHz&20 MHz","5 GHz&40 MHz","5 GHz&80 MHz","5 GHz
    &160 MHz");
int channelNumber;
modulation = default("BPSK"); }
```

In Listing 3.6 the main parameters of the Ieee80211TransmitterBase module are illustrated. The opMode parameter indicates the kind of IEEE802.11 standard that is determined by a lower-case letter. In this regard, the default Omnet++ source code has been modified by adding the ac operation mode. Note that also the 5 GHz frequency band configurations have been added. The transmitter uses the class

Ieee80211CompliantBands for retrieving the available bands and the Ieee802ModeBase class obtaining the operation mode. This latest class inherits the parameters offered by the classes Ieee80211 VHTMode and Ieee80211VHTCode that contains the new data rate values specified by the 802.11ac standard according to the VHT specifications. For this purpose all the data rate values provided by the standard by varying the carrier frequency and the number of spatial streams have been added the original code. The Ieee80211VHTCode is the module that computes the error probability functions depending on the kind of modulation used in simulation. A similar block diagram could be designed for the receiver.

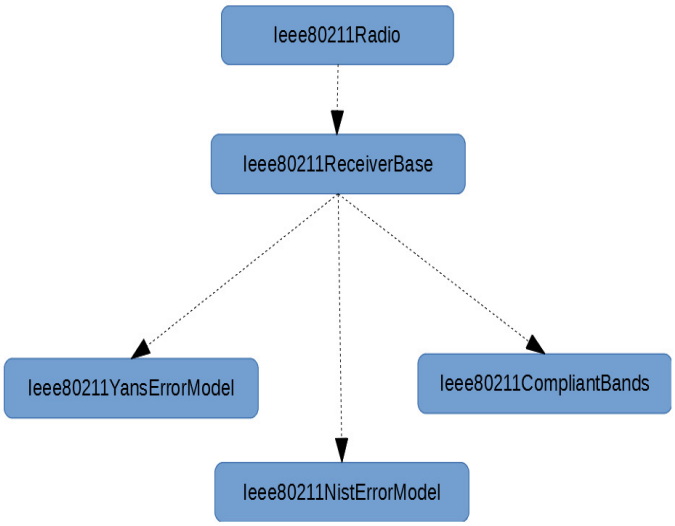

FIGURE 3.8: Error model designing at the receiver.

In the diagram of Figure 3.8 it is possible to analyze the hierarchical relationships at the receiver. It is important to highlight that the error model is mainly used by the receiver rather than the transmitter. Omnet++ uses some of the error models offered from the NS3 (Network Simulator 3) simulator that are the Yans and the Nist models [31]. Basically, these error modules compute the Bit Error Rate (BER) probability values in function of the modulation. For enabling the 802.11ac the default code of Omnet++ has been extended by adding the BER computation functions for 256, 512 and 1024-Quadrature Amplitude Modulation (QAM) modulation:

LISTING 3.7: Nist error model BER computation example

```
double Ieee80211NistErrorModel::get256QamBer (double snr) const {
  double z = std::sqrt (snr / (85.0 * 2.0));
  double ber = 15.0 / 32.0 * 0.5 * erfc (z);
  EV << "256-Qam" << " snr=" << snr << " ber=" << ber;
  return ber; }
```

The Listing 3.7 contains a part of the full code of the Ieee80211NistErrorModel class. The function get256QamBer computes and returns the BER relating to a 256-QAM modulation; the BER is evaluated by computing the Zeta function that depends on the SINR.

3.5.2 Massive MIMO module design and implementation

Once modified the physical layer in order to support the specifications of the VHT standard including the error model and modulations, the massive MIMO antenna modules have been designed. The antenna modules are defined in the *phyisicallayer* package as mentioned.

LISTING 3.8: MassiveMIMOURPA.ned definition

```
module MassiveMIMOURPA extends AntennaBase {
    parameters:
        double length @unit(m); // length of the antenna
        double distance; // distance between elements
        double freq; // frequency
        double thetazero; // steering angle
        int M; //number of columns;
        int N; //number of rows
        .......}
```

The Listing 3.8 illustrates the main definition parameters of the MassiveMIMOURPA antenna module. Note that the module inherits the basic features of the AntennaBase module; besides the main antenna array parameters such as the length the distance and the frequency the module provides for the setting of the steering angle thetazero in order to support the beam piloting.

Algorithm 7 MassiveMIMOHPA.cc pseudo-code

```
1: procedure INITIALIZE(int stage)
2:     initialize the module
3: end procedure
1: procedure GETMAXGAIN
2:     double maxG;
3:     int numel = getNumAntennas();
4:     double numer = 4 * M_PI * numel * numel;
5:     maxG = 20 * log10(numer/risInt);
6:     return maxG;
7: end procedure
1: procedure COMPUTEGAIN(EulerAngles direction)
2:     const std::complex < double > i(0,1);
3:     double heading = direction.alpha;
4:     for (int m=-emme; m<=emme ; ++m) do
5:         int val = (2*emme) - abs(m);
6:         sum2 = 0;
7:         for (int n=0; n<= val; ++n) do
8:             double aux = (double)n * (sin(heading) * cos(elevation) + betaM);
9:             complex <double> aux2 = exp(i * M_PI * aux);
10:            sum2 += aux2;
11:        end for
12:    end for
13:    return gain;
14: end procedure
1: procedure COMPUTEINTEGRAL
2:     double risInt = computes the double integral
3:     return risInt;
4: end procedure
```

The algorithm 7 depicts the main functions of the MassiveMIMOHPA.cc class. The function getMaxGain computes the maximum gain according the to the Equations (2.19) and (2.22) defined in the chapter 2; the function getNumAntennas returns the total number of antennas of the massive MIMO; the result of double integral (given by the risInt variable) is evaluated by implementing the Simpson method in C++ in the function computeIntegral; Observe that the integral could be computed by using some mathematical software tools such as Matlab and then passed to Omnet++, but in this case, it has been decided to implement the evaluation in C++ because the computation is once and because the use of MATLAB with this kind of very complex antenna module could significantly slow down the simulation. Finally, the function computeGain evaluates the gain in function of the direction EulerAngles components and the steering angle according to the Equation (2.22) (that however does not consider the scan term); the portion of code of computeGain function shown by Algorithm 7 is related to the implementation of the summations of the Equation (2.22).

3.5.3 Massive MIMO Modules validation

The validation of the designed models is accomplished by illustrating some log screens related to the debug runs and by analyzing some useful statistics extracted from the simulations. The following table includes the most important simulation set parameters:

TABLE 3.2: Main simulation parameter set.

Antenna Model	Massive MIMO URPA/UHPA/UCPA
Network Standard	Ieee802.11ac
Num. of elements	90 (URPA), 91 (UHPA), 91 (UCPA)
Steering angle	45°
Carrier freq.	5 GHz
Ch. bandwidths [Mhz]	20, 40, 80, 160
Num. of nodes	20, 50, 100
Data Rates [Mbps]	from 57.8 to 6933.3
Traffic data type	UDP
Sim. Area Size	500 x 500 m
Sim. time	300 s

The simulations have been accomplished by using 20 different seeds and extracting the confidence intervals obtained by the repetitions considering a confidence level set to 95 %. The traffic is represented by UDP data packets randomly generated (based on the simulation seed) by different couples of nodes. Therefore, the most of the antenna parameters including the number of elements and the spacing in the system are the same used in [132] with the only exception that the beam steering angle setting has been provided. For simulations such of the data rates provided

by the 802.11ac standard in function of the number of spatial streams have been considered. In order to validate the model, the first test consists of the analysis of such run simulation logs:

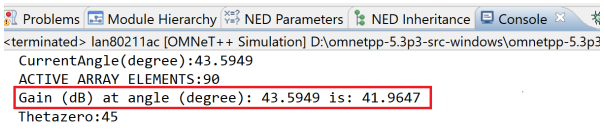

FIGURE 3.9: Portion of log extracted by simulations.

Fig. 3.9 represents a portion of log extracted by a randomly chosen simulation run related to the case of URPA; the result of the log is printed on the console perspective of *Omnet++*; the red rectangle highlights the main line of the log, that displays the result of the computed gain in function of the current angle; the main line synthesizes that the value of the gain corresponding to the angle of 43.5949 ° is 41.9647 dB; considering the steering angle of 45° it is possible to manually compute the maximum gain that is the gain corresponding to the maximum radiation angle (thus the steering angle) by using the Equation (2.20) and replancing the terms of the equation with the values used in Table 3.2:

$$G_{MAX}(\theta_0 = 45°, \phi) = \frac{4\pi \times 90^2}{772.97} - \delta_{\theta_0} = \mathbf{42.16 \quad dB} \tag{3.4}$$

Where δ_{θ_0} represents the attenuation in dB related to the steering angle with respect to the maximum gain corresponding to $\theta = 0°$ (which is 42.39 dB). In the Equation (3.4), the value of 772.97 at the denominator is the result of the double integral computed by the simulator, using the Simpson method. Finally, the gain value of 41.9647 dB related to the angle of 43.5949 ° is almost about close to the maximum gain value, as we could expect.

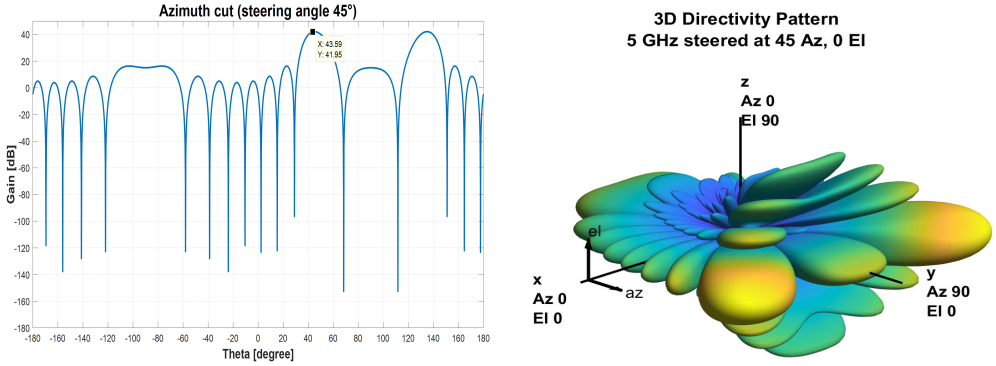

(a) Az cut rectangular plot (b) 3D polar plot

FIGURE 3.10: : Designed model radiation pattern.

For a further investigation, by using the Sensor Array Analyzer tool provided by Matlab [29] it is possible to represent the radiation pattern plots related the designed

Massive MIMO URPA model. In Subfigure 3.10 (a) it can be observed that, the obtained gain value, achieved corresponding to the angle of 43.5949° is very consistent with the obtained gain value related to log of Figure 3.9. Finally, the Subfigure 3.10 (b) illustrates the three dimensional polar radiation pattern of the designed model.

Chapter 4

Addressing Deafness Problem in Directional MANET Communications Environments

4.1 Introduction

Generally, The early works on wireless ad hoc networks suppose the use of omnidirectional antennas in order to perform symmetrical and directional communications between nodes. Traditional MAC protocols using omnidirectional antennas such as for example IEEE 802.11 DCF, cannot attain high throughput in MANET because of the low capability and coverage provided by antennas. Directional antennas are very able to handle this issue, by exploiting the high spatial reuse and range efficiently, toward a certain direction. For this reason, several MAC protocols using directional antennas for ad hoc networks have already been proposed recently. Directional MAC protocols, however, introduce new types of problems related to directional transmissions as already mentioned in the chapter 1. Developments in beamforming technology have addressed current research to review some of the problems in wireless networking. Although several studies have been shown the great potential provided by SAS increasing benefits provided by classic directional antenna systems in terms packet and physical performance, therefore, problems such as deafness issues is still not completely solved. While relating to wireless directional contexts deafness not only degrades the performance at the MAC level, but it also considerably affects the performance of higher layers. As previously stated, the use of Directional NAV can help to reduce frame collisions caused by deafness, however also DNAV is subject to several limitations; the most common is represented by the fact that DNAV, in the basic implementation, suffers from beams synchronization problem that translates in low setting accuracy resulting in possible performance degradation [133]–[135]. Nevertheless, whenever a node sends a directional RTS and does not receive back a directional CTS, it waits for a random backoff (according to IEEE 802.11) and tries to retransmit the directional RTS at some later time.

This can lead to excessive wastage of network capacity in control packet transmission [136]. Larger backoff intervals also result into unfairness wherein a flow completely captures the wireless shared medium. The present chapter aims to illustrate a comparative study of the most important works attempting to mitigate deafness problems in the case of directional and SAS systems usage; the purpose of this chapter is also to focus about Round-Robin MAC (and its enhancements) approach that has been proposed to encounter deafness problem in directional and asymmetrical communications.

4.2 Deafness problem in Directional MANET Related Works

The deafness problem was deeply investigated and treated in the latest years and, especially thanks to the growth of employment of the Smart Antenna Technology, a remarkable number of researches have been encouraged to propose novel solutions for minimizing or, at least, reducing this problem. Basically, from the point of view of features which they are oriented, the whole of the works in this field can be grouped into 4 categories:

- **Works neighbor-informing based**
- **Works special-messages based**
- **Works multichannel based**
- **Other works**

4.2.1 Works neighbor-informing based

These kinds of works aim to use caches or tables in order to notify possible deafness behaviors by exchanging protocol messages with one-hop neighbor nodes. In this case, classical DMAC protocols features are maintained by improving (and exploiting) the potentiality of caching mechanism. In work [137] a CDMA based directional MAC protocol is presented; the deafness is encountered using localization information tables for each node and the Code Division Multiple Access (CDMA) technique. A pretty close concept is presented by authors in [138], implementing a Neighbor Initiated approach; a new schema that improves the classical Directional schema is proposed, in order to advertise neighbor nodes about a possible deaf situation during communications. A similar approach is presented by authors in [139], implementing a Directional Mac with Deafness avoidance (DMAC-DEAV) mechanism that provides an exchange of particular frames (Wait to Send frames) in order to notify the set of nodes that could high likely affect from deafness; results show a considerable reduction of the problem especially when the active flows number in the network is large. Due that DMAC-DEAV use special frames, this approach could be also categorized as a special-messages based work. In [41] a Circular Directional RTS MAC (CDR-MAC) is presented; in this case nodes are notified about

possible deafness situation by using RTS messages in a circular way; the circularity of message exchanging is guaranteed by using updated record table informations. In addition, in order to reduce the probability of deaf node occurrence, the basic DNAV is employed. DMAC protocol with Deafness Avoidance and Collision Avoidance (DMAC-DACA) protocol [140] is the basic directional RTS/CTS exchange is followed by sweeping RTS/CTS counterclockwise to inform all the neighbors about the upcoming communication. Deafness is avoided using a deafness neighbor table that uses the sweeping RTS/CTS to record the deafness duration of neighboring nodes. The location information, retrieved by GPS, is added to the RTS/CTS frames. Using this information, the node that receives RTS/CTS can update the record in its deafness neighbor table if any of the neighbors is in the coverage area of the upcoming transmission. The DMAC-DACA protocol performs collision avoidance through the DNAV mechanism. In [141] a Receiver-Initiated Directional MAC (RI-DMAC) mechanism is proposed, in which each node maintains a polling table that is used to advertise some particular potential deafness nodes by emitting Ready to Receive (RTR).

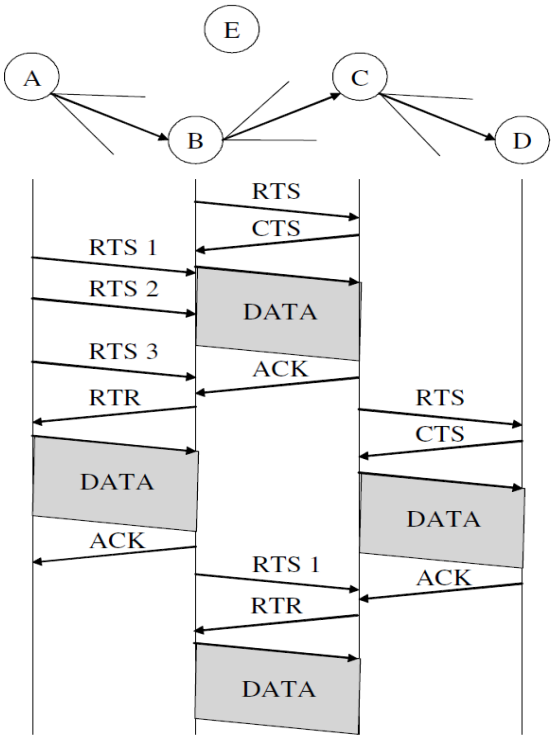

FIGURE 4.1: RI-DMAC principle

In RI-DMAC, the sender transmits RTS even when the receiver is in the RI-mode and it may receive RTR as illustrated in Figure 4.1; this is because when RTR is not received successfully due to collision or deafness, the transmitter should wait for the next RTR from the receiver, and it may result in the wastage of the wireless channel and increase the delay as in other receiver initiated MAC protocols.

4.2.2 Works special-messages based

The set of works belonging to this category enhance basic features of classic directional MAC protocols by using additional messages besides RTS, CTS and DNAV informations in order to increase the protocol capability of deafness recognition. In [142], authors present a MAC protocol for directional Antennas (MDA-MAC) which employs an enhanced directional network allocation vector (NAV) scheme and, a novel technique of Diametrically Opposite Directions (DOD) transmission of RTS and CTS. In MDA, the Enhanced DNAV scheme consists of two components: a DNAV mechanism which is manipulated differently from basic schemes, and a Deafness Table (DT) which is used to handle deafness scenarios. Whenever a node has a packet to be sent over one direction, both DNAV and DT are consulted. In [143] authors, propose a dual-Tone DMAC mechanism that enable the transmission of special packets (Out-of band tones) by nodes in omnidirectional mode; these tones can be processed by neighbors reducing considerably the large backoff time introduced by deafness. In work [144] two schemes are proposed in order to mitigate the deafness caused by persistent hearing of data and for handling the Short Retry Limit (SRL) in directional environments. The SRL is managed by an exchanging process of particular messages using the classic basic DMAC schema. A DMAC/DA (Directional MAC with Deafness Avoidance) is proposed by authors in [145] to overcome the deafness problem. As well as in DMAC-DEAV, in DMAC/DA, WTS (Wait To Send) frames are used by the transmitter and the receiver after the successful exchange of directional RTS (Request To Send) and CTS (Clear To Send) to notify the on-going communication to potential transmitters that may experience deafness. In DMAC/DA, therefore, each node maintains a neighbor table with one record for every node that it has heard. Initially, the neighbor table is empty and it is continuously updated upon overhearing any transmission; for this reason it also can be categorized as a neighbor-informing based work. Multiple Access Scheme with Sender driven and Reception first for Smart antenna (MARS) [146] is a protocol which changes RTR frames into Ready to Receive and Transmit (RTRT) frames. RTRT frames include addresses of the source and destination nodes. A node transmits an RTRT frame when it has data to send. Because the RTRT frame includes the transmitter address, the neighbors of the middle node can adjust their antennas to its direction and transmit their RTS frames. If a particular neighboring node does not have data to send it sets the size of data to zero. Upon reception of the RTS frames the middle node adjusts the gain pattern of its antenna and transmits all corresponding CTS frames. This way of operation allows reducing polling overhead and interference in comparison to the IEEE 802.11 standard. In [147] authors present an Advance Notice Directional MAC (AN-DMAC) using an additional RTS (A-RTS) and CTS (A-CTS) frame, that are classified as "AN packets", in order to delay the critical communications for reducing the deafness. In AN-DMAC maintains a LIT (Local Information Table), which records the information of surrounding network activity.

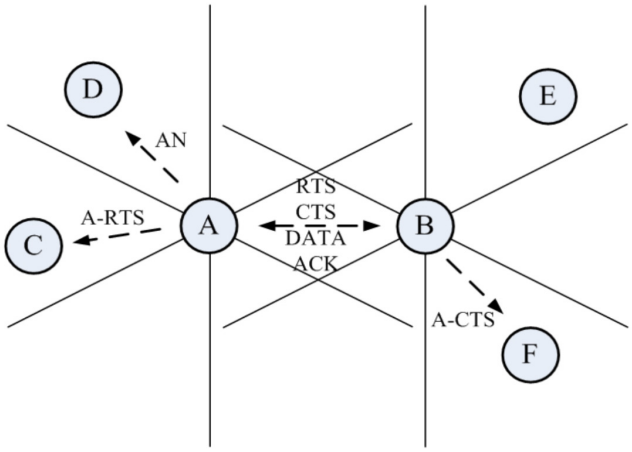

FIGURE 4.2: AN-DMAC operation

For example, let us consider the scenario shown in Figure 4.2; when node A points its beam to the direction of D and transmits the AN packet, neighboring node of node D, for example node C, is likely to overhear such AN packet. If the LIT of the node G indicates that node D is in the state of deafness now, C should send a cooperative AN packet to node D when D finishes current communication. The duration field of cooperative AN packet is invalid, and the field is set as 0 to be different from ordinary AN packet.

4.2.3 Works multi-channel based

Related works of this category provide for the use of multiple channel for DMAC, opposite of what is laid down by IEEE802.1x standards establishing the use of a single channel. In [148] authors, propose a New Deafness Aware (NDA-MAC) mechanism which tries to mitigate the deafness problem through the use of control channels and logical data; more specifically, a discrete time Markov chain model for analyzing the deafness impact is provided. In [149] authors propose a dual-channel MAC protocol that reduces the excessive overhead introduced by deafness while limiting this issue especially for high-frequency directional communications. The dual-sensing directional MAC protocol (DSDMAC) protocol helps to improve the throughput and delay performance of the wireless networks by minimizing the negative effect of the hidden-terminal, exposed-terminal, and deafness problems. The protocol uses a non interfering out-of-band busy-tone signal combined with sensing the activity on the actual data channel to identify deafness situations and to avoid unnecessary blocking. In addition, the protocol avoids the asymmetry-in-gain problem introduced by other solutions. DSDMAC protocol uses two well-separated wireless channels: a data channel and a busy-tone channel; the data channel carries the data packets and the RTS, CTS, and ACK packets on a specified direction while the busy-tone channel is used to transmit a sine-wave busy-tone signal on all other directions. Only the source and destination nodes will transmit the busy-tone

signal. The protocol assumes that the directions of all reachable destinations or forwarders are predetermined. In the Multi-Channel MAC protocol with a Directional Antenna (MCDA) [150] each node is equipped with a single antenna and has to switch between the data and control channels. Therefore, to cope with the channel collision problem, here situation in which the control-channel information cannot be heard because a node is tuned to a data channel. This protocol adopts the channel switch sequence (CSS) mechanism. Additionally, MCDA implements RTS/CTS/-DATA/ACK exchange. All CTS/DATA/ACK frames are transmitted directionally. MCDA operates in three phases: negotiation, communication, and block. In the first phase the source–destination pair exchanges RTS/CTS frames on the control channel to select the data channel. In [151] a novel Deafness-Aware (DA-MAC) is presented, in order to mitigate the Deafness problem through a discrete-time Markov chain model.

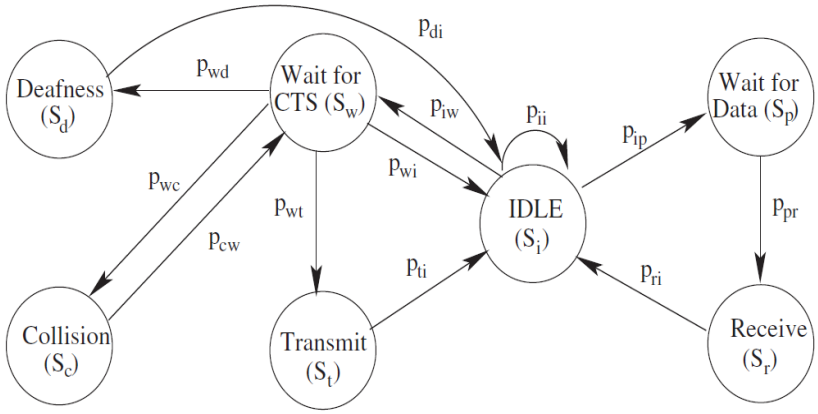

FIGURE 4.3: DA-MAC state diagram

The model uses a double-channel schema in order to handle the Directional RTS (DRTS); more specifically, the single channel provided by the Directional MAC is splitted into two different logical channels used for filtering the data traffic and the control packets respectively; the designed DA-MAC algorithm provides for several features that allows to recognize and mitigate efficiently the collisions occurred because of deafness. In Fig. 4.3 the state diagram of the DA-MAC is illustrated: there are four states to which the *wait for CTS* state moves; if a sender does not receive any DCTS frames on either channel (collision), it moves to the *collision* state. Similarly, the sender moves to the *deafness* state when the sender receives a DCTS frame only on the control channel (deafness). The sender moves to the *transmit* or *idle* states when it receives a DCTS frame on each channel and when it reaches the maximum retransmission limit k, respectively.

4.2.4 Other works

This section includes directional MAC works attempting to limit deafness problem that does not belong to any of previous mentioned categories. In [152] authors present a Power-Controlled Directional MAC protocol (PCD-MAC) for adaptive antennas. PCD-MAC uses the standard RTS–CTS–DATA–ACK exchange procedure. The novel difference is the transmission of the RTS and CTS packets in all directions with a tunable power while the DATA and ACK are transmitted directionally at the minimal required power. In [153] a full-duplex MAC exploiting a synchronized contention window mechanism is proposed. The analysis accomplished on different kinds of network topologies show acceptable results in terms of aggregate throughput. In [154] authors show how a Directional Cooperative MAC (D-Coop MAC) approach can improve throughput while reducing the overall frame collision amount in the network. The Coordinated Directional MAC (CDMAC) [155] allows for parallel directional DATA/ACK transmissions. Additionally, it uses omnidirectional RTS/CTS transmissions to minimize the deafness problem. It is assumed that each node has a single transceiver but it can dynamically switch from directional to Omni-directional transmission and reception.

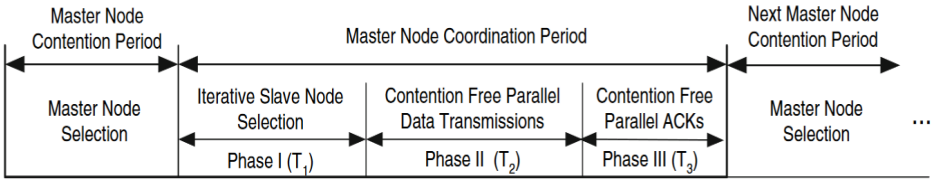

FIGURE 4.4: CDMAC timing structure

The timing structure of CDMAC is shown in Fig. 4.4. From the perspective of an arbitrary node, there are two periods alternated locally, master-node contention period and master-node coordination period. The master-node contention period is for electing a master node-pair. During the master-node contention period, multiple nodes contend for channel access and the first winning node-pair is called the master node-pair. The master-node contention period ends once the master node- pair is selected. The master node-pair coordinates the activities in the following period, called master-node coordinated period, which consists of three phases.

4.3 The Round Robin MAC approach

Differently from the most of the discussed related works attempting to limit deafness problem using high level neighboring information tables or multichannel solutions, the Round-Robin MAC (RR-MAC) [156] approach aims to mitigate deafness problem by limiting the beamfoming time of nodes in directional communications (further motivations are explained in section 4.3.1). Basically, the RR-MAC model

provides for a sectorization of the transmission/reception plane with a beam assigned to each sector.

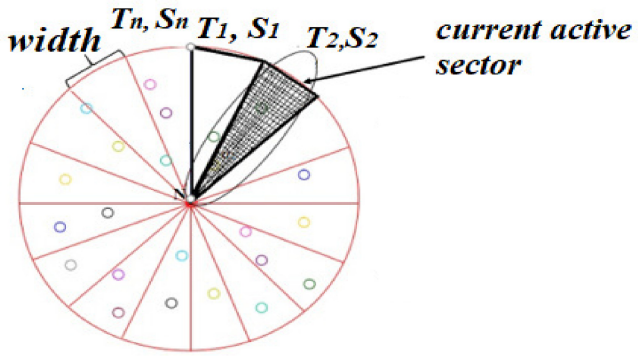

FIGURE 4.5: Plane sectorization principle.

The mathematical formulation of RR-MAC is synthetized by the following expressions:

$$\begin{aligned} \alpha_i = \alpha_j = ... = \alpha \\ T_i = T_j = ... = T_s \\ \alpha_i(T_i) = \alpha_j(T_j) = ... = \alpha(T) \\ \forall i, j = 1, 2..N, \quad i \neq j \end{aligned} \tag{4.1}$$

The plane in Fig. 4.5 is divided into N equal sectors (each sector is denoted by S), each one having a certain amplitude w (*sector width*) and a beamforming duration time T (*sector time*). Note that all sectors have the same width as well as the same *sector time*. Each node that belongs to a certain sector beamforms with an angle α_i where i =1...N and N is the number of sectors in which the plane is divided; each node beamforms in a certain sector until the *sector time* is reached, then it switches to the next sector. We defined the sector in which the beam is currently active as the *current active sector*. The beam turns around all sectors in a iterative way in order that each sector is crossed by the beam periodically throughout the simulation time. The transmission/reception is allowed only for the set of directions that belong to the *current active sector*; signals having a Region of Interest (ROI) or a Direction of Arrive (Direction of Arrive (DOA)) outside from the *current active sector*, are temporally queued and wait for its turn. In particular, these signals are delayed in a queue (a queue with equal size for each sector) until its direction sector does not become the *current active sector*, then, are transmitted in the channel. In this way it is possible to limit the transmission/reception time of each node in a certain direction, and so the beamforming time. Because the beam is assigned to each sector for allowing the communications in a round robin mode, this approach has been named as Round-Robin MAC approach (Round Robin MAC (RR-MAC)). The *sector time* is measured in seconds and the maximum *sector width* is set to 180° in order to sectorize the plane at least into 2 sectors (N=2).

4.3.1 Analytical model and motivations

Let us reconsider the deafness scenario illustrated in Figure 1.4; let us suppose to apply to this scenario the Round-Robin approach along with the plane sectorization of Fig. 4.5; this process can be modelled as a Markov chain defined by the following parameters:

- **state:** the set of the directions associated with a sector (in other terms, a state is a sector).
- **transition:** the switching process from a sector to another sector.

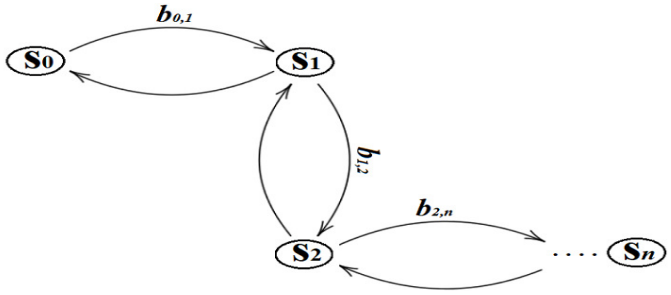

FIGURE 4.6: RR-MAC Markov chain modeling.

The transitions can be expressed as:

$$b_{i,k} = \frac{T_i - k}{T_i} b_{i,0}, \quad 0 \leq i \leq N, \quad k \in [0, T_i] \tag{4.2}$$

In eq. 4.2, $b_{i,0}$ represents the transition from the state i to the state 0; T_i is the duration of the sector i (*sector time*) while N is the maximum number of sectors. Figure 4.6 illustrates the Markov model applied to our case study. Assuming a beamfoming context, considering a period T with $0 \leq T \leq T_i$ let define:

- $\boldsymbol{P_{sec}}$ = prob. that a node x attempts for a transmission in a randomly chosen sector. $P_{sec} = 2/(T_i + 1)$
- $\boldsymbol{P_{tr}}$ = prob. that there is at least a transmission in a certain sector. $P_{tr} = 1 - (1 - P_{sec})^N$
- $\boldsymbol{P_{nb}}$ = prob. that at least one of the neighbors of x attempts for a transmission. $P_{nb} = (N-1)(1 - P_{tr})$
- $\boldsymbol{P_B}$ = prob. that x is beamformed at least from one of its neighbors. $P_B = (1/N) + w(T_i)$

The term P_B it depends on the number of sectors and on a weight assigned to each sector w; in our case the weight is the same for each sector. We can express the probability that the node x experiences a collision in the considered period as follows:

$$P_c = P_B(T_i) P_{tr} (N-1) P_{nb} (1 - P_{nb})^{N-1} \tag{4.3}$$

Note that P_B is function of the *sector time* that also represents the beamforming time. As it clear from eq. 4.3, the larger is the beamforming time the higher become the number of frame collisions. From this analysis the reasons to create a Round Robin approach and limiting the beamforming time of nodes could be clearly highlighted.

4.3.2 RR-MAC implementation

The RR-MAC has been implemented and tested by using the *Omnet++* Simulator; as starting point, the Smart Antenna *PhasedArray* module designed in [102] has been employed; basic MAC layer class that is the *DcfUpperMac* module has been modified for implementing the RR-MAC. The pseudo-code of the RR-MAC algorithm is shown as follows:

Algorithm 8 round-robin algorithm pseudo-code

```
1:  procedure ROUNDROBINMAC()
2:      Frame frame = getCurrentFrame();
3:      int nsectors = getSectorsNumber();
4:      for (i=1; i < nsectors; i++) do
5:          createWaitQueues();
6:      end for
7:      int frameSector=getFrameSector(frame);
8:      int currentActiveSector=getCurrentActiveSector();
9:      if (currentActiveSector != frameSector ) then
10:         waitQueue[frameSector].insert(frame)//queue the frame
11:         delay(frame);
12:     else
13:         transmissionQueue.insert(frame);
14:         waitForMyTurn(frame);//wait for turn, then transmit the frame
15:     end if
16: end procedure
```

Each frame is processed by the system that checks if the sector for which is destined the frame is the *current active sector*. If true, it inserts the frame in the transmission queue and transmit the frame according to Last In First Out (LIFO) queue mechanism; if the direction of the receiver for which the current frame is destined is outside the set of the directions currently available (*current active sector*), the frame is queued in its waiting sector queue, and delayed until its sector does not become the *current active sector*. It is important to notice that, the simulator is synchronized together with the frame exchange process, in order to provide an efficient exchange mechanism that also takes into account of the delayed frames in the channel.

4.3.3 RR-MAC validation and simulation results

For validating RR-MAC, the classical Directional MAC approach for SAS implemented in [157] has been considered, then, simulation runs of Directional MAC case have been compared with runs related to RR-MAC. As metric for fairness evaluation the DRTS/DCTS ratio has been defined:

$$DRTS/DCTS_{ratio} = \frac{(DRTS + DCTS)_{received}}{(DRTS + DCTS)_{sent}} \tag{4.4}$$

Where it can be observed that the ratio is expressed as the sum of all DRTS and DCTS frame received for each node divided by the sum of all DRTS and DCTS frame sent in the network. This parameter is useful for MAC layer fairness performance evaluation. The following table summarizes the main parameters set used in our simulations:

TABLE 4.1: Simulation parameters set for RR-MAC analysis.

MAC protocols	Directional MAC,RR-MAC
Antenna Type	Adaptive Phased Array
Antenna Freq.	1 MHz
Distance	0.5 λ
Number of Nodes	10, 30, 50, 80, 100
Simulation Area Size	500 x 500 m
Simulation Time	300 s
Sector Width values	45°,60°,90°,120°,180°

Simulation results about Packet Delivery Ratio (PDR) for throughput evaluation, number of collisions and DRTS/DCTS ratio, have been collected for MAC layer performance analysis. For reason of space, due to the large number of configurations considered, in this case it is possible to analyze statistics related to one of the *sector time* case (sector time = 2 s) varying the number of active connections and making comparisons between the classical directional MAC and our RR-MAC. Next figures illustrate the plots related to the PDR, the number of collisions and the DRTS/DCTS ratio respectively:

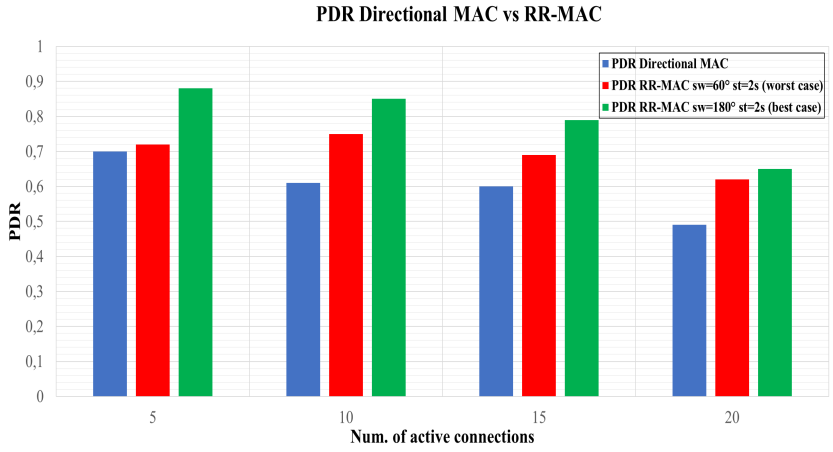

FIGURE 4.7: PDR Directional MAC vs RR-MAC

In Fig. 4.7 it has been compared the PDR statistic of classical directional MAC with the best and the worst case of our RR-MAC related to *sector time* equal to 2 s. It can been observed that, the PDR value in the directional MAC case remains always

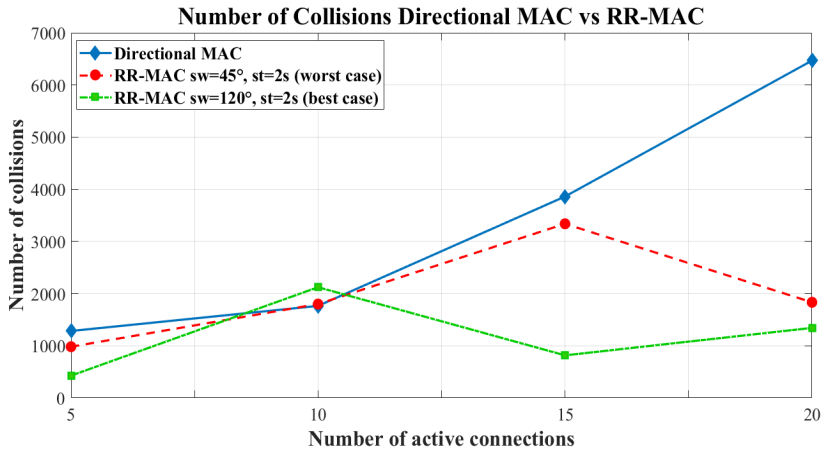

FIGURE 4.8: Num. of collisions Directional MAC vs RR-MAC

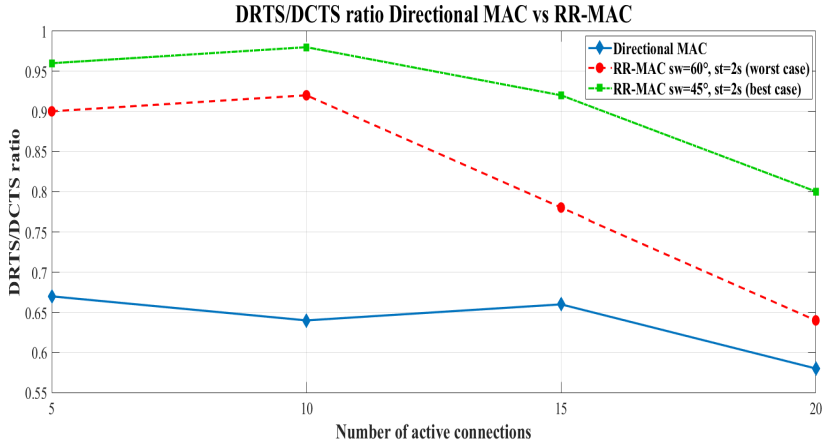

FIGURE 4.9: DRTS/DCTS ratio directional MAC vs RR-MAC.

smaller than the minimum value of the worst RR-MAC case registered (*sector width* = 60°). In fact, in the worst RR-MAC case we have an average PDR of 0.695 against the 0.6 average value registered in the directional MAC. From Fig. 4.8 it clearly appears that the number of collisions in the directional MAC case raises exponentially with the number of active connections. In the RR-MAC best and worst cases we observe a slightly growth of the collisions as the load data traffic increases; the overall amount it seems to be converge when the network presents an high data traffic load. The maximum number of collisions for RR-MAC is limited to 3339 against the 6468 registered in the directional case. On average we obtain a reduction of the number of collisions that gives from 40,5% to 64,7% in the best case. In Fig. 4.9 the curves of DRTS/DCTS ratio related to the case *sector width* = 2 s are illustrated. In particular, the ratio remains almost linear for all curves as the load grows up, but in RR-MAC worst case we obtain an average ratio of 81% against the 63,7% of the directional MAC case. From Fig. 4.9 it also can be noted that, when the number of active connections is small we are able to obtain a DRTS/DCTS ratio value of 98% in the RR-MAC best case.

4.3.4 RR-MAC vs other existing directional MAC works

In order to assess the contribution of RR-MAC with respect to the current state of art, it is possible to make a comparison of the main features of the most important works cited in the related works section with respect to RR-MAC:

TABLE 4.2: Directional MAC protocols comparison

MAC protocol	coll. red.	synch.	fairn.	scalab.	SAS support
DA-DMAC	✓	✓	✗	✓	✗
NDA-MAC	✓	✓	✓	✗	✗
RI-DMAC	✓	✗	✗	✓	✗
DMAC-DEAV	✓	✗	✓	✓	?
DS-DMAC	✓	✓	✓	✗	✗
RR-MAC	✓	✓	✓	✓	✓

In Table 4.2 it can be seen that, protocols such as NDA-MAC and DS-DMAC ensure a reduction of the overall MAC collisions and care the synchronization issue properly. DA-DMAC enhances the contribution in terms of number of collisions, while RI-DMAC and DMAC-DEAV do not provide any mechanism to synchronize the communications. Nevertheless, these approaches do not propose any support for enabling the SAS technology, so, this aspect, it could represent a not negligible limitation in the context of the beamforming networks. In spite of this, DMAC-DEAV offers a sectorized approach that could be adapted for SAS. Our RR-MAC provides quite good results in terms of number of collisions, and properly addresses the synchronization issue as well as such of the directional MAC existing works. Finally, it is possible to evaluate the impact on the deafness problem of our protocol with respect to the works of Table 4.2 in terms of average number of collision reduction:

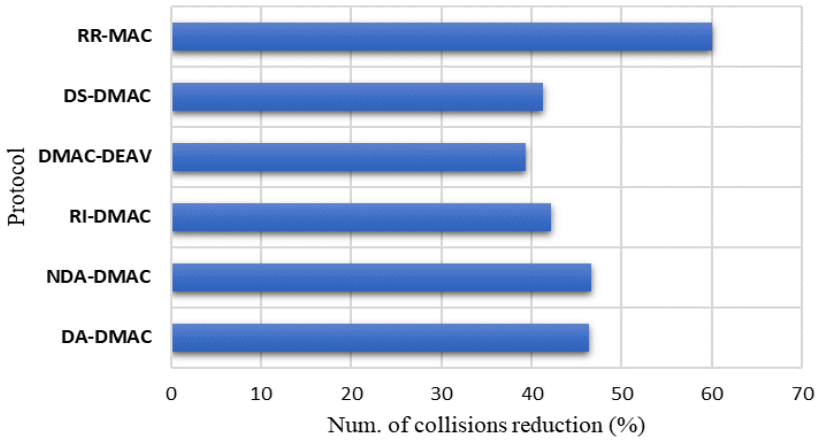

FIGURE 4.10: Collision reduction protocols comparison

In Fig. 4.10 it can be observed how our protocol outperforms other works in terms of MAC performance especially with regard to fairness. This surely results

from the fact that other considered approaches do not provide for an efficient antenna hardware technology, while our work offers a full SAS Adaptive Array support which allows to well mitigate the deafness by improving the system fairness and the overall PDR.

4.4 Round-Robin MAC issues

Therefore, The RR-MAC is a static model and it does not adapt itself to the traffic channel conditions; this could represent a limit in scenarios in which nodes are concentrated in a certain sector; in particular, these kinds of scenario could be affected from the queue issues such as the queue size and the waiting queue time [158], [159]. For this purpose, through the use of *Omnet++* Network simulator, two different run configurations using the same simulation parameters described in [156] have been created; in the first one (RC1), mobile nodes are uniformly distributed in the network scenario; also the activity degree of the nodes is uniformly distributed among sectors; in the second run (RC2) instead, the nodes are periodically concentrated in a certain sector (randomly chosen) of the sectorized plane and the activity degree of nodes is unbalanced among sectors. The number of sectors in the plane varies from 3 to 8 while the queue size is evaluated based on the following equation:

$$Queue\,size = QSF \times [N + w_Q(N_s)] \qquad w_Q \in \overline{W_Q} \tag{4.5}$$

The queue size is function of the number of nodes N and the number of sectors N_s in the plane. QSF is denoted as *Queue Size Factor*, it is a term related to the *Queue size* and it is chosen in the interval $0.1 \leq QSF \leq 0.25$ in order to maximize the Packet Delivery Ratio performance [156]. The number of sectors is weighted by the term w_Q that varies from 1 to 6 as the number of sector value increases. In particular, given the number of sector array $\overline{S} = [3,4,5,6,7,8]$, the weight vector $\overline{W_Q}$ is expressed by: $\overline{W_Q} = [1,2,3,4,5,6]$. In order to assess the impact of the two simulation scenarios relating to the queue issues, it is possible to compare the waiting queue time of the two running configurations in function of the number of sectors and queue size.

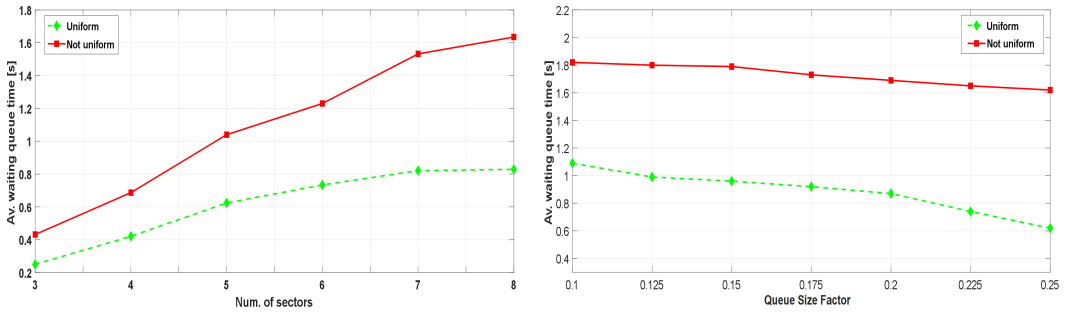

(a) Av. waiting queue time vs numb. of sectors.

(b) Av. waiting queue time vs Queue size.

FIGURE 4.11: RR-MAC queue issues

The Figure 4.11 (a) illustrates the average waiting queue time in function of the number of sectors. The waiting queue time is averaged by varying the *QSF* parameter from 0.1 to 0.25. In Figure 4.11 (a) it can be observed that the waiting queue time in the case of not uniform distributed nodes remains higher than the uniform case independently from the number of sector value; in particular, the gap between the waiting queue time of the two considered cases seeks to grow up for number sector values higher than 5. Note that the obtained results are also averaged in terms of sector time values by increasing the sector time from 1 to 4 s. The curves in Fig. 4.11 (b) are plotted in function of the *QSF* parameter that represents a properly index of the queue size; as it can be deduced from Equation (4.5), the higher is the *QSF* value, the higher is the *Queue size*. As it happens in Figure 4.11 (a) the waiting queue time in the case of not uniform traffic lies above the uniform case curve independently from the queue size. However, as opposed to Figure 4.11 (a) the difference between curves has kept almost constant as the queue size increases. In the uniform traffic case it can be noted how the waiting time slightly decreases for the highest values of *QSF* while, in the not uniform case, the decrease corresponding to the same values is closely negligible. In summary, as the size of the queue grows up the waiting time in the not uniform case does not tend to get smaller, or rather, the decreasing related to high queue size values is not significant. The trends evaluated in Fig. 4.11 (b) are certainly justified by one of the most common issue implied by a Round-Robin algorithm scheduling: the time slice problem; basically, the time slice represents the quantum assigned to each sector (the sector time) in equal portions; therefore, the communications are handled in a circular way among sectors without priority. In case of not uniform distributed traffic if most of mobile nodes are focused in a specific sector of the plane, the communications related to that nodes are enqueued until the beam is allowed in the specific sector; as consequence, the largest is the quantum assigned to each sector the largest is the waiting queue time. In the same way, as observed in if the quantum assigned to each sector is too low, the system will provide bad performance in terms of overall throughput; a similar behaviour is produced if the quantum assigned to each sector is averaged in a specific interval with increasing the number of sectors which results in largest waiting queue time values as seen in Fig. 4.11 (a).

4.5 The A-MSDU MAC approach

The transmission of a set of frames each one handled individually, along with the use of fixed timers in the communication exchange process could produce a large overhead that does not allow an efficient use of the channel time while limiting the throughput with respect to the actual data rates that are steadily increasing. One of the most useful solution that could be able to face the time slice and the queue issues implied by the Round-Robin approach is represented by the employment of the Aggregate MAC Service Data Unit (A-MSDU) and the Aggregate MAC Protocol

Data Unit (A-MPDU) features [160]. Indeed, a quite evolutionary enhancement introduced in the most recent IEEE 802.11n and IEEE 802.11ac MAC standards is the frame aggregation.

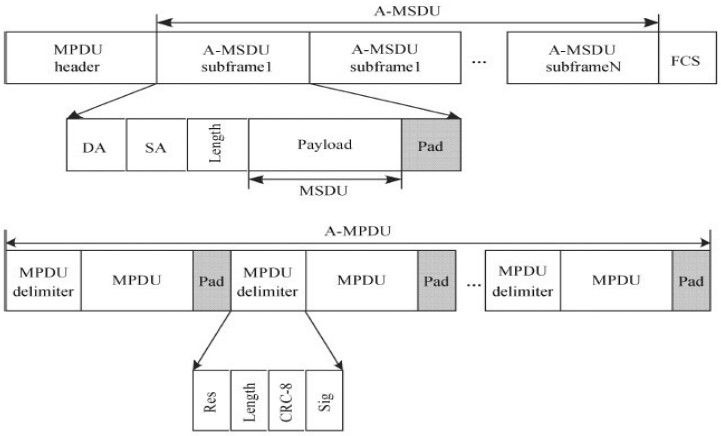

FIGURE 4.12: Frame aggregation principle.

The Fig. 4.12 illustrates the basic operational principle of the frame aggregation. The frame aggregation provides for the concatenation of several frames into a single PHY frame that is successively transmitted in a single channel access. The A-MSDU superframe consist of a set of subframes that are encapsulated between the MPDU (MAC packet Data Unit) header and the FCS (Frame Check Sequence) field. The single A-MSDU subframe contains the address informations related to the communication (Destination Address and Source Address), the packet payload and the padding delimiters. Concatenating multiple MSDUs into a single frame increases the channel utilization and improves the MAC throughout, especially for small frames such as TCP ACK and VoIP (Voice over IP) frames. Indeed, the IEEE80211.n standard contemplates the possibility to use the A-MPDU in place of the A-MSDU. There are few differences between the two aggregation techniques; for example the A-MSDU establishes that individual MSDUs must all be of the same 802.11e QoS access category while A-MPDU provides that the individual MPDUs within an A-MPDU must all have the same receiver address. Although the A-MPDU is a little few expensive than A-MSDU in terms of overhead the A-MSDU mechanism represents a more adequate functionality to use along with directional RTS/CTS and sectorized antennas rather than the A-MPDU. More specifically, the use of A-MSDU, simplifies the control of the antenna while minimizing the average loss of synchronization; conversely, the A-MPDU has more inconveniences: the most significant is the fact that, is highly likely that the system tries to change the sector during the transmission of an A-MPDU sequence; this issue can bring to unwanted node states and consequently to an excessive loss of synchronization. These are the main reasons that led us to choice the A-MSDU strategy. Observe that, the use of A-MSDU with the DRTS/D-CTS exchange process, implies that the system consumes a time that is smaller than the time necessary to transmit a full flow of single frames; in fact, by transmitting a

unique superframe instead of several frames, makes it possible to reduce the total time (DRTS/DCTS + frame aggregation) resulted from a set of communications.

4.5.1 Model implementation

The 5.0 version of Omnet++ simulator does not support any features related to MAC layer modules that allow to simulate the A-MSDU mechanism; therefore, neither the IEEE 802.11n and neither the IEEE 802.11ac MAC standards are supported. For this reason the original DCFUpperMac module used in Omnet++ has been extended. The DCFUpperMac class, is the module responsible for the sector control and also provides for the synchronization in the communication process by scheduling and handling the exchange between the sector queues and the main queue. Basically, the idea is to create a A-MSDU just before a change of sector is involved by the system, in order that this superframe packet remains stored in the main queue until the sector is active. In our implementation [161], the source sends several consecutive frames and the MAC module, aggregates these individual frames by creating a superframe (the A-MSDU frame); the first frame is not included in the superframe because this frame, as logical operation of the DCFUpperMac, is extracted from the main queue and transmitted in the channel.

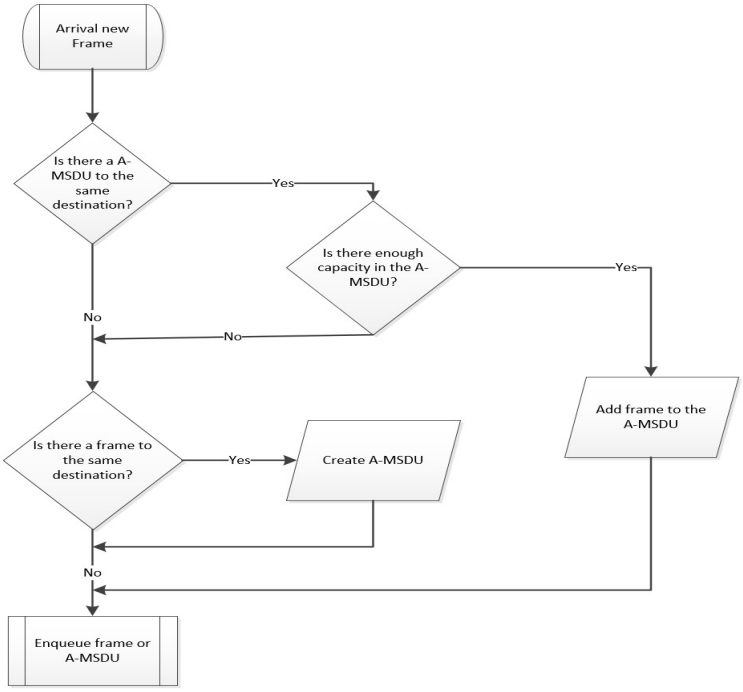

FIGURE 4.13: A-MSDU MAC protocol operations.

The Flowchart of Fig. 4.13 synthetizes the A-MSDU MAC protocol operations. When a new individual frame is ready to be sent in the channel the MAC module primarily checks if an A-MSDU exists in one of the sector queues having the same destination address of the incoming frame; if an A-MSDU exists and there is enough space available, the frame is encapsulated in a new subframe and concatenated to

the current A-MSDU; if there are not A-MSDU available but there is at least another frame in the sector queues containing the same destination address of the considered frame, they are merged in order that a new A-MSDU is created; finally, if none of the sector queues contains a frame having the same destination address of the incoming frame, the frame is enqueued in the delay queue. Note that the A-MSDU is sent towards a specific destination as soon as it reaches the maximum size.

4.6 The Weighted Round-Robin approach

The main goal of a Weighted Round-Robin (Weighted Round Robin MAC (WRR-MAC)) approach [161] is to partially minimize the most common issues introduced by the use of a Round-Robin approach which may significantly limit the overall network performance. As explained in the section 4.4, the main challenges related to the RR approach are referred to the size of the queues and the delay produced by static time slices which cannot be modelled in function of the traffic in the network. However, as observed in [156] the quantum of time assigned for the beamforming process is the same for each sector as well as the amplitude of the width. Therefore, in the work [156] it can be clearly deduced as a proper set of the sector time value affects the overall performance more than the sector width choice; this implies that the time slot assigned to sectors needs to be carefully handled with respect to the width relying in the resource allocation optimization process. For these reasons our Weighted Round-Robin approach modifies the original RR algorithm formulation relative to the evaluation of the sector time while keeping unchanged the sectorization of the plane and thus the width of the sectors. More specifically, the sector time related to the *i-esimum* sector of the plane is function of two main terms:

$$T_i = f(A_D, M_L) \tag{4.6}$$

the term A_L denotes the activity degree of nodes in the sector i while the term M_L considers the misalignment level between the transmitter and the receiver during a communication. In particular, the activity degree of nodes in a sector can be defined as follows:

$$A_D = \frac{N_{ACTIVE}}{N_{TOTAL}} \qquad 0 \leq A_D \leq 1 \tag{4.7}$$

in the ratio defined by Equation 4.7, the term at numerator represents the total of active mobile nodes in the sector, while N_{TOTAL} is the total number of nodes in the sector. Note that a node is considered active if it is involved in a communication process (either in transmission and either in reception). By considering the cited dependency factors, the sector time expression becomes:

$$T_i = w_{A_D}\left[\frac{S_i}{\sum_{i=1}^{N_s} S_i} A_D w_s N_s T\right] - w_{M_L}\left[\frac{(DRTS + DCTS)_{received}}{(DRTS + DCTS)_{sent}} T\right] \tag{4.8}$$

The Equation 4.8 consists of two main terms; The first one is related to the degree activity of nodes and is denoted by :

$$T_i^I = w_{A_D} \left[\frac{S_i}{\sum_{i=1}^{N_s} S_i} A_D w_s N_s T \right] \tag{4.9}$$

the degree activity of nodes in the i-esium sector denoted by A_D is certainly affected by the size of the queue in that sector, thus, the term S_i is referred to the size of the queue of the sector i; N_s is the number of sectors in the plane that is weighted by w_s which represents the weight assigned dependently on the number of sectors of the plane; w_{A_D} is the weight related to the degree activity factor; finally, T is a project parameter that represents the duration lowerbound assigned to the beamforming process that is directly derived from the work [156]; therefore, T matches with the duration lowerbound chosen for the Round-Robin MAC approach and is set to 1 second. The second term of equation 4.8 considers the level of misalignment between transmitter and receiver and is expressed as:

$$T_i^{II} = w_{M_L} \left[\frac{(DRTS + DCTS)_{received}}{(DRTS + DCTS)_{sent}} T \right] = w_{M_L} (DRTS/DCTS)_{ratio} \tag{4.10}$$

the factor denoted by Equation 4.10 tests the alignment between sender and receiver through the evaluation of the DRTS/DCTS ratio that was defined in [162] this parameter, already used in [156] for estimating the MAC system performance in terms of fairness, represents a significant term for minimizing the deafness issue. The DRTS/DCTS ratio is multiplied by the term w_{M_L} that is the weight referred to the misalignment level between transmitter and receiver. In the Equation 4.10 it can be noted that when the size of the queues is the same for all sectors (Round-Robin case) we obtain:

$$T_i^I = w_{A_D} A_D w_s T \qquad S_i = S_{i+1} = ... = S_{N_s} \tag{4.11}$$

with:

$$\frac{S_i}{\sum_{i=1}^{N_s} S_i} N_s = 1 \qquad S_i = S_{i+1} = ... = S_{N_s} \tag{4.12}$$

the Equation 4.11 determines the duration weighted lowerbound assigned to the beamforming process for each sector which has been already mentioned. However, by considering the Equation 4.11 it has been assumed that the weights can take the values synthetized by the following vectors:

$$\overline{W}_{A_D} = \overline{W}_{M_L} = [1,2,3]^T \qquad \overline{W}_s = [5,4,3,2,1]^T \qquad \overline{N}_s = [2,3,4,6,8]^T$$

the vector $\overline{W}_s$ is function of the number of sectors in which the plane is divided; more specifically, let i be the index of the vectors $\overline{W}_s$ and $\overline{N}_s$, the i-esimum element

of $\overline{W}_s$ is the weight associated with the i-esimum element of $\overline{N}_s$. For example, if the plane is divided into 2 sectors, we obtain w_s= 5. Note that the descending order used for the weights assignment in function of the number of sectors is not casual: as Round-Robin assumption, the greater is the number of sectors in which the plane is divided, the smallest should be the quantum of time (and thus the weight) assigned to each sector. As regards the equation 5, assumed that the possible values of T_i belong to an interval having lowerbound T, it is possible to determine also the upperbound value related to this interval. The upperbound is determined based on the following assumptions:

Assumption 1 *the lowerbound is limited to T.*

Assumption 2 $\min(DRTS/DCTS)_{ratio} = 0.5$*; this value is obtained from the RR-MAC.*

Assumption 3 $w_{A_D} \neq w_{M_L}$.

the assumption 3 is made in order that the two terms of the equation 5 is unbalanced; in particular, the choice $w_{A_D} > w_{M_L}$ is reflected in the maximization of the contribution of the first term of equation 5 with respect to second term. In other terms, this project parameter weight choice maximizes the PDR (that is closely related to the activity degree of nodes) while choosing $w_{M_L} > w_{A_D}$ aims to maximize the fairness (that is closely related to the DRTS/DCTS ratio) of the system. By parameterizing, it is possible to obtain the interval of values which T_i belongs:

if $w_{A_D} > w_{M_L}$:

$$\begin{cases} T \leq T_i \leq w_{A_D} A_D[(2w_s - 1) + 0.5]T & w_{M_L} = 1 \\ T \leq T_i \leq w_{A_D} A_D[(2w_s - 1)]T & w_{M_L} \neq 1 \end{cases} \tag{4.13}$$

if $w_{M_L} > w_{A_D}$:

$$\begin{cases} T \leq T_i \leq w_{A_D} A_D[(2w_s - 1) + 0.5]T & w_{M_L} = 3 \\ T \leq T_i \leq w_{A_D} A_D[(2w_s - 1)]T & w_{M_L} \neq 3 \end{cases} \tag{4.14}$$

for example, let us assume to choice $N_s = 4, w_{A_D} = 1, w_{M_L} = 2, w_s = 3$ with $w_{M_L} > w_{A_D}$, the upperbound of the interval related to T_i is obtained for $A_D = 1$ and is denoted by:

$$T(upper)_i = w_{A_D} A_D[(2w_s - 1)]T = A_D 5T = 5s \tag{4.15}$$

that determines the interval: $1s \leq T_i \leq 5s$. Note that the upperbound value is function of the degree activity A_D and the weight w_s; the smaller is the number of sector the greater is the upperbound value and thus the quantum assigned to the sector i. The full operations of the WRR MAC are summarized by the pseudo code included in Appendix 1.

4.7 Designed MAC approaches performance comparison

Designed MAC approaches have been compared with one of the most significant Directional MAC work, that is the DA-MAC protocol (that has been implemented in Omnet++). The number of antenna elements of the array is set to 10 either of the switched beam SAS and either of the adaptive array SAS; the overall MAC performance of the considered approaches have been evaluated in function of the number of mobile nodes in the network in order to investigates about the scalability level of each protocol; the number of nodes has been increased from 10 to 100. The first statistic is referred to the PDR:

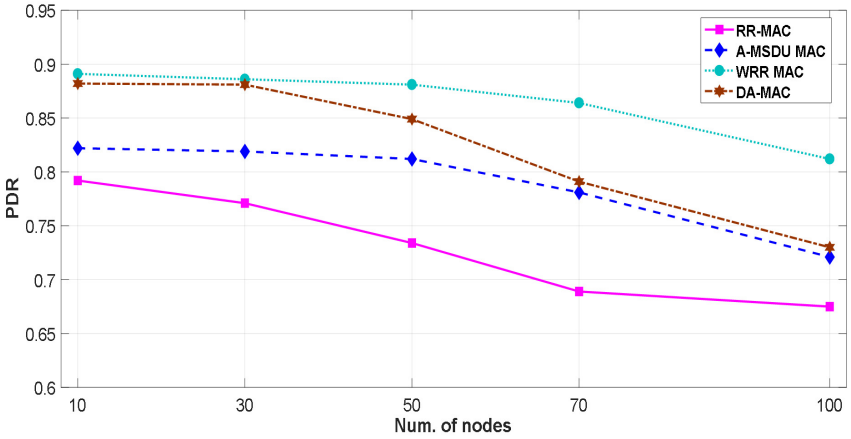

FIGURE 4.14: PDR considered approaches comparison

The Figure 4.14 illustrates the comparison plot of the considered approaches related to the PDR statistic. When the number of nodes is low the DA-MAC performs very quite similarly to the WRR MAC; indeed, as demonstrated in [151] the peak of DA-MAC is obtained for a number of nodes set to 20; however, this value, for DA-MAC tends to linearly decrease when the number of nodes is higher than 50; the average reduction gives from 4% to 12%; This is probably closely related to the different kind of SAS technology used by the two approaches; in fact, the more is the number of nodes the highest is the correlation matrix associated to the network, the lowest is the accuracy in the DOA (Direction of Arrival) estimation; more specifically, the Adaptive SAS technology due to its complex and efficient logical processing unit, is able to reduce the overall error introduced by the directions estimation better than the switched beam technology and contributes to limit the reduction of the aggregate throughput with increasing network complexity; Very similar performance are offered by the A-MSDU MAC, which is globally worse than the WRR and the DA-MAC, but remains more stable compared to that both cited; it also can be observed how the feature of aggregation offered by the A-MSDU is able to improve the performance of the RR-MAC because of the efficient exploitation of the sectorization compared with the latter. For a further investigation it has been analyzed the fairness by varying the number of nodes.

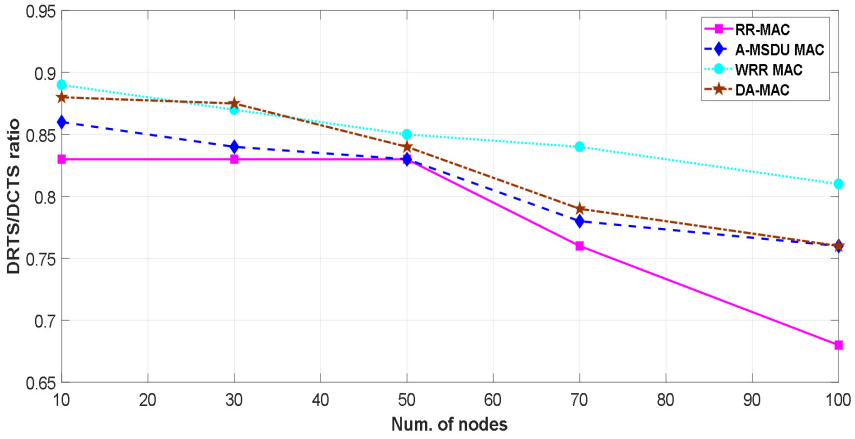

FIGURE 4.15: DRTS/DCTS ratio considered approaches comparison

The Figure 4.15 plots the DRTS/DCTS ratio statistic of the four approaches. It is important to emphasize that, as opposed to [151] in which the fairness is evaluated using the Jain's index [163] (that is very interrelated to the aggregate throughput), in this case for DA-MAC the DRTS/DCTS ratio has been employed as fairness evaluation metric, in order to uniform the comparison with respect to other approaches. As it happens for the PDR, the WRR-MAC and the DA-MAC are almost similar until N = 30 nodes; then, the WRR begins to marginally decrease and becomes very close to the A-MSDU MAC. The decreasing behaviour of the DA-MAC could be easily justified due that it concerns the backoff procedure management. Suppose that, there is an incoming frame transmission destined to the sector S_x but that sector is sensed busy; in a non-sectorized MAC approach (such as the DA-MAC), the protocol, enables the backoff procedure which in turn stops the contention window timer; therefore, any node in the coverage area stops its operation in order to minimize the collision probability. This issue could represent a severe limitation to performance, especially in terms of fairness, which is closely constrained by the contention window timer and it becomes more accentuated with increasing mobile nodes. Thus, an advantage of our sectorized approach is represented by the fact that, only the nodes belonging to the sector that is sensed busy are involved in the backoff; for this reason, the WRR MAC slightly outperforms the DA-MAC and for the same reason, the A-MSDU MAC which is close enough to DA-MAC in terms of PDR keeps the similarity also as regards the fairness.

4.8 The Self Clocked Fair Queuing MAC approach

For overcoming issues related to queue management and time slice it possible to use alternative scheduling techniques avoiding Round Robin problems. For example a Weighted Fair Queuing (WFQ) scheduler enhances fairness provided by Round Robin [164], [165]. One of the biggest problems with WFQ is implementing the algorithm for updating the round number on packet arrival, since this may lead to

iterated deletion of connections. The SCFQ algorithm is a way to speed up round number computation. SCFQ uses a simplified method of calculating the service time, based on the transmission delay of the packet, and the finish time of the packet currently being serviced. In SCFQ, when a packet arrives to an empty queue, instead of using the round number to compute its finish number, it uses the finish number of the packet currently in service. Because SCFQ is a derivative of WFQ, the round number update rule can be evaluated as [166]:

$$F(i,k,t) = MAX[F(i,k-1,t), \quad CF] + \frac{P(i,k,t)}{\phi(i)} \tag{4.16}$$

Where CF represents the finish number of the packet currently being served, $F(i,k-1,t)$ denotes the finish number for the $(k-1)th$ packet related to the communication flow i, $P(i,k,t)$ is the size of the kth packet that arrives on flow i at time t and $\phi(i)$ represents the weight related to the ith flow. Observe that we consider as *finish number* the time needed for sending a packet related to a certain communication flow. The relative fairness bound provided by SCFQ can be expressed as [167]:

$$RFB = \frac{PMAX(i)}{g(i)} + \frac{PMAX(j)}{g(j)} \tag{4.17}$$

Where $PMAX(i)$ and $PMAX(j)$ are the sizes of the packets that can be sent by connection flows i and j while $g(i)$ and $g(j)$ are the service rates allocated to connections i and j respectively. The absolute fairness bound for SCFQ is currently unkwnown. Although the SCFQ round number update is easy to implement, it can be unfair over short times scales. In SCFQ algorithm, the internal generation of the virtual time involves negligible overhead, as the virtual time is simply extracted from the packet situated at the head of the queue. This approach eliminates the computational complexity introduced by WFQ scheduling. In particular, the logarithmic computational complexity and bounded end-to-end property suggests that SCFQ is well suited for the queue managament of sectorized antennas.

4.8.1 SCFQ-MAC implementation and algorithm pseudo-code

Likewise RR-MAC, the Self Clocked Queuing MAC (SCFQ-MAC) is implemented in Omnet++ network simulator [123] in the *DcfUpperMac* module that is the module that manages the operations at MAC layer in Omnet++. The SCFQ algorithm replaces the original Round-Robin scheduler designed in [156]. Observe that, main functions of *DCFUpperMac* class containing the SCFQ implementation are *UpperFrameReceived* and *FrameExchangeFinished*; the first one manages packets exchange between the MAC layer and upper layers, the second it is useful to specify which is the next frame properly selected among queues to be processed by the scheduler. In order to understand the SCFQ algorithm pseudo-code that is illustrated in this section, it is necessary to explain the use of some auxiliary variables that we defined

in the code with the aim to facilitate the implementation of the main expression of the SCFQ that is the Equation (1) (explained in the section III):

- **actualEndTime** = representing the term CF denoted in the Equation (1)
- **actualArrivalTime** = representing the arrival time of the frame currently being served; it is useful for evaluating the waiting time of the queues.
- **baseTimer** = representing the term $MAX[F(i,k-1,t), \quad CF]$ denoted in the Equation (1).

The pseudo-code of SCFQ-MAC is shown as follows:

Algorithm 9 SCFQ-MAC algorithm

```
1: procedure UPPERFRAMERECEIVED(frame)
2:     .............
3:     if !frameExchange then
4:         bw = random(20 * 10^6, 30 * 10^6) * w[frameSector];
5:         enqueue (frame);
6:     else
7:         baseTimer = MAX (sectorsQueue[frameSector].back().endTime,
8: actualEndTime);
9:         PktData pktData;
10:        pktData = frame;
11:        pktData.endTime = baseTimer + (frame.getByteLength())/bw;
12:        pktData.arrivalTime = simTime();
13:        updateQueues();
14:        recomputeWeights();
15:    end if
16: end procedure
1: procedure FRAMEEXCHANGEFINISHED
2:     .............
3:     if !queueIsEmpty then
4:         for i=0;i< queueSize;i++ do
5:             if sectorsQueue[i].front().endTime < min then
6:                 que = sectorsQueue[i];
7:                 min = sectorsQueue[i].front().endTime;
8:                 queue = i;
9:             end if
10:        end for
11:    end if
12:    if que then
13:        actualEndTime = que->front().endTime;
14:        actualArrivalTime = que->front().arrivalTime;
15:        computeWaitingQueueTime(actualEndTime, actualArrivalTime, simTime())
16:    end if
17: end procedure
```

The Algorithm 1 describes the main steps of SCFQ-MAC. *UpperFrameReceived* function basically implements the Equation (1); other than that, when the channel is in idle state, the initial bandwidth is set to a number (expressed in Mbps) randomly chosen between 20 and 30 that is yielded for the weight assigned to the sector which the current frame belongs. Then the virtual *endTime* of the processed frame is evaluated by extracting the maximum value chosen between the the *finish number* for the

$(k-1)th$ frame and the *actualEndTime*; this value is stored in the *baseTimer* variable and then it is added to the the size of the *kth* packet divided by the bandwidth, according to Equation (1). Finally, queues are updated with the new informations and weights for sectors are re-assigned. The function $frameExchangeFinished$ instead, provides the instructions that the scheduler has to use in order to select the next frame (from queues) that has to be served. More specifically, in our implementation we established that, the next frame that must be served, in case of several frame pending in queues, it is the frame having the minimum virtual *end time*; once the right frame it has been selected from its *sectorQueue* all frame tag informations are used for evaluating periodically the average waiting time of queues; the Waiting Queue Time (WQT) is evaluated as:

$$WQT = simTime() - actualArrivalTime \tag{4.18}$$

Where, *simTime()* is an utility Omnet++ function returning the current simulation time, while the *actualArrivalTime* is the arrival time of the frame currently processed.

4.8.2 The SCFQ-MAC approach: differences with RR-MAC

The RR-MAC designed in [156] has a static approach that does not take into account neither the channel state nor the transmission/reception time of frames. In fact, no priority in-frame scheduling exists and queues of sectors are not affected by weights.

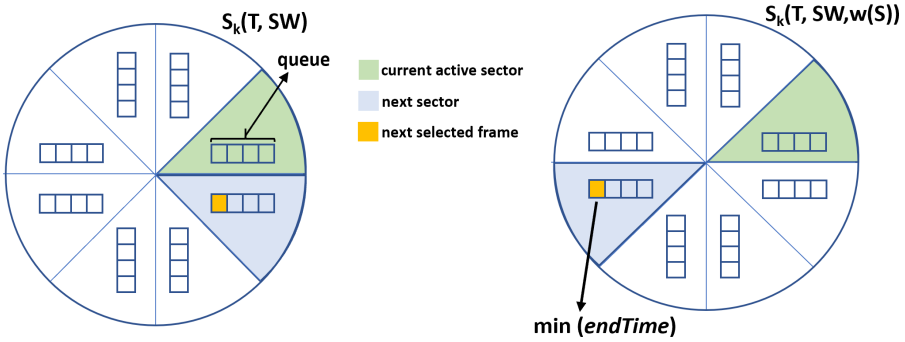

(a) RR-MAC principle (b) SCFQ-MAC principle

FIGURE 4.16: RR-MAC and SCFQ-MAC comparison.

The Figure 4.16 illustrates the approach comparison about the designed SCFQ-MAC and the RR-MAC. In Figure 4.16 (a) the RR-MAC principle is depicted. The plane is sectorized into 8 sectors; each sector is denoted by $S_k(T, SW)$ in order to highlight the dependency on the *sector time* T and the *sector width* SW; k is the index related to the sector and in this case, it can assume values such that $k = 1....8$. All of sectors have assigned a queue in which frames are located and wait until they are transmitted in the channel. Recall that in [156] the *current active sector* has been defined as the sector whose frames are allowed to be transmitted in the channel until

the *sector time T* has elapsed. Let us suppose that the antenna beam is currently active in the sector 2 as shown in Figure 4.16 (a); according to Round-Robin operation, the next sector in which the beam will become active is the sector 3; this means that the next frame selected by the scheduler will be the frame belonging to sector 3 and having the highest waiting time in the queue. In this case, as it has been mentioned, no priority frame mechanism are adopted. Now, let us refer to the situation depicted in Figure 4.16 (b) illustrating the SCFQ-MAC principle; observe that in this case, the sector is also function of the assigned weight $w(S)$; although the *current active sector* is again the sector 2, however, according to SCFQ operation, the next active sector it will be the sector 6; more specifically, the scheduler does not wait the expiration of the *sector time* related to sector 2, but immediately "jumps" to sector 6 because it contains the frame having the minimum virtual *endTime* computed according operations performed by Algorithm 1. Only once the frame having the minimum *endTime* has been sent in the channel, if the *sector time* for sector 2 has not expired, the scheduler returns in sector 2 and continues to serve pending frames in that queue. This last point introduces a priority mechanism relating to frames management.

4.8.3 The SCFQ-MAC approach: Numerical Results

In order to obtain a fair comparison among results related to performance, the experimental analysis for SCFQ-MAC evaluation is accomplished through the use of the Omnet++ simulator as has been done for RR-MAC. In particular, the same module used for RR-MAC that is the *DcFUpperMac* class is modified by replacing the Round-Robin algorithm with the designed SCFQ algorithm. The main parameters setting used in simulations are synthetized by Table 4.3:

TABLE 4.3: Main simulation parameter set.

Antenna Model	SAS phasedArray
Array Elements Spacing	0.5 λ
Number of Nodes	30
Transmission Rate	54 *Mbps*
Traffic data type	UDP
Message Length	512 *Byte*
Simulation Area Size	500 x 500 *m*
Simulation Time	100 *s*
Number of sectors	8
Sector Time values	1,2,3,4 *s*
Size of queues	5 *frames*

Simulations have performed by using 20 different seeds and extracting confidence intervals obtained by repetitions considering a confidence level of 95 %. The traffic is randomly generated (based on the simulation seed) by different couples of nodes. Observe that the plane is divided into 8 equal sectors according the example scenario illustrated in Figure 1. Relating to performance analysis, primarily, it has been decided to evaluate the average waiting queue time (averaged by *sector time*

values) both for RR-MAC and SCFQ-MAC approaches; we remark that in the case of SCFQ-MAC, at the begin of simulations weights are equals and set to 1, the weight range gives from 0.05 to 1.

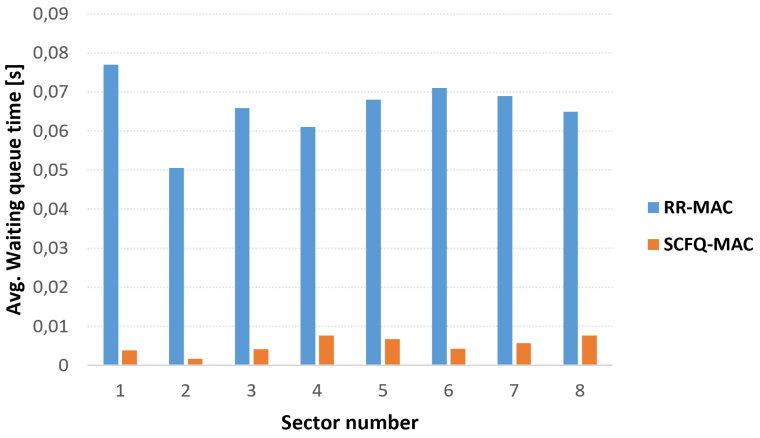

FIGURE 4.17: RR-MAC SCFQ-MAC Waiting queue time comparison.

The Figure 4.17 illustrates the comparison plot relating to waiting queue time statistic in function of sectors of the plane. In case of RR-MAC the waiting queue time range is $[0.05s, 0.077s]$ while when using SCFQ-MAC the maximum value is 0.0076 s; this means that there is one order of magnitude of difference in the comparison among approaches. This result is mainly due to the fact that, in the case of SCFQ-MAC, the time slice problem involved by Round Robin, is considerably reduced due to the use of virtual timers allowing the active beam to switch among non adjacent sectors; this aspect means that the static loop of RR-MAC in sectors crossing is broken. Therefore, highlight also that in the case of SCFQ-MAC, the scheduler does not necessarily wait the expiration of the sector time before transmitting frame related to other sectors; this aspect certainly contributes to reduce the average waiting time of queues. In order to confirm waiting queue time results, the end to end Omnet ++ statistic has been analyzed:

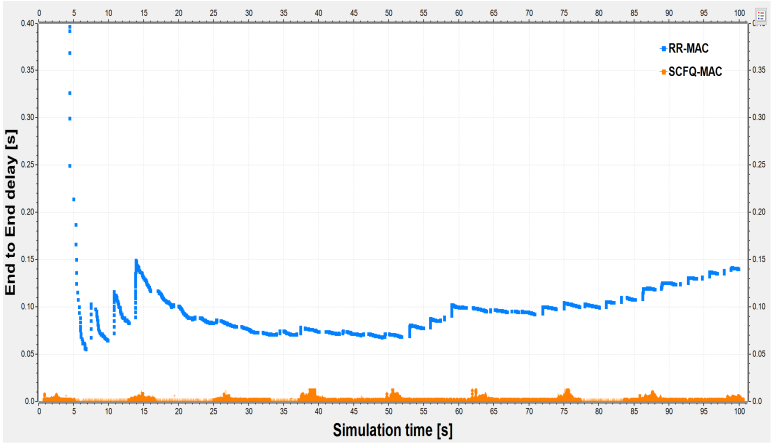

FIGURE 4.18: RR-MAC SCFQ-MAC End to End delay comparison.

The Figure 4.18 depicts the Omnet++ statistic related to end to end delay vector including the comparison between RR-MAC and SCFQ-MAC. In the case of RR-MAC the average end to end delay is about 0.1 s; however, along all the simulation time it never gets values lower than 0.07 s. In the case of SCFQ-MAC, the average end to end delay is about 0.001 s; in the worst case we obtain a value of 0.0025 s. The behaviour of Figure 4.18 confirms the trend registered in Figure 4.17. As last result, it has been evaluated the fairness of our proposed approach. To make this, it has been used the same fairness metric evaluation index employed for RR-MAC analysis that is the DRTS/DCTS ratio which has been defined in [156]:

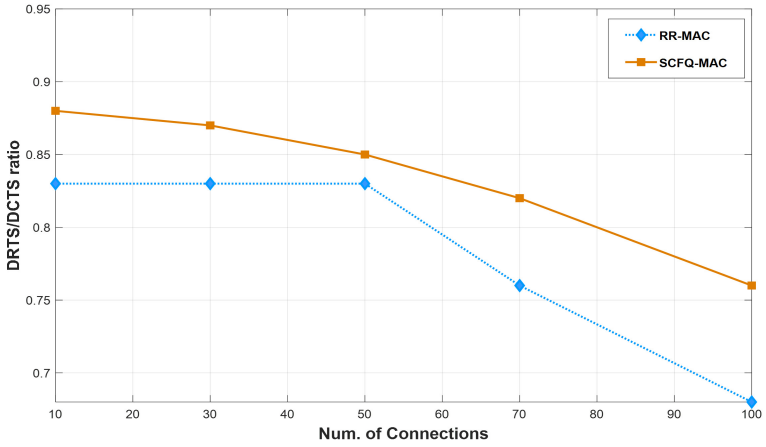

FIGURE 4.19: RR-MAC SCFQ-MAC DRTS/DCTS ratio comparison.

The comparison plot shown in Figure 4.19 illustrates the DRTS/DCTS ratio curves related to examined approaches. the trend of DRTS/DCTS ratio is obtained by increasing the number of connections (and then the network load) in the network from 10 to 100. From Figure 4.19 it can be observed how the SCFQ-MAC outperforms RR-MAC independently from the network load. In particular, in case of SCFQ-MAC we obtain a maximum value of 0.88 against the best RR-MAC that is 0.83. However, as the number of connections increases, this value tends to reduce; although in the case of RR-MAC this reduction is quite accentuated leaving from 50 connections, this trend results more mitigated when SCFQ-MAC is employed. Indeed, using SCFQ-MAC we are able to achieve a minimum DRTS/DCTS ratio of 0.76; this result improves considerably the worst RR-MAC case value of 0.68.

Chapter 5

Mobility and energy consumption issues in Directional MANET

5.1 Introduction

Two of the most important issues in Directional MANET environments especially as regards the most modern employed antenna technologies are certainly represented by the mobility and the energy consumption of nodes. However, when considering mobility in MANET, also energy consumption of nodes implied by mobility should be evaluated. Indeed energy consumption is very related to mobility pattern employed in the network protocol. Therefore, the mobility model plays a very important role in determining the protocol performance in MANET. Thus, it is essential to study and analyze various mobility models and their effect on MANET protocols. In particular, the performance of MAC protocols commonly degrades with increasing system dynamics, and malfunctions may occur in highly dynamic scenarios. As it has been said in the chapter 1, when a node is subjected to mobility during a communication, especially in beamforming network contexts, it can be affected from undesired phenomena such as the handoff problem. A most common solution used to mitigate the impact of the nodes mobility in directional communications is mobility prediction [168], [169]. Essentially, the mobility prediction is a method for estimating the trajectory of the future position of the nodes. Mobility prediction has been studied in cellular networks and wireless ad-hoc networks and represents a precious instrument for estimating the future location, mobility speed, and the direction of the mobile users. Anyway, the nodes in this type of networks are generally power constrained because they depend on limited battery resources, whereas wireless communications consume a lot of energy. Without the resource, power, mobile devices will become useless. So, maximizing the lifetime of batteries of each host and entire network is an important challenge, especially for MANET, which is supported by batteries only. The problem of limiting the overall network consumption comes to be greater if we consider the latest antenna technologies such as SAS and Massive MIMO systems. In this regard, the task of minimizing energy consumption of nodes is very critical because nodes use very high-gain directive beam for communications. The purpose of the present chapter is to provide a brief

background about the most recent and significant works about mobility and energy consumption issues in directional MANET with special attention to proposals that deal with the use of the most modern antenna systems.

5.2 Mobility in MANET

Before exposing the most significant works related to directional MANET communications it is necessary to provide a generic brief overview about the mobility concept in Mobile Ad Hoc Networks. Firstly, mobility in MANET represents a challenge as well as a property [170]; in fact, usually mobile nodes move in the network periodically changing their position according to a certain mobility pattern. However, this feature significantly impacts on the network performance especially in terms of routing protocol and overhead.

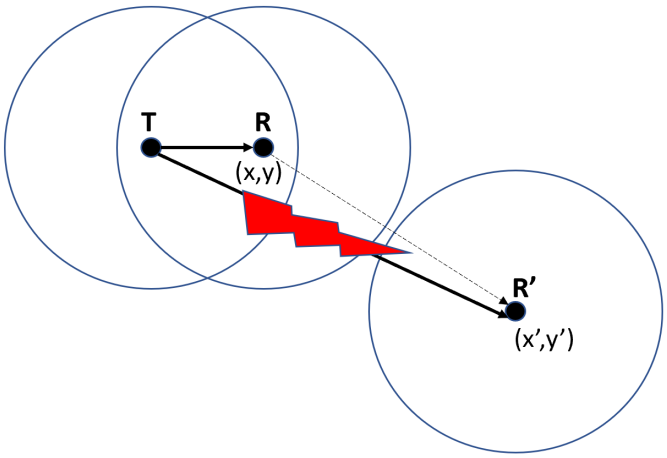

FIGURE 5.1: Mobility in MANET using omnidirectional antennas

For simplicity, let us consider a simple case of mobility of nodes. In Figure 5.1, all nodes are equipped with omnidirectional antennas. Node T attempts a communication with node R lying in the position (x, y); in this case, because R is within the coverage range of T the communication has successful. Now, let us suppose the R, after a certain time move in the network according to a mobility pattern in the position $R^{'}$ having coordinates $(x^{'}, y^{'})$, in this case, because the radiation pattern formed by R is outside the coverage range of T, current link between T and R goes break and communication fails. This event presents two main consequences: firstly, amount of messages that does not arrive to R translates into a degradation of packet performance; secondly, if there is a routing protocol that recomputes the new route between T and R, this lead to an increasing of the overall protocol overhead, especially if node R moves in the network frequently. Generally, due to node mobility, the links along paths could suffer frequent failure and reactivation in highly dynamic environments. Consequently, the communication paths consisting of relaying nodes between a source and destination node have to change frequently. Without a fixed

infrastructure, frequent path changes cause significant number of routing packets to discover new paths, leading to increased network congestion and transmission latency. Therefore, finding reliable means of choosing reliable communication paths is a critical task. Things get complicated when directional antennas are employed. As it has been shown in Figure 1.9, when directional beams are used, routing performance are often affected by handoff problem. Anyway, because of the use of directional antenna systems, handoff has to be considered in addition to other undesired phenomena occurring at lower layers such as deafness and hidden terminal problems. For this reason, mobility prediction algorithms are commonly used to pre-estimate future movements of nodes in order to limit excessive degradation of network performance. Nevertheless, mobility prediction techniques are closely related to the kind of mobility pattern of nodes in the network. The following section illustrates main mobility models in MANET.

5.3 MANET mobility models

Mobility models represent the tendency of mobile nodes according to the type of movement that they accomplish in function of time [171]. Since mobility modeling represents a significant factor in the analysis of MANET, many mobility models have already been studied to reproduce the motions of real mobile nodes. The mobility model is made to in order to describe the movement pattern of mobile users. Since mobility patterns may play an important role in identifying the protocol performance, it is advisable for mobility models to emulate the movement pattern of particular real life applications in an affordable way. Thus, when analyzing MANET protocols, it is very important to select the proper underlying mobility model. Mobility models are based on different parameters associated with node movement. Common parameters usually include, starting position of nodes, movement direction and mobility speed; all of these parameters are assumed to be made in function of time. Generally, a mobile node can move according to an individual pattern or a group pattern; in the second case, in particular, node is affected from the behaviour of a group of nodes using a common mobility pattern. In light of this, mobility models can be divided into two main macro categories: entity mobility model and group mobility model [172]. The first category specifies individual node movement, the second, instead, describes group motion as well as individual node movement within groups. The most important mobility models are briefly described in the following subsections.

5.3.1 Random Walk mobility model

The Random Walk model was mathematically introduced by Einstein in 1926 [173]. In this mobility model, a mobile node can move randomly, which means that the direction and speed of moving are casually selected using uniform distribution. Both the speed and the direction are limited by a pre-defined range, [*speedmin*; *speedmax*]

and $[0; 2\pi]$ respectively. Each movement in the random walk mobility model happens in either a constant time period t or at a constant distance travelled d, by which a new direction and speed are computed. In the particular case that a node arrives at the border of the area, it selects a new direction. Many derivatives of the random walk mobility model have been studied including the one-dimensional, two-dimensional, three-dimensional, and d-dimensional walks. The Figure 5.2 depicts an example of the movement pattern of a mobile node based on the Random Walk Mobility.

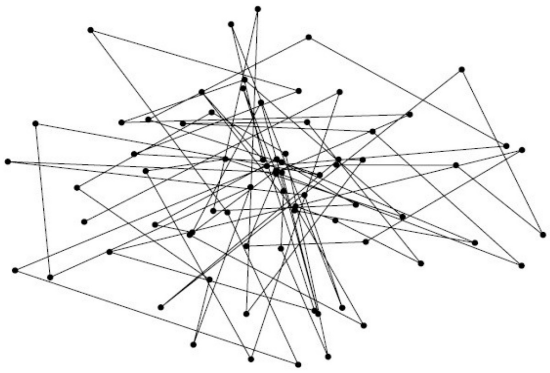

FIGURE 5.2: Random Walk mobility model example

5.3.2 Random Waypoint mobility model

The Random Waypoint is one of the most popular mobility models used in MANET [174], [175]. With this model, the node moves from its current position to a new one by randomly selecting destination and speed. The distribution of speed is uniform within a range [*speedmin*; *speedmax*]. When node reaches its destination, waits for a certain time (pause time) and then starts moving again. Basically, the random waypoint model is very similar to the random walk model except from the fact that the first one includes pause times between changes in direction and/or speed. Pause is used to overcome abrupt stopping and starting in the random walk model. Upon expiry of this pause, the node arbitrary selects a new location to move towards and a new speed which is uniformly randomly selected from the interval [*speedmin*; *speedmax*].

After reaching the destination, the node stops for a duration defined by the 'pause time' parameter. After this duration, it again chooses a random destination and repeats the whole process again until the simulation ends. Figure 5.3 illustrates an example of Random Waypoint in which nodes move independently to a randomly chosen destination with a randomly selected speed.

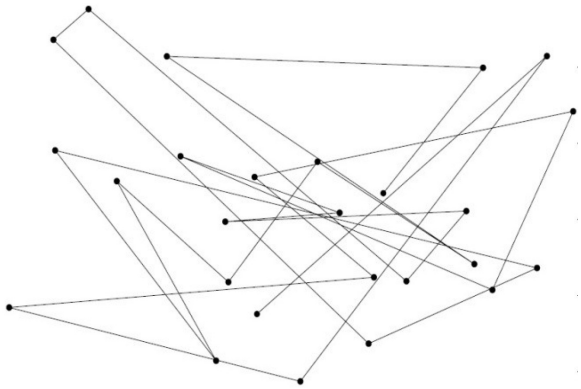

FIGURE 5.3: Random Waypoint mobility model example

5.3.3 Random Direction mobility model

This model basically overcomes the non-uniform spatial distribution problems typically found in Random Waypoint mobility model [176]. In this model, a node randomly selects a direction to move along until it arrives to the boundary of the simulation area. The speed and direction of the mobile node remain unchanged until it hits the boundary. After the boundary is reached by node, it stops for a specified pause time and then it chooses another angular direction $[0; \pi]$ to travel. In this way, the typical problem (i.e. higher node density in the middle of simulation area) found with Random Waypoint mobility model has been resolved. Random Direction is similar to Random Waypoint except from the fact that the pause time is performed also when the border is reached and not only when node arrives to destination. An illustrative example is given in Figure 5.4

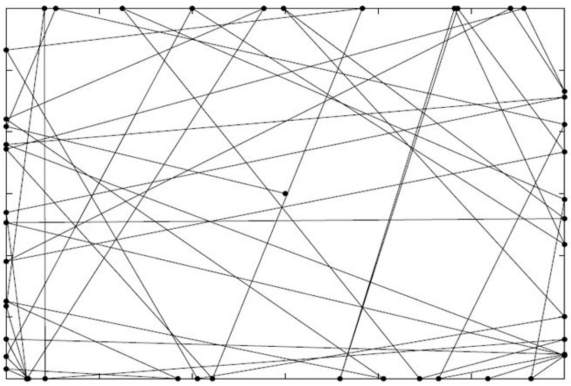

FIGURE 5.4: Random Direction mobility model example

5.3.4 Probabilistic Random mobility model

This model utilizes a probability matrix to determine the position of a particular mobile node in the next time step which has three different states (0,1 and 2) for its

x and y position [177]. The probability matrix used is:

$$\mathbf{P} = \begin{bmatrix} P(0,0) & P(0,1) & P(0,2) \\ P(1,0) & P(1,1) & P(1,2) \\ P(2,0) & P(2,1) & P(2,2) \end{bmatrix}$$

Where each entry, that is denoted by $P(i,j)$ expresses the probability of a mobile node to go from state i to state j. The probability matrix allows a mobile node to move in any direction as long as it does not return to its previous position. State '0' represents the current position (x or y) of a mobile node, state '1' represents the previous position (x or y) and state 2 represents the mobile nodes next position (x or y) if the mobile node continues to move in the same direction. This implementation produces probabilistic motion rather than pure random motion, which may represent a more realistic behaviour.

5.3.5 Reference Point Group Mobility model

The Reference Point Group Mobility (RPGM) has been proposed in [178]; this model provides that nodes are divided into groups each with a group leader. In the standard RPGM model, the leader is based on the Random Waypoint model and the group members follow the movement of the respective group leaders closely. In poor terms, RPGM represents the random motion of a group of mobile nodes and their random individual motion within the group. All group members follow a logical group center that determines the group motion behaviour. The entity mobility models should be specified to handle the movement of the individual mobile nodes within the group. Here, each group has a logical center (group leader) that determines the group's motion behaviour. Initially, each member of the group is uniformly distributed in the neighbourhood of the group leader. Subsequently, at each instant, every node has a speed and direction that is derived by randomly deviating from that of the group leader.

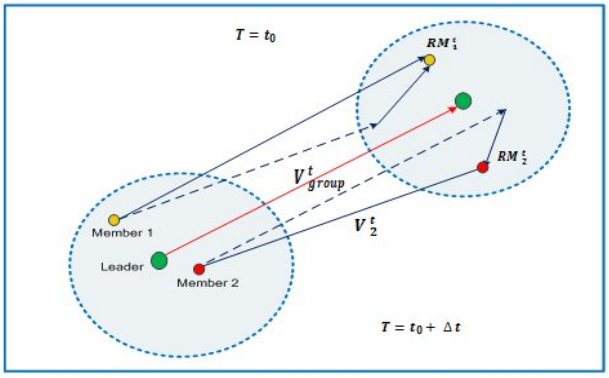

FIGURE 5.5: Reference Point Group Mobility model example

The Figure 5.5 illustrates an example of Reference Point Group Mobility model with the group leader represented in green and the members represented in red and

yellow respectively. V^t_{group} is the motion vector of the group leader and the whole group. Observe that is the each node is associated with a reference member through a random motion vector RM^t_i representing the deviation of the group member i from its reference member. The motion vector is free identically distributed random procedure whose duration is uniformly distributed in the interval $[0, r_{max}]$ with r_{max} representing the maximum acceptable distance whose path is uniformly distributed in the interval $[0; 2\pi]$.

5.3.6 Manhattan Grid mobility model

Manhattan Grid mobility model [179] has originally been developed to emulate the Manhattan street network, i.e. a city section which is only crossed by vertical and horizontal streets on an urban map. The Manhattan mobility model uses a grid road topology. This mobility model was mainly proposed for the movement in urban area, where the streets are in an organized manner. This mobility model can be described by the following parameters: mean speed, minimum speed (with a defined standard deviation for speed), a probability to change speed at position update, and a probability to turn at cross junctions.

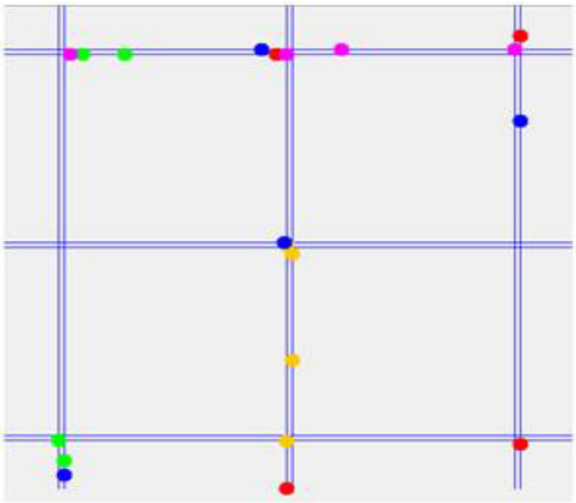

FIGURE 5.6: Manhattan Grid mobility model example

The Figure 5.6 illustrates an example scenario using Manhattan Grid mobility model. The mobile node is allowed to move along the grid of horizontal and vertical streets on the map. At an intersection of a horizontal and a vertical street, the mobile node can turn left, right or go straight. This choice is probabilistic: the probability of moving on the same street is 0.5, the probability of turning left is 0.25 and the probability of turning right is 0.25.

5.4 Mobility prediction in Ad Hoc Networks using directional antennas: related works

The current state of art related to mobility prediction models in directional antenna MANET contexts is a bit limited; indeed, actually, implementing a robust predictive algorithm for addressing mobility issue in directional MANET represents a severe task that is very difficult to encounter due to issues implied by directional antennas in this context. The large majority of these few works are related to classical directional antennas; unfortunately, with regard to complex antenna technology as SAS, literature is very lacking. The present section provides a brief overview for each of these works. In [180] authors propose a location and mobility aware (LMA) MAC scheme that considers the relative movement between the mobile nodes within the design of the directional-antenna-based MAC algorithm. The antenna beams of mobile nodes during data transmission are adjusted based on their predicted locations. Moreover, the deafness problem is improved by adapting a switching mechanism based on the information stored in the location table of each mobile node. Special Omni-Listen/Omni-RTS and Directional-Listen/Directional-RTS messages are used by mobile nodes to initiate a new data transmission. In addition, the usage of the directional-beacon (DB) mechanism within the proposed scheme facilitates mobile nodes to always obtain the correct position and mobility information after one node has changed its moving direction or velocity. In summary, LMA MAC protocol uses the RTS and the CTS control packets for exchanging location information among nodes. Location information are stored by each node in special Location Tables (LT).

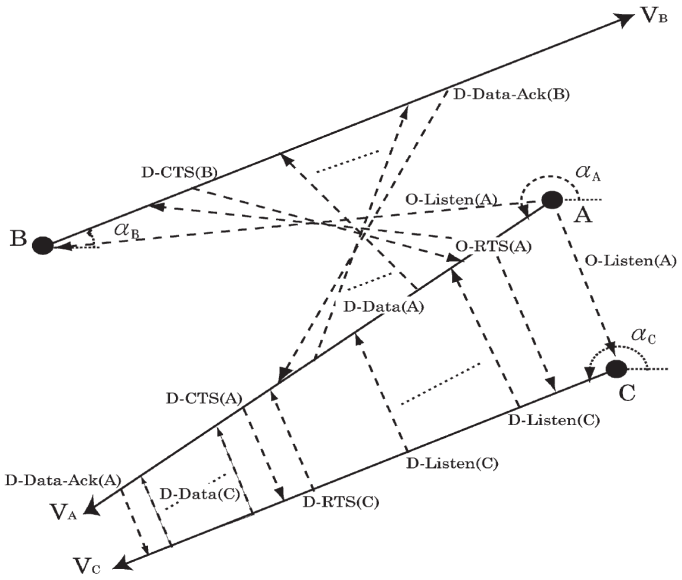

FIGURE 5.7: Timing diagram of LMA MAC

The Figure 5.7 illustrates the timing diagram of LMA MAC. The solid lines associated with nodes A, B, and C indicate the timelines and the moving directions of these three mobile nodes. In the case that node A intends to deliver data packets to

node B, it will conduct the default O-Listen(A) mode to its neighbor, since node A does not have any prior location information about node B in its LT_A. O-RTS packet relared to A contains location information of node A. The intended transmission of data packets from node A to B will be sent at time t_d after the O-RTS/D-CTS exchange. Finally, beams of A and B are adjusted based on fresh informations derived by the exchange of these special packets. In [181] a method for estimating the location of each node in the network using a pair of reference nodes and the AoA of best signal from each reference node are proposed. In this case, the location tracking of nodes is performed by using the ESPAR (Electronically Steerable Passive Array Radiator) antenna; mobile nodes accomplish directional location tracking periodically and wait in omnidirectional receive-mode while idle. To initiate location tracking, a node, broadcasts directional beacons sequentially, using its directional beam-pattern in the ESPAR Antenna. In addition each node records its neighborhood information in a table known as Neighborhood Link State Table (NLST). After the formation of NLST, a node calculates the beam pattern of the sending node from which it has received strongest signal and the corresponding value of the received signal strength; this node is tagged as reference node; finally it sends this information to its neighbors; direction informations are recorded in Angle Signal Table (AST). In work [182] authors attempt to reduce the handoff issue through an efficient beam system control; The system employs an antenna controller in communication with a beamforming network that generates two independently lobes from a single beam. The single beam is radiated by a phased array antenna on the mobile platform. In particular, a Base Transceiver Station (BTS) look-up position table is utilized to provide the locations of a plurality of BTS sites. However, the work is designed for Wireless cellular networks and does not provide for a mobility prediction model. In paper [183], authors try to mitigate the handoff problem by proposing a predictive location model algorithm named TRAC (Triangle and Circle) in order to advance the future position movements of the nodes.

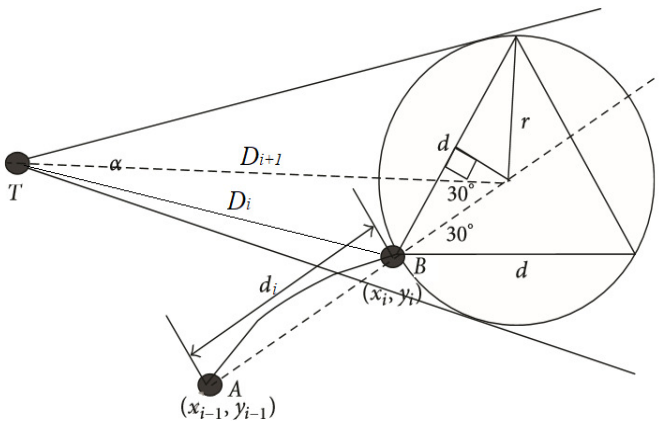

FIGURE 5.8: TRAC operational principle.

Figure 5.8 synthesizes the operational principle of TRAC. Basically, each node stores in a history cache its current position together with the location of the previous

position occupied. The algorithm provides for the estimation of the next position in which a node will move based on history cache info. Let us consider a certain transmitter node T that is sending data towards a receiver node R, with R that moves according to a mobility pattern (in this case it has been used the Mass mobility model provided by Omnet++ simulator [17]). The current position of the node R is denoted by B and its location is represented by the coordinates (x_i, y_i) while the previous location of R is denoted by A and has coordinates (x_{i-1}, y_{i-1}); the distance between the transmitter and the i-esimum position of the receiver is denoted by D_i while d_i is the distance between A and B. TRAC algorithm estimates the next position of node R based on these location informations; in particular, the next position is approximately within a circle that contains an equilateral triangle having one of its vertex coinciding with the position B. This search area is estimated by using the following steps:

1. calculate the slope of $\overrightarrow{AB}$ denoted by k:

$$k = \frac{y_i - y_{i-1}}{x_i - x_{i-1}}, \quad x_i \neq x_{i-1} \tag{5.1}$$

2. make an equilateral triangle whose one vertex is at B position centered at coordinates (x_{i+1}, y_{i+1}) and side length d expressed by:

$$\begin{cases} x_{i+1} = x_i + \frac{\sqrt{3}d}{3} \frac{x_i - x_{i-1}}{|x_i - x_{i-1}|} cos(arctan(\mid k \mid) \\ \\ y_{i+1} = y_i + \frac{\sqrt{3}d}{6} \frac{y_i - y_{i-1}}{|y_i - y_{i-1}|} cos(arctan(\mid k \mid) \end{cases} \tag{5.2}$$

$$d = \sqrt{(x_i - x_{i-1})^2 + (y_i - y_{i-1})^2} \tag{5.3}$$

3. draw a circle that contains the equilateral triangle with radius:

$$r = \frac{\sqrt{3}d}{3} \tag{5.4}$$

4. calculate the needed sector angle as:

$$\alpha = 2 * arcsin\left(\frac{r}{D_{i+1}}\right) \tag{5.5}$$

Where D_{i+1} is the approximate distance from the transmitter T to the new position of the receiver node R.

5.5 The Enhanced RR-MAC approach

The Round-Robin MAC approach presented in section 4.3 is perfectly suitable for limiting the deafness problem in beamforming networks, but does not consider the

effects introduced by the mobility of nodes. This approach can be enhanced in order to adapt it also for medium-high mobility environments. The Enhanced RR-MAC [184] attempts to limit handoff problem through the use of mobility prediction model that has been denoted as Enhanced-TRAC (ETRAC) (because improves TRAC algorithm) and a in-frame priority scheduling mechanism.

5.5.1 Enhanced TRAC algorithm

Although TRAC algorithm results very functional for adaptive beamforming systems it presents some aspects that need to be investigated in the analysis of directional communications concerning dynamic environments such as MANET. Primarily, the TRAC algorithm does not consider the effects of the mobility speed of nodes that could affect the estimation of the next position of the node R; furthermore, it does not find any radio propagation channel model which could offer meaningful indications for improving the predictive position estimation. For this reason, the TRAC algorithm has been enhanced by attempting to address these issues.

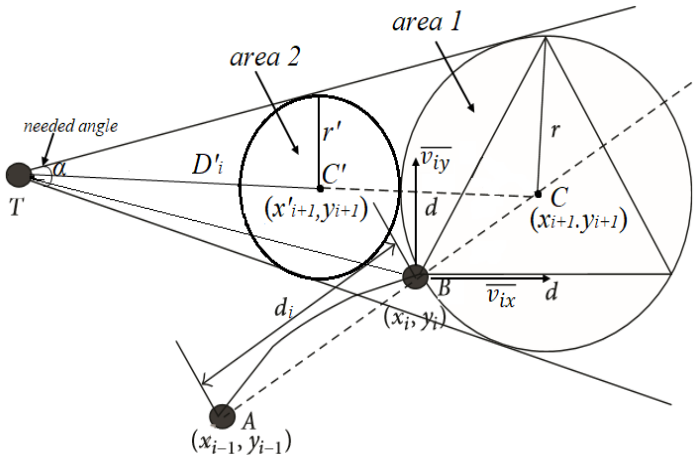

FIGURE 5.9: Enhanced TRAC principle.

Figure 5.9 illustrates the Enhanced TRAC principle. The new model now considers the mobility speed vector related to the current position $\overline{v}$ that consists of two vectorial components along x and y axes which could be expressed as:

$$\begin{cases} \overline{v_{ix}} = \frac{x_i - x_{i-1}}{\Delta t} \\ \overline{v_{iy}} = \frac{y_i - y_{i-1}}{\Delta t} \end{cases} \tag{5.6}$$

Where Δt is the period time between two consecutive movements of the node R. Considering the dependence on the mobility speed vector, Expressions (5.2) assume

the following form:

$$\begin{cases} x_{i+1} = x_i + \frac{\sqrt{3}d}{3} \frac{\overline{v_{ix}}\Delta t}{|x_i - x_{i-1}|} cos(arctan(\mid k \mid) \\ \\ y_{i+1} = y_i + \frac{\sqrt{3}d}{6} \frac{\overline{v_{iy}}\Delta t}{|y_i - y_{i-1}|} cos(arctan(\mid k \mid) \end{cases} \tag{5.7}$$

As it can be noted, the coordinates of the next position of the node are now function of the mobility speed. In order to improve the accuracy in the position estimation we can consider the Friis radio propagation model:

$$P_{RX} = P_{TX} \left(\frac{\lambda}{4\pi d L} \right)^2 \tag{5.8}$$

Where P_{RX} is the power related to the receiver, P_{TX} is the transmitted power, λ is wavelength, d is the distance between the transmitter and the receiver while L denotes the losses in the channel. Based on this equation we can evaluate the approximate distance between the transmitter node T and the receiver R in the new position. More specifically, let us assume to check the received power at node R every time that it changes its current position; considering the Equation 5.8, the distance between the transmitter node T and the receiver R depends on the received power; In particular, the search area of the new position of node R depends on the received power evaluated in its new position. In Figure 5.9 it is possible to distinguish two main search areas: the first one named *area 1* having center at position C and another one named *area 2* centered at position C' having radius $r' = \sqrt{3}d/6$ and coordinate component along x axis that can be expressed as:

$$x'_{i+1} = (x_i - d) + \frac{\sqrt{3}d}{3} \frac{\overline{v_{ix}}\Delta t}{\mid x_i - x_{i-1} \mid} cos(arctan \mid k \mid) \tag{5.9}$$

The distance between the two centers C and C' is approximatively d. The new position of node R depends on the received power measured at this position. Let P be the new position of the node R and $P_{RX}(P)$ the received power of the node R in the position P, it is possible to locate the approximate search area of the position P as follows:

$$\begin{cases} P_{RX}(P) \leq P_{RX}(B) + \Delta(L) \quad P \in area1 \\ \\ P_{RX}(P) > P_{RX}(B) + \Delta(L) \quad P \in area2 \end{cases} \tag{5.10}$$

Where $P_{RX}(B)$ is the received power of the node R at the position B while $\Delta(L)$ is a term that is function of the losses in the channel. Because of the use of the Friis model it is important to notice that the expression 10 is theoretically suitable for Line of Sight (LoS) scenarios having $\Delta(L) = 0$. Therefore, the real environments are typically referred to non-LoS situations, therefore the accuracy of the nodes position estimation is certainly related to the number of losses in the scenario. In order to

overcome this kind of issue, for directional communications it is possible to estimate the attenuation in function of the main beam orientation. For this purpose, it has been created the *attenuation database* in which the position and direction infos related to an incoming communication are cached and periodically updated; these informations are used to improve the accuracy of the estimation. From different samples of simulations, it has been derived that the interval of values that maximizes the accuracy of the estimation is reached for $0.12P_{RX}(B) \leq \Delta(L) \leq 0.16P_{RX}(B)$. By these expedients, the estimation of the new position of the node R can result more accurate with respect to the original TRAC formulation.

5.5.2 Enhanced RR algorithm based on mobility-aware priority

Once designed the predictive location model, it has been used it in order to improve Round-Robin MAC algorithm, providing a mechanism for mobility network management. From work [156] it can be noted that the performances of the system in terms of fairness are very related to the sector width value.

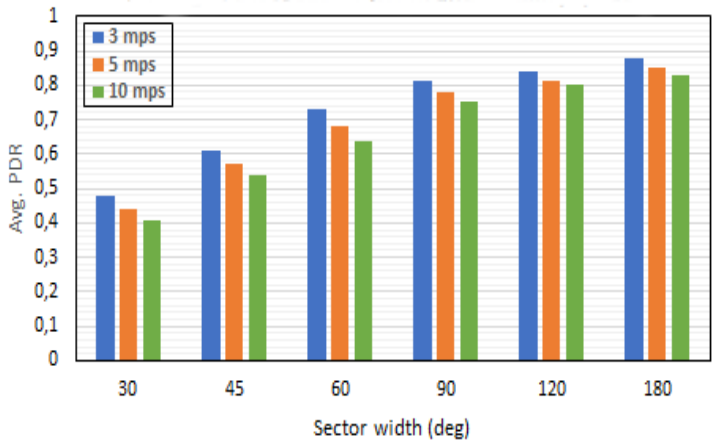

FIGURE 5.10: Average PDR vs mobility speed RR-MAC.

In Figure 5.10 it can be highlighted that, as the sector width decreases, the average Packet Delivery Ratio also decreases. In particular, the RR algorithm provides for a good PDR value in slow mobility speed conditions but as the speed increases it tends to dramatically decreases for sector width values less than 60°. In view of this, a mechanism that extends the Round-Robin algorithm has been designed in order to minimize this situation. The next figure illustrates the Enhanced Round-Robin principle:

Figure 5.11 shows an example in which the sector x is the current active sector and each sector presents a sector width value $\beta = 30°$. Let us assume that the node T is transmitting towards the node R and that node R moves in the network changing its sector. It will move in the sector *x-1* or in the sector *x+1* with same probability. The next position in which the node R will move is estimated by the Enhanced TRAC

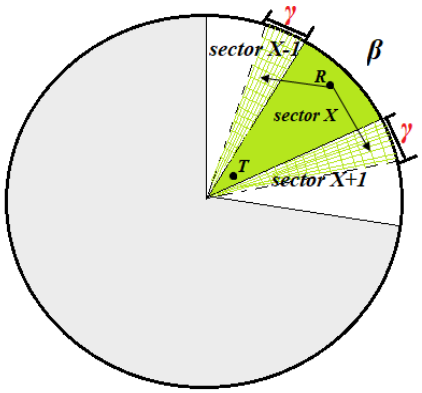

FIGURE 5.11: Enhanced Round-Robin algorithm principle.

algorithm that also estimates the needed angle α; the Enhanced RR algorithm provides for a temporary enlargement of the current sector beam if the node T senses a variation of the received power of R during the communication, that could be interpreted as a change of position of node R. This enlargement is produced for a time T_{en} that is a fraction of the sector time T_s; in particular, based on results obtained after a set of simulations, it has been considered $T_{en} = 0.25T_s$; the enlargement angle γ is evaluated as:

$$\gamma = \begin{cases} \left| \frac{\alpha-\beta}{2} \right| & \alpha > \beta \\ \\ \beta & \alpha \leq \beta \end{cases} \tag{5.11}$$

From Eq. 5.11 it can be seen that, the enlargement angle depends on the needed angle α that is evaluated by the Enhanced TRAC algorithm; if this value is less or equal to the sector width β , no enlargement is provided. The Enhanced Round-Robin algorithm also addresses the handoff problem. In order to face up to this issue it has been provided a priority scheduling that assigns a certain priority level to each kind of communication. These levels vary from 1 to 3, where 1 represents the highest priority level. More specifically, the priority values are assigned as follows:

- ***priority level 1***: communications not completed in which either the transmitter or either the receiver move in a sector adjacent to the current active sector.
- ***priority level 2***: communications of the sector queues.
- ***priority level 3***: communications in the current active sector.

The highest priority is assigned to communications related to nodes that move in a neighbor sector. In this case the communication continues, after a re-pointing process of the beams, until it does not completely finish; note that the change of sector of a node does not affect the continuity of the communication; in this way the fail induced by handoff is avoided. If there are no nodes in the current active sector that change their sector during a communication, the scheduler selects the communications that are in the sector queue. Once the sector queue is empty, the

scheduler selects the communication of the current active sector that are not in the sector queue (lowest priority level).

5.5.3 RR-MAC vs Mobility Speed Simulation Results

The first set of simulations is accomplished executing the original RR-MAC protocol proposed in [156] without using any predictive model for estimating the future position of nodes. The system performances are analysed in terms of PDR, number of collisions at MAC layer and DRTS/DCTS (Directional Request to Send Directional Clear to Send) ratio; this last parameter was defined in chapter 4 and it could result very useful for the estimation of the fairness of the system. These results are examined by increasing the average nodes mobility speed from 3 *mps* (meter per seconds) to 10 *mps* and the sector time (st) from 1 to 4 seconds. The following table summarizes the main parameters set used in our simulations:

TABLE 5.1: Simulation parameters set.

Antenna Model	SAS phasedArray
Array Elements Spacing	0.5 λ
Number of Nodes	10, 30, 50
Transmission Rate	54 *Mbps*
Message Length	512 *Byte*
Simulation Area Size	500 x 500 *m*
Simulation Time	300 *s*
Mobility model	Mass Mobility
Node mobility speed values	3,5,10 *mps*
Sector Time values	1,2,3,4 *s*

It has been assumed that nodes are uniformly distributed in the network; obtained values are evaluated by estimating confidence intervals by varying the simulation seed from 1 to 20. Therefore, for reason of spaces the next figures illustrate the results related to the configuration case having number of nodes set to 30.

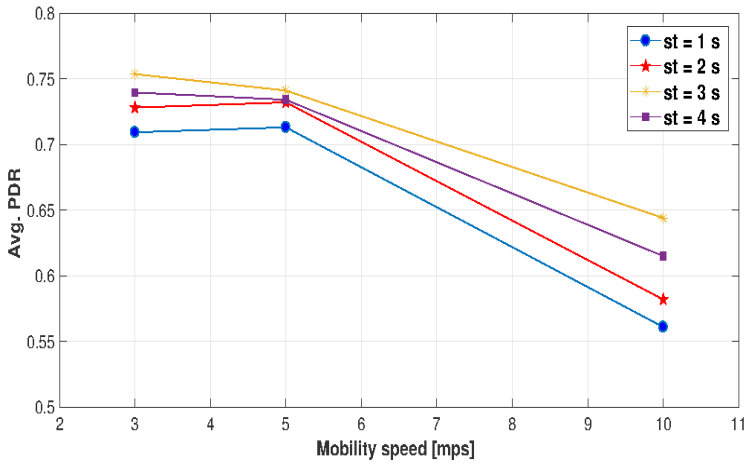

FIGURE 5.12: Average PDR vs Mobility speed.

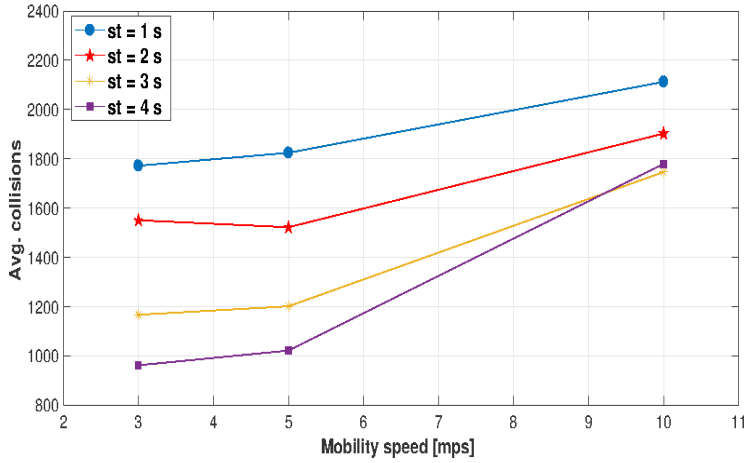

FIGURE 5.13: Average Num. of Collisions vs Mobility speed.

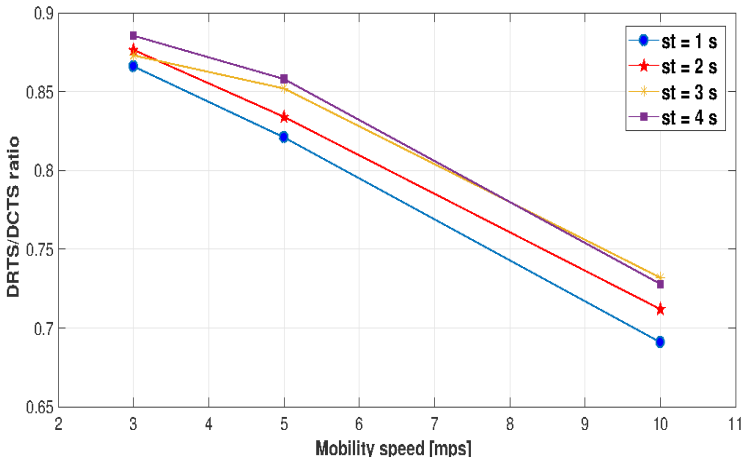

FIGURE 5.14: DRTS/DCTS ratio vs Mobility speed.

Fig. 5.12 displays the statistic plot related to average PDR; the figure shows a slightly improvement of the PDR as the sector time increases; however this trend is not linear and suffers from a decrease for sector values higher than 4 *s*. From Fig. 5.12 it also can be noted that the PDR tends to reduce significantly as the mobility speed of nodes increases. This trend is confirmed from Fig. 5.13 in which it can be observed an increment of the number of collisions of 54% in the worst sector time case with respect the best case (st = 3 *s*). In Fig. 5.14 it can be observed how the fairness of the system in terms of DRTS/DCTS ratio is quite good as long as the mobility speed is low; however this value decreases at an exponential rate for high speed values; in particular, in the mobility speed case related to 10 *mps* it is registered a reduction of the DRTS/DCTS ratio of about 24% with respect to the lowest mobility speed considered case. In summary, the overall reduction of the system performance is probably due to the fact that, in this case, the system does not support any mechanism that handles the mobility of the nodes; in order to confirm this hypothesis the following table shows the average failed communications due to handoff in the network (in terms of percentage) obtained from simulations.

TABLE 5.2: Failed communications due to handoff

Failed handoff communications		
3 mps	***5 mps***	***10 mps***
11,42 %	18,01 %	34,6 %

We considered as handoff communication a transmission/reception that presents at least a change of sector (by a transmitter or a receiver node). From Table II it can be deduced how the lack of a mobility management mechanism heavily influences the performance of the system; in particular, in the case of 10 *mps* about one-third of the communications fail.

5.5.4 Enhanced RR-MAC vs Mobility Speed Simulation Results

As last analysis the modifications introduced to the original TRAC and Round Robin (RR) algorithms have been enabled. In this case, the scheduler uses either the designed predictive model (ETRAC) and either the priority mechanism provided by the Enhanced RR algorithm. The next figures illustrate the statistics related to PDR, number of collisions and DRTS/DCTS ratio.

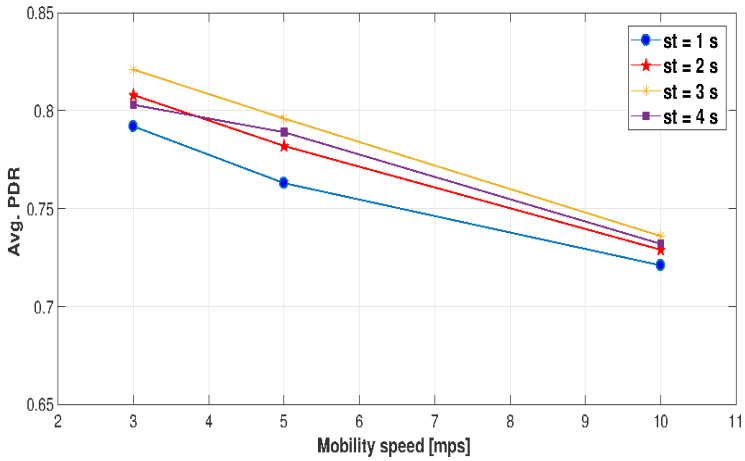

FIGURE 5.15: Average PDR vs Mobility speed Enh. RR-MAC.

From Fig. 5.15 we observe that, the minimum value of PDR registered in the worst case is 0.721 against the 0.561 obtained in the original RR case. In Fig. 5.16 it may be experienced a little improvement of the average number of collisions for all of the considered cases; this behaviour is probably due to the beam enlargement involved by the Enhanced Round Robin algorithm which slightly extends the set of directions usually related to a certain sector; however, this improvement is about 2.5% with respect to the original RR-MAC and it results quite negligible. The Fig. 5.17 highlights that, in high mobility conditions (10 *mps*) it can be obtained a minimum DRTS/DCTS ratio of 0.774 against the 0.691 registered in the RR-MAC case; in particular, the average value by varying the mobility speed is about 0.826, that

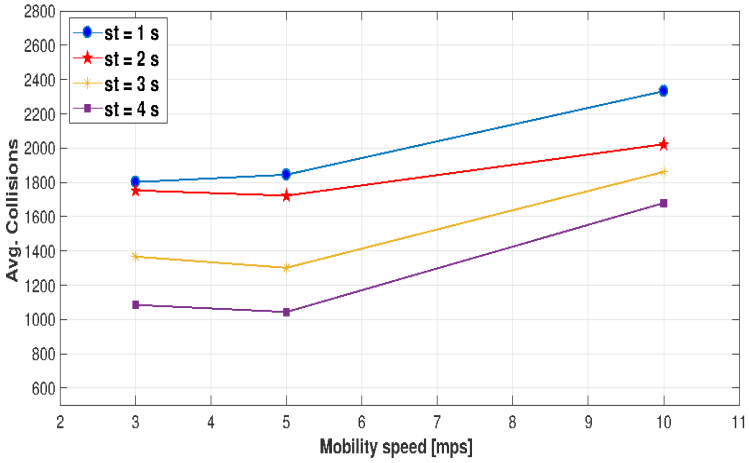

FIGURE 5.16: Average Num. of Collisions vs Mobility speed Enh. RR-MAC.

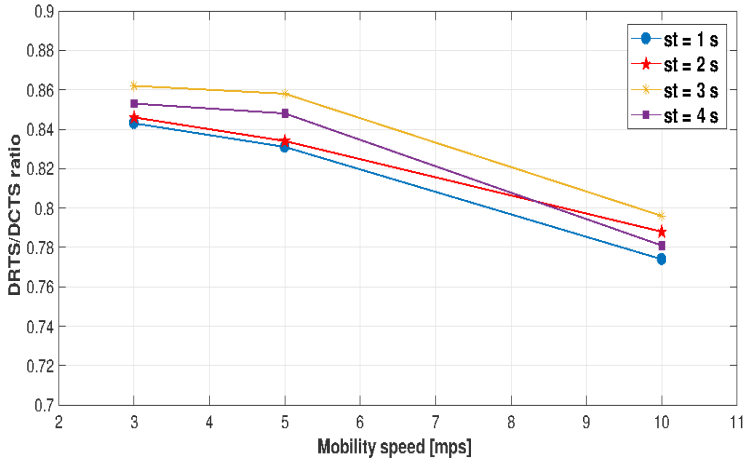

FIGURE 5.17: DRTS/DCTS ratio vs Mobility speed Enh. RR-MAC.

improves considerably the value of 0.731 obtained in the RR case. This growth is certainly justified because of the priority mechanism provided by the scheduler that contributes to reduce the number of communications failed for handoff.

5.6 Energy consumption in MANET using directional antennas

Energy efficiency represents a critical challenge in all layers of communication protocols, as well as on a wide range of technological applications in wireless network environments [185]–[187]. Nowadays, energy efficiency draws a significant attention among the researchers due to the introduction of battery operated devices. Energy efficiency is one of the most crucial design criteria for MANET, as nodes are battery operated. If a node runs out of battery, its ability to route traffic gets affected. This adversely affects the network lifetime as well as degrades the performance. Network lifetime can be improved by minimizing the power consumption and/or

maximizing the battery power of a node. Although a considerable progress has been accomplished in the battery technology front in latest years, yet, it is incomparable with the progress made in semiconductor technology. Battery life has not kept pace with advances in mobile devices. To enhance the lifetime of mobile devices, it necessitates the requirement of power conservation techniques to enhance the network lifetime [188]. Such techniques can be applied at different layers of protocol stack. In recent years, various techniques have been proposed to achieve energy efficiency at protocol level. These techniques adopt different approach to achieve energy efficiency. A few of them are: energy-efficient path selection, adjusting transmission power dynamically, reducing maximum transmission power at node level, adaptive sleeping. In the chapter 1 it has been remarked how the use of directional antennas represents an advantage with respect the use of classical omnidirectional systems in the sense that they are able to focus in a particular direction the energy flow occurring in a communication exchange between nodes. This affirmation shall be considered as true, when classical directional antenna systems are employed. However, when more complex antenna systems such as SAS and Massive MIMO are used, this aspect that originally has been tagged as an advantage could be turn in a severe drawback. Indeed, in this case, although only a particular area suffers from energy consumption and leakage, very high gains related to main beams contributes to provide a significant waste of energy that has to be added to other sources of waste. In this regard, the most common causes of waste of energy in directional MANET could be summarized as follows:

- **high gains**: it is the most significant cause of waste; in fact, the most recent antenna technologies having a large number of radiating elements supply directional beams using gains that are considerably higher with respect to classical directional antennas.
- **directional carrier sensing**: MAC protocols for wired networks such as CSMA/CD, ALOHA are not suitable for wireless networks due to the physical characteristics of wireless medium. Carrier sensing is a challenging task in wireless network. A node expends a lot of energy in carrier sensing, which is also affected by deafness hidden terminal problems.
- **collisions**: Retransmission occurs due to collision, and this increases per packet energy consumption. Retransmission also affects other network parameters such as: end-to-end delay, jitter, throughput etc.
- **idle channel sensing**: an aspect neglected by a lot of studies is represented by the fact that, during protocols execution nodes that are not involved in communications which are in idle state attempt anyway to listen to the channel for sensing and consume an important amount of energy in passive mode.

- **overhearing**: When a node transmits a packet, it is overheard by the neighbors within its transmission range. Thus, a node expend its energy by receiving a packet even though it is not destined to the node.
- **packet size**: using larger packet size, consumes more power as compared to smaller packet size. Larger packet size also increases the probability of retransmission due to collision.
- **dynamic topology**: Due to node mobility, frequent path break may take place. This necessitates route discovery and route maintenance, which consumes energy.

The current state of art attempts to face the energy consumption problem by addressing one or more of the mentioned causes. In the next section the most related works in this field are discussed.

5.7 Energy consumption in directional MANET related works

Besides to consider the most common causes of waste of energy discussed in the previous section, existing related works in this field focus on energy consumption implied by hardware resources. Data processing implies the large usage of Central Processing Unit (CPU), memory, hard drive, etc. To partially solve this issue, regarding energy consumption, the most actual solution is to find a compromise between data processing and radio communication [189]. In this regard, in work authors present a data compression mechanism in order minimize packet length [190] with the purpose to limit energy consumption in radio communication. In work [191] authors also highlight the large protocol overhead introduced by this kind of systems. The rest of the works are categorized based on the type of antennas used by mobile nodes.

5.7.1 Related works using directional antennas

The most common addressed problem when basic directional antennas are used is related to directional carrier sensing. For example, in [192] authors present energy efficiency approach for improving performance of directional MAC protocols in unicast packet transmission when different RTS/CTS exchange schemes are employed to perform virtual carrier sensing. To compare the energy consumption of different RTS/CTS exchange schemes an energy dissipation model is designed. In paper [193], an energy-efficient clustering routing algorithm based on directional antennas (EECDA) is proposed based on existing cluster algorithm. The key idea is that in wireless environments sending data with directional antennas can reduce the interference among wireless signals. From the energy point of view, replacing the low-gain omni-directional antennas with the high-gain directional antennas to send data make routing algorithms more effective energy-efficient. In [194] an energy-efficient

algorithm for routing and scheduling in ad hoc network with nodes using directional antennas is proposed; the designed algorithm is able to coordinate transmissions in ad hoc networks where each node has a single directional antenna. Using the topology consisting of all the possible links in the network, firstly, the finding of shortest cost paths is optimized in terms of energy consumption. In addition, a scheduling mechanism is used for transmissions of nodes, attempting to minimize the total communication time.

5.7.2 Related works using SAS

In [195] authors present a mechanism aimed to improve antennas BTS performance using SAS. The goal of the work is to present a solution based on smart antenna, by optimizing the radiation pattern of the base station and making it more directive. This can help to minimize the radiated energy and therefore will allow the operator to decrease its transmission power while covering the entire sector. In paper [196] aurhors attempt to overcome the problem of unnecessary transmitted power wastage with omnidirectional antenna system in ad-hoc wireless networks by using Smart Antenna Systems (SAS). Through different simulations, transmitted power variations with different number in different conditions are evaluated. The work [197] presents an energy efficiency (EE) investigation of a beam generated by the combination of Recursive Least Square (RLS) algorithm and Kaiser side lobe cancellation technique in smart antenna system. The RLS-Kaiser combination is investigated using energy model which is a function of beam width, range and signal to noise plus interference ratio (SNIR). The approach proposed in [182] provides for a *BeamSwitch*, for directional communication on mobile devices. BeamSwitch employs a special multi-antenna system that consists of multiple identical directional antennas or beams, a single regular omnidirectional antenna, and a single RF chain. BeamSwitch addresses two key technical challenges toward improving energy efficiency. Firstly, hardware realization of directional communication, including phased-array antenna systems and sectorization; secondly, BeamSwitch addresses the problem of the frequent changing of relative direction of nodes with respect to the access point; this issue is addressed leveraging the acknowledgement mechanism and the channel reciprocity to assess the quality of a beam based on the received signal strength of ACK frames from the access point. It determines the efficacy of a beam by comparing the RSSI of received ACK with a history record.

The Figure 5.18 illustrates the key components of BeamSwitch and how they interact with the network protocol stack in the wireless network interface card (WNIC).

5.7.3 Related works using Massive MIMO systems

In literature exist very few proposals attempting to attenuate the energy consumption issue related to large scale antenna systems in massive MIMO 5G environments. For example, in work [198] authors focus of the consumption of Base Stations (BS)

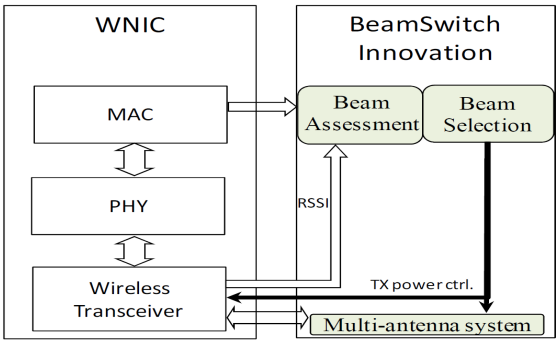

FIGURE 5.18: BeamSwitch operation principle.

that is reduced through a multilevel beamforming approach; in this approach, the received signal is amplified by the high gain of the beams, specially the beams of the highest levels; The focused beams create very low interference on neighboring cells, resulting in much higher Spectral Efficiency (SE) and Energy Efficiency (EE). The proposed approach also benefits from low complexity and hence potentially low cost. In the same way the model proposed in [199], aims to minimize the waste of energy caused by amplifiers related to BS through a clustering algorithm that allow for high throughput. Finally, in paper [200], an Energy Efficiency maximization scheme is presented with reference to power budget problem.

5.8 The Adaptive Beamforming Time RR-MAC approach

The Adaptive Beamforming Time RR-MAC (ABT-RRMAC) approach presented in [201] modifies the original Round Robin MAC algorithm formulation regarding the evaluation of the sector time without affecting the plane sectorization and thus the width of the sectors. Basically, the idea is to assign a portion of time for each sector that is proportional to the size of the queues, that in this case is not fixed for each sector and can vary dynamically. The main purpose of the work is to limit the excessive energy consumption in the network derived by the queue and the time slice problems involved by the use of the Round-Robin.

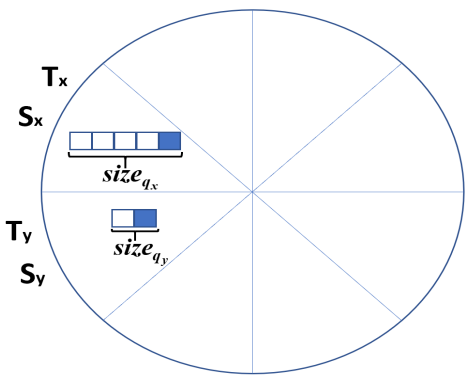

FIGURE 5.19: Adaptive Beamforming Time RR-MAC example.

In Figure 5.19, an example of the Adaptive Beamforming Time RR-MAC (ABT-RRMAC) application is shown. The plane is normally sectorized into equals amplitude sectors as well as the Round Robin MAC. However, in this case, the considered traffic pattern is not uniformly distributed among nodes; in Figure 8, it is assumed that, two particular sectors denoted S_x and S_y respectively have different size of the frame waiting queues; in this regard, the term $size_{q_i}$ denotes the size of the waiting queue related to the *i-th* sector. While considering the situation in Figure 8, assuming that T_X and T_Y are the beamforming (sector) times related to the sector x and y respectively, the ABT-RRMAC assigns the beamforming times as follows:

$$\begin{cases} T_1 = \frac{size_{q_i}}{\sum_{i=1}^{N} size_{q_i}} \times \overline{T} \neq T_s \\ \quad \dots \\ \quad \dots \\ T_N = \frac{size_{q_N}}{\sum_{i=1}^{N} size_{q_i}} \times \overline{T} \end{cases} \Rightarrow T_1 \neq T_2 \neq .. \neq T_N \iff size_{q_1} \neq size_{q_2} \neq .. \neq size_{q_N}$$

Where:

$$\overline{T} = \sum_{i=1}^{N} \frac{T_i}{N} \tag{5.12}$$

The term $\overline{T}$ denotes the mean beamforming time averaged by all sectors. Initially, the beamforming times are the same for all sectors and set to T_s (RR-MAC); after a training phase set to 10 s, the mean beamforming time and then sector times are updated periodically in order that for each sector is assigned a quantum of time that is proportional to the size of the queue of that sector multiplied by the mean beamforming time. In this way, sector times can be different and unbalanced among them and the major fraction of time is assigned to the sector having the biggest queue size. For instance, if we consider the example of Figure 5.19, because $size_{q_x} > size_{q_y}$ then the ABT-RRMAC will assign sector times such that $T_X > T_Y$. The motivation of this choice is due to fact that $size_{q_x} > size_{q_y}$ the serving queue rate of S_X is lower than the serving queue rate of S_Y; consequently, S_X needs for a beamforming time higher than S_Y in order to empty its queue. This set will optimizes the network energy consumption due that the waste of energy caused by Round-Robin is limited by the dynamic beamforming time assignment.

5.8.1 ABT-RRMAC implementation

The ABT-RRMAC algorithm is implemented in the Omnet++ Network Simulator in the *DcfUpperMAC* module, that is the main class in which the most important operations at MAC layer are provided, such as frame and collisions management; therefore, as explained in [14] the sectorization of the plane is managed by the SAS antenna module (*PhasedArray* module). The following pseudo-code enhances the original Round-Robin MAC formulation:

Algorithm 10 ABT-RRMAC pseudo-code

```
1: procedure INIT(numSectors)
2:     numQueues ← numSectors
3:     CREATEQUEUES(numQueues)
4: end procedure
1: procedure ASSIGNSECTORTIME(trainingPeriod, updatePeriod, numQueues)
2:     if Sim.Time () < trainingPeriod || Sim.Time()< updatePeriod then
3:         averageSectorsTime = 0;
4:         for i=1; i< numQueues; i++ do
5:             sectorTime[i] = T_s;
6:         end for
7:     else
8:         averageSectorsTime = computeAverageSectorsTime()
9:         for i=1; i< numQueues; i++ do
10:            sectorTime[i] = (size_{q_i} / Σ_{i=1}^{N} size_{q_i}) × averageSectorsTime;
11:        end for
12:    end if
13: end procedure
1: procedure STARTTRANSMIT(frame)
2:     int frameSector=getFrameSector(frame);
3:     int currentActiveSector=getCurrentActiveSector();
4:     if currentActiveSector != frameSector then
5:         queueSector[frameSector].insert(frame)//queuetheframe
6:     else
7:         transmissionQueue.insert(frame);
8:         transmitFrame ← queueSector[activeSector].front()
9:         queueSector[activeSector].pop()
10:        CONFIGUREANTENNA(activeSector)
11:    end if
12: end procedure
1: procedure STARTRECEPTIONSTATE
2:     CONFIGUREANTENNA(omnidirectional)
3:     MAC in reception Mode
4:     SCHEDULEEVENT(CSMATimer)
5: end procedure
1: procedure RECEPTIONFRAME(frame)
2:     orientation ← GETORIENTATION(frame)
3:     sector ← GETSECTOR(orientation)
4:     CONFIGUREANTENNA(sector)
5: end procedure
1: procedure RECEIVEFRAMEFROMUPPERLAYERS(frame)
2:     sector ← GETSECTORFRAME(frame)
3:     queueSector[sector].push_back(frame)
4: end procedure
1: procedure MACPROCCESS
2:     INIT(NumSectors)
3:     STARTRECEPTIONSTATE
4:     loop
5:         WaitEvent
6:         if Event Is Upper Frame then
7:             RECEIVEFRAMEFROMUPPERLAYERS(frame)
8:         else if Event Is Lower Frame then
9:             RECEPTIONFRAME(frame)
10:        else if End Transmission then
11:            STARTRECEPTIONSTATE
12:        else if EndCSMA ∧ QueueSector ≠ empty then
13:            STARTTRANSMIT(frame)
14:        else
15:            STARTRECEPTIONSTATE
16:        end if
17:    end loop
18: end procedure
```

At the beginning of the process, after the plane is sectorized into equal width sectors, the same quantum of time is assigned for all sectors (Round-Robin). If the *trainingPeriod* has elapsed the *averageSectorsTime* denoting the mean beamforming time averaged by all sectors, can be computed; remember that this parameter is updated periodically after an *updatePeriod* (that has been set to 10 s) has passed; from the first time that the *averageSectorsTime* is computed, the beamforming times of the sectors are assigned according to expressions defined in section 4.2. The whole of these operations are included in *AssignSectorTime* function. The transmission of frames is ruled by *StartTransmit* function in which the system checks if the sector for which is destined the current frame is the *current active sector*. If true, it inserts the frame in the transmission queue and transmit the frame, otherwise the frame is queued in its waiting sector queue, and delayed until its sector does not become the current active sector. The reception of the frame is performed by *ReceptionFrame* and*ReceiveFromUpperLayers* functions in which, the receiver antenna is configured in omnidirectional mode and the information about the orientation of the transmitter antenna is retrieved in order to achive the synchronization during communication process. Other coordination functions are performed by *MacProcess* procedure. The complexity of the algorithm can be evaluated by considering the *assignSectorTime* procedure due that it includes the most of the overall operations; the complexity of ABT-RRMAC increases linearly with the number of sectors and not with the number of nodes. This is one of the benefits implied by the sectorized approach.

5.8.2 Performance evaluation

In order to evaluate the contribution of the ABT-RRMAC it is possible perform simulations by considering three different configurations of antennas in the nodes: omnidirectional with Round-Robin scheduling, SAS with Round-Robin (RR-MAC), and our proposed ABT-RRMAC that uses SAS adaptive array antennas; Simulations are accomplished by varying the number of sectors and then, node mobility speed. The following table summarizes the main simulation parameters:

TABLE 5.3: Main simulation parameter set.

Parameter	Value
Transmission Rate	54 *Mbps*
Message Length	512 *Byte*
Mobility model	Random Waypoint
Node Mobility speed	from 1 to 10 mps *mps*
Network Load	50 %
Simulation Area Size	500 x 500 *m*
Simulation Time	300 *s*
Number of Sectors	3,4,6,8
Initial battery capacity	300 J

Simulations have been accomplished by using 20 different seeds and extracting the confidence intervals obtained by the repetitions considering a confidence level set to 95 %. The traffic is represented by UDP data packets randomly generated (based on the simulation seed) by different couples of nodes. The number of nodes is set to 50 and couples of nodes involved in the data traffic exchange is one half with respect to the total number of nodes in the network. In addition, the channel is moderately affected from noise (-80 dBm), with SAS that have the main beam towards 45°. For the first set of simulations an unbalanced distribution of data (worst conditions) traffic has been considered by concentrating the main fraction of communications in the first sector of the plane; therefore, nodes move very slowly (2 mps) in the network and the size of the queues is set to 5. The first evaluated statistic is the energy consumption of nodes by varying the number of sectors.

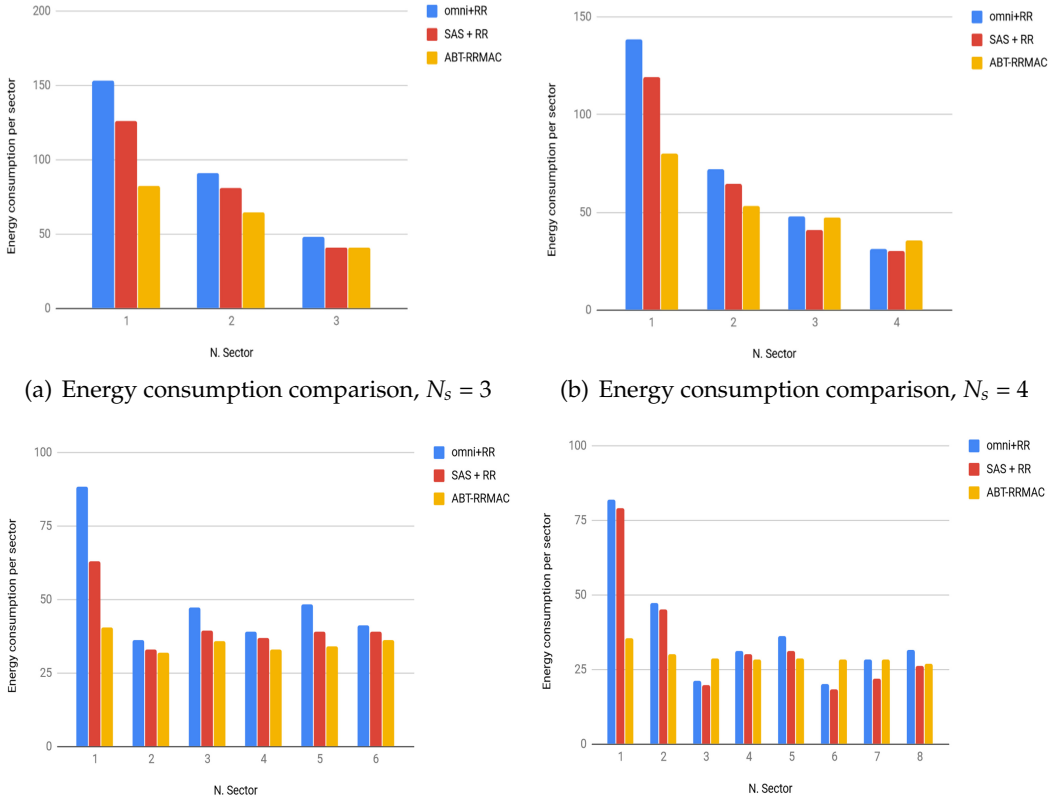

(a) Energy consumption comparison, $N_s = 3$

(b) Energy consumption comparison, $N_s = 4$

(c) Energy consumption comparison, $N_s = 6$

(d) Energy consumption comparison, $N_s = 8$

FIGURE 5.20: Energy consumption per sectors vs number of sectors

The plots in Figure 5.20 illustrate the energy consumption of nodes (expressed in Joule) in function of the number of sectors (observe that the term "*N. Sector*" used in plots of Figure 5.20 is related to the progressive number id assigned to each sector and does not identify N_s). In Figure 5.20(a) it can be observed how the main fraction of consumption is related to the sector 1, that is the sector in which the traffic is mostly focused with respect to others. When omnidirectional antennas and the Round Robin scheduler are used the distribution of energy consumption among sectors is very unbalanced; this trend is mainly due to the static time slot assigned by

the scheduler, that, in this case is the same of all sectors; this feature results in a not efficient distribution of the energy in the sectors and consequently, the total energy consumption is considerable (almost 298 J). However, the same behavior is maintained in Figure 5.20(b) in which, when SAS module are used it can be highlighted a better distribution of the consumed energy among sectors. In Figure 5.20(c) it appears clear, how, as the number of sector increases the maximum amount of consumed energy is reduced, but in the case of omnidirectional antennas the imbalance remains unchanged; however the use of the SAS allows to decrease considerably the maximum energy amount that is further reduced when ABT-RRMAC approach is employed (44.54 against 88.27 registered in the omnidirectional case). Finally, the Figure 5.20(d) emphasizes even more the impact of the proposed approach flowing in a overall balancing of the energy consumption. In summary, the dynamic allocation of the beamforming time allows, independently from the number of sectors, to optimize the distribution of the energy also leading to a reduction of the overall consumed energy; indeed the registered values of total consumed energy in the RR-MAC case in function of the number of sectors are 248.33, 255.14, 250.91 and 272.32 *J* against values of 187.89, 216.26, 211.81 and 235.37 *J* registered when ABT-RRMAC is used. For a further investigation, it is possible to evaluate the standard deviation (averaging values by sectors) of the energy consumption by increasing the number of sectors for all of the configurations:

TABLE 5.4: Energy consumption: standard deviation vs number of sectors.

Number of sectors	omni + RR	SAS + RR	ABT-RRMAC
3	52.96	42.79	20.55
4	47.02	39.6	19.03
6	19.04	20.69	3.03
8	18.71	18.15	2.62

The Table 5.4 collects standard deviation values by varying number of sectors for all of the considered approaches; the use of SAS slightly enhances the omnidirectional case, however, observe how ABT-RRMAC contributes to dramatically decrease values when the number of sectors improves with respect to other considered configurations; this trend confirms that our proposed approach seeks to efficiently distribute the energy consumption among sectors as already noticed in plots of Figure 9. Therefore, energy consumption is very related to Packet Delivery Ratio and could represent an helpful indication of the overall network performance; for this purpose next figure illustrates PDR comparison extracted by *rcvdPkts* and *sentPkts* statistics collected by Omnet++:

In Figure 5.21, the average (averaged with respect to nodes) PDR is plotted both in function of the number of sectors and the queue size. The Figure 5.21(a) simply reflects the situation verified in Figure 5.20, in fact, the lowest is the energy

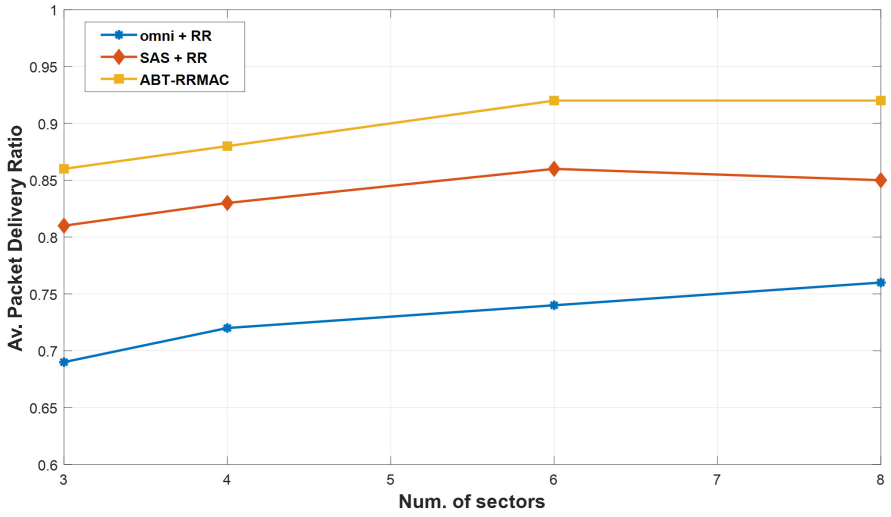

(a) Average PDR vs Num. of sectors

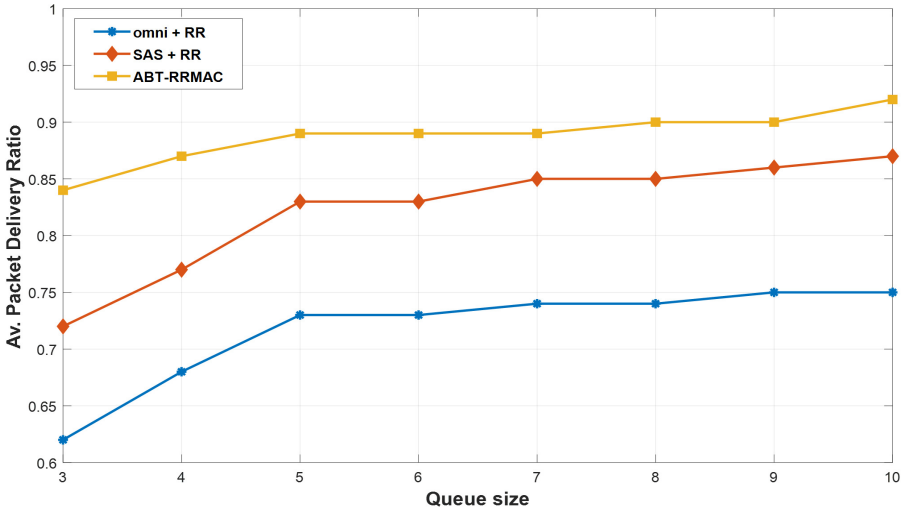

(b) Average PDR vs Queue size

FIGURE 5.21: Packet Delivery Ratio comparison.

consumption the highest is the PDR; therefore, when the number of sector is high, ABT-RRMAC is able to provide a PDR of about 0.92 against 0.85 registered in the RR-MAC configuration. The same statistic can be evaluated by increasing the size of the queues; in Figure 5.21(b) (values are averaged with respect to number of sectors) it seems clear that PDR performance are quite sensitive to queue size, indeed, low moderately values of PDR are obtained when omnidirectional antennas are used; SAS contributes to increase the minimum PDR from 0.62 to 0.72, however the minimum PDR value, when our proposed approach is used, is 0.84; this value slightly improves together with the queue size and tends to begin almost uniform for highest queue size values. More specifically, especially for critical queue size cases (from 3 to 5) the difference between RR-MAC and ABT-RRMAC is very significant; this result suggests that our proposed algorithm provides for a great robustness also when the queue size are small, allowing quite acceptable performance in case of limited

resource allocation. The latest set of simulations is accomplished with the aim to test our proposal in condition of mobility of nodes; for this purpose it is possible to evaluate the energy consumption of nodes by increasing the node mobility speed from 1 to 10 *mps*; in this case, results are obtained by averaging energy consumption values with respect to number of sectors. In addition, the worst queue size case (queue size = 3) and the best queue size case (queue size = 10) have been compared.

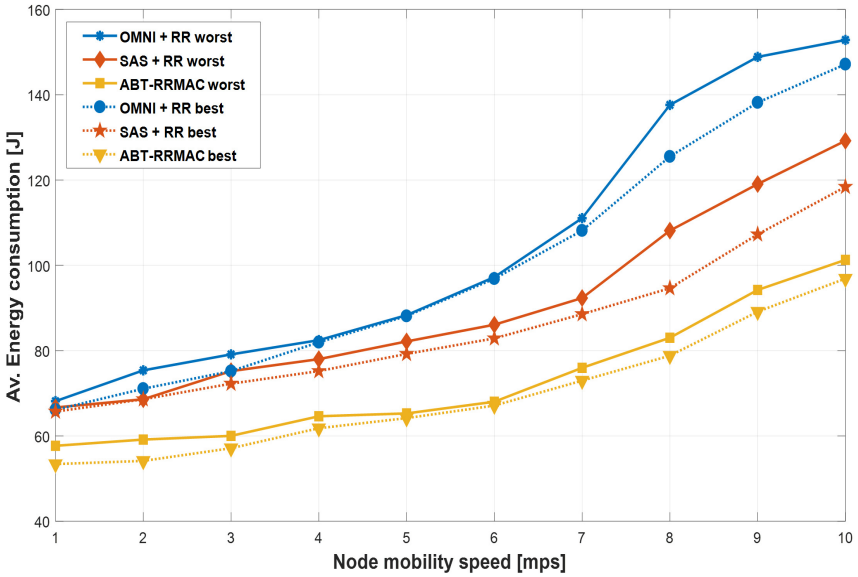

FIGURE 5.22: Energy consumption vs Node mobility speed.

The Figure 5.22 displays comparison curves related to energy consumption of nodes in function of the mobility speed by considering the worst and the best registered case in function of the size of the queues. Note that continued-line curves depict the worst case plots while dashed-line curves are related to the best case plots. As regards omnidirectional case, the overall consumption remains tolerant until 7 *mps* and then whereupon increases widely; this is mainly due to link failures occurring for high mobility speed values that results in enhancement of protocol overhead. However this rapid increase is weak limited in the best omnidirectional case. When using SAS in cooperation with Round-Robin, disruptive impacts due to growth of node mobility speed, are quite mitigated with respect to omnidirectional case, especially for high mobility values. Therefore the effects of directional high-gain beamforming are quite straightforward; in particular, by considering the best and worst cases, the energy saving amount in the case of RR-MAC gives from 23 to 29 J compared to omnidirectional. Nevertheless, ABT-RRMAC, thanks to dynamic sector time assignment, improves, performance of RR-MAC extending battery life of nodes of about 21% (on average) compared to the latter. This effect seems to keep uniform also as the mobility speed of nodes grows up. Note that, for ABT-RRMAC curves related to best and worst case are almost overlapped, indeed, the effect of queue size results mitigated compared to other considered cases.

5.9 The Energy Optimization algorithm With Variable Data Rate

Although when considering limited data rate (less than 100 Mbps) it is possible to obtain a significant mitigation of the overall energy consumption of nodes in the network, for example by using sectorized approaches [162], this aspect could represent a severe challenge that should not be underestimated when data rate is considerably high, especially if the main goal is to achieve very high network performance. However, very complex and efficient technologies such as MIMO and SAS have to be developed in order to satisfy high performance at high data rates. Ad regards massive MIMO, although a large number of elements promotes high performance in terms of gain, the higher is the number of elements, the highest is the energy consumption of nodes in the network. On the other hand, besides the number of radiating elements, energy consumption of massive MIMO is certainly related to physical parameters such as data rate, modulation and coding schema. For example, using a fixed data rate (and then, a fixed modulation schema) could certainly lead to facilitate significant waste of energy in the network, especially in a scenario in which nodes are uniformly distributed. Considering the previous scenario, it is high likely that a large number of transmissions are performed with a SNR (Signal to Noise Ratio) that is well beyond than the minimum requested SNR allowing to complete the transmission successfully. In the same way, highest data rates accelerate significantly the depletion of the battery life of nodes. In order to limit energy consumption in very high gain communications involving massive MIMO systems, a twice-action *energyOptimization* algorithm with variable data rate is presented in [202]. As denoted by the name, the algorithm has the purpose to optimize the energy consumption of nodes in the network by performing two main operations:

- **Data rate adaption at the transmitter**
- **Energy minimization at the receiver**

The first operation grants to avoid undesired waste of energy by adapting the data rate during communications in function on the SNR measured at the receiver; the second, ensures to limit the energy consumption at the receiver when capturing the signals in directional mode and, at the same time, aims to provide for a very high throughput and a high degree of synchronization between nodes.

5.9.1 Data rate adaption at the transmitter

One of the most common drawbacks when using massive MIMO systems is the fact that, SNR is directly related to the distance between sender and receiver and could considerably impact on the overall energy consumption of nodes if the data rate remains unchanged for a long time. For overcoming this issue, a procedure that dynamically adapts data rate at the transmitter based on the SNR requested at the

receiver has been designed, in order that the transmitter adopts the "best possible data rate" and so, the best modulation schema relating to a particular receiver. The best data rate, is the data rate which corresponds to the maximum SNR required at the receiver for maximizing the throughput. For a better investigation of the idea we can consider a scenario in which the Free Space Path Loss is used as channel propagation model.

$$P_{RX} = P_{TX} G_t G_r \left(\frac{\lambda}{4\pi d} \right)^2 \tag{5.13}$$

In Equation (5.13), P_{RX} and P_{TX} denote the transmitter and the receiver power respectively, while G_t and G_r are the gains at the transmitter and the receiver; remember that the wavelength is expressed as $\lambda = c/f$ where c is the speed of light while f is the frequency; finally d represents the distance between transmitter and receiver. The received power can be used for evaluating the SNR that could be expressed as:

$$SNR_{MAX} = \frac{P_{RX}}{N} \tag{5.14}$$

In Equation (5.14), the term N denotes the power of the noise intended as the background noise. Observe that, the received power divided by the background noise corresponds to the best SNR possible. Once that SNR_{MAX} is evaluated, it is possible to extract the best data rate and the relative modulation from the standard. In this way, for each destination, the best data rate is used and the energy consumption is minimized. Important to highlight that, in this case, the channel is bidirectional; by exploiting this affirmation it has been assumed that, the evaluation of the maximum SNR is performed by the receiver, that encapsulates the information about the SNR_{MAX} in an acknowledge packet which is sent to the transmitter. Once the transmitter receives the ack, it sets the data rate to the best possible data rate value for that destination, according to the SNR information.

5.9.2 Energy minimization at the receiver

Another common source of waste of undesired energy is represented by the operations at the receiver during a communication. It is well known that, in directional and asymmetrical environments it is not useful to set the receiver completely into directional mode because, in spite of the benefits in terms of energy that could be achieved, a large amount of control packet is required [140]; the best solution for maximizing packet performance, is to set the receiver in omni (omnidirectional) mode, in order to maintain high throughput. However, while considering omnidirectional mode, because the receiver attempts to exploit the antenna gain in all directions for channel sensing, this solution involves a considerable waste of energy un the network, even if gains involved are small. In view of these considerations, it can be derived that an acceptable solution could be achieved by mixing the operational mode at the receiver; obviously, in order to be efficent in terms of energy

consumption, the mixing operation must to be properly designed. Indeed, our solution provides that the receiver captures in a different and separate mode the two main parts composing the packet: the preamble (that is contained in the header) in omni mode using very low gain (1 dB) and the data in directional mode, exploiting the maximum gain in the desired direction. The reason of this choice is twice; capturing the preamble in omni mode ensures a strong likelihood that nodes remain correctly synchronized during a communication; furthermore, the passive mode of the receiver during channel sensing, produces a negligible waste of energy due to the very small size of this part of the packet (usually from 20 to 60 bytes); secondarily, receiving data in directional mode, means that reception beam is active for an higher period compared to preamble, then, because the beam is pointed only toward the intended direction, energy consumption is limited compared to omnidirectional; receiving data in directional mode also allows to avoid potential interferences of nodes that are close to receiver node.

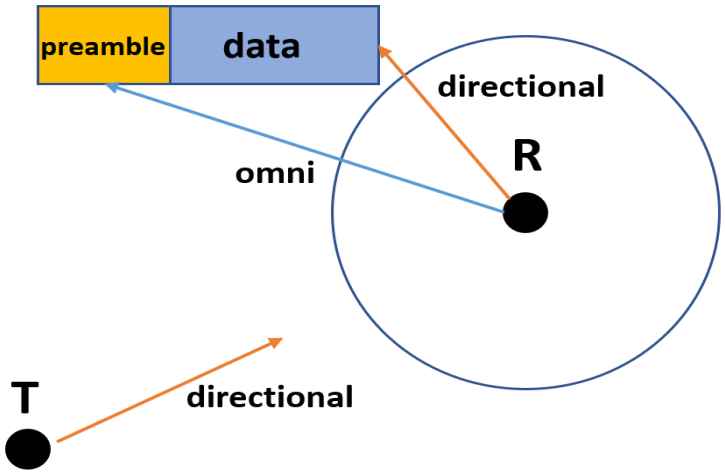

FIGURE 5.23: Packet Reception operation.

In Figure 5.23 it can be observed that, the trasmitter node T performs a transmission in directional mode at the best data rate possible (related to the receiver), while the receiver R attempts to receive the preamble in omni mode; after the preamble is correctly captured, R receives the rest of the packet (the data) in directional mode by avoiding to overhear other possible transmissions in the neighborhood until the whole packet is fully received. Note that the switching process of the radiation pattern from omnidirectional to directional is accomplished by an RF (Radio Frequency) switch and occurs during the reception of the preamble; this choice is deeply motivated in the section IV. However, After the packet is received, node R returns in omni mode and senses for other possible transmissions.

5.9.3 Energy optimization algorithm pseudo-code

The following pseudo-code summarizes operations of the *energyOptimization* algorithm:

Algorithm 11 Energy optimization pseudo-code

```
1: function COMPUTE ERROR(S/N, dataRate) return error using Nist Error Model
2: end function
1: function EXTRACT MAXIMUM DATARATE(Destination Address, Threshold)
2:             ▷ Search the maximum dataRate using error model with the S/N for this destination and Threshold
3:     return dataRate
4: end function
1: procedure DATARATE ADAPTION AT THE TRANSMITTER
2:     if first Transmission then                          ▷ Compute maximum data rate in function S/N
3:         current datarate = EXTRACT MAXIMUM DATARATE(Destination Address, Threshold)
4:     end if
5:     attempt transmission with current dataRate();
6:     if transmissionFailed then
7:         countFailed++;
8:         DECREASEDATARATE(())
9:     end if
10: end procedure
1: procedure ENERGY MINIMIZATION AT THE RECEIVER
2:     if reception (receiver) then
3:         setSeparateReceptionMode();
4:     end if
5:     if messagePart == PREAMBLE  &&  receiver is idle then
6:         startReception(reception);
7:     else if messagePart == DATA then
8:         SETRECEIVERMODE(DIR(receiverDir));              ▷ Change the antenna to directional
9:         CONTINUERECEPTION(());                          ▷ Receive data part of the frame
10:    end if
11:    if RECEPTIONISCOMPLETED(()) then
12:        SETRECEIVERMODE(OMNI);                          ▷ End reception change to OMNI
13:    end if
14: end procedure
```

The data rate adaption procedure handles the data rate in the simulation through the evaluation of the maximum SNR according to the current packet destination. The SNR is derived by using the Nist error model [203] implemented in Omnet++. Note that, for the first iterations the data rate is set to the best possible related to the receiver; every time that a communication fail occurs data rate is decreased; more specifically it is is re-evaluated based on the latest SNR measured at the receiver and then, it is assigned to the transmitter; the new value is the closest possible to the latest data rate used. When the optimum data rate for a given receiver is evaluated for the first time, it is stored in a cache and then used within a certain expiration time for the subsequent transmissions of that receiver: When the expiration time is reached, data rate caches are deleted and eventually updated (this because nodes move in the network and network topology can be modified periodically). By default the receiver is in omni mode; when the receiver detects a reception, attempts to receive in omni mode the preamble of the packet; once the preamble is captured, the receiver is set to directional, then, the rest of the packet (the data) can be received. The receiver, only after has finished to receive the full packet returns in omni mode.

5.10 Performance evaluation

The experimental analysis is accomplished through the use of the Omnet++ Network simulator. Basically, the considered scenario is consistent with the IEEE802.11ac specifications because, as the most up to date standards, it defines requirements for 5G wireless network environments. Observe that it has been decided to use this standard because it is very suitable for MANET and furthermore because it represents the precursor of the most modern 802.11ax and 802.11ah standards that however are not definitive. Along with this, mobile nodes are equipped with the *MassiveMIMOURPA* antenna module designed in [204] and then the energy consumption model presented in [205] (which represents a good approximation of the model proposed in [115]) has been implemented. *EnergyOptimization* algorithm is implemented in the *Radio.cc* class; this module handles communications between nodes at physical layer.

TABLE 5.5: Main simulation parameter set.

Num. of elements	90 (URPA)
Elem. Spacing	0.5 λ
Network Standard	IEEE802.11ac
Carrier freq.	5 GHz
Ch. bandwidths [Mhz]	20, 40, 80, 160
Num. of nodes	20, 50, 100
Data Rates [Mbps]	from 57.8 to 6933.3
Traffic data type	UDP
Message Length	512 *Byte*
Sim. Area Size	500 x 500 *m*
Sim. time	300 *s*

Simulations have been accomplished by using 20 different seeds and extracting confidence intervals obtained by repetitions considering a confidence level of 95 %. The traffic is randomly generated (based on the simulation seed) by different couples of nodes. The number of spatial streams is 8 while *BackgroundNoise* is set to -80 dBm. Finally, initial energy value of each node is set to 300 J, the shutdown energy value is 0 J. Other useful parameters are synthesized in Table I. The first result that has been evaluated is the statistic related to the residual capacity by considering 8 configuration cases extracted from the IEEE802.11ac standard having fixed data rate corresponding to the guard interval of 400 ns; then, these results have been compared with a configuration case implementing the *energyOptimization* algorithm.

Figure 5.24 represents the residual capacity in function of the simulation time displaying the best and the worst fixed data rate case and the curve obtained by averaging all data rate cases. Results are compared with the configuration implementing the proposed algorithm. The plots are averaged against all nodes. The worst case is related to the configuration having data rate of 6933.3 Mbps having a

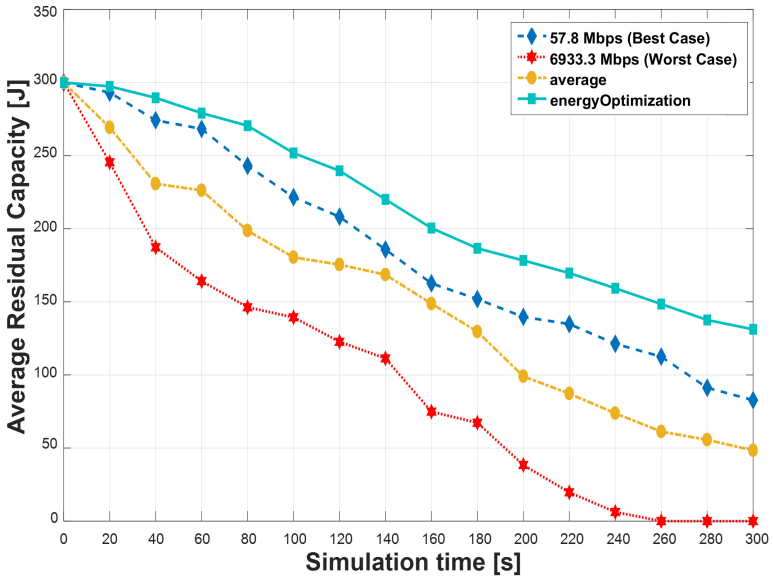

FIGURE 5.24: Residual capacity progression.

256-QAM (Quadrature Amplitude Modulation); indeed, the highest is the data rate the fastest is the energy depletion of nodes, as we can expect. However, in the worst case, nodes drain completely their battery at t = 250 s; curves related to the average case and the best case fixed data rate case (57.8 Mbps using a Binary Phase Shift Keying modulation) have a similar trend. Finally, compared to the best fixed data rate case, the curve related to *energyOptimization* algorithm overlooks the latter; in particular, it can be observed how the proposed algorithm improves residual capacity more than 38% compared to the best fixed data rate case. The main reason of this result is due to the fact that, while using a fixed data rate, the most of the energy consumption is related to receiver which receives in omni mode for all of the duration of the packet that in this case has a considerable size (512 Byte + header); in addition, because *energyOptimization* algorithm establishes that receiver captures data in directional mode, this contributes to considerably reduce collisions due to interferences in the channel; nevertheless, in this case, the used data rate at the transmitter is the best possible (or very close to the best possible in case of reduction provided by algorithm) corresponding to receiver that is adapted with respect to the evaluated SNR. The second statistic is related to PDR (Packet Delivery Ratio), that is close related with the energy consumption:

In Figure 5.25 it can be observed that, all curves, except for the worst case, are almost overlapped until 80 s; then, a decrease due to the drain of residual capacity, is registered. Because the PDR is directly proportional to the reduction of the energy of nodes we observe a dramatic decline of the performance especially in the worst case, for $t > 250s$ that is the time in which nodes completely exhaust their energy. However, this decrease is quite well mitigate if *energyOptimization* algorithm is used; in fact, at the end of simulation, it has been registered a PDR of 0.61 against 0.43 obtained in the best fixed data rate case. For a further investigation, the clustering

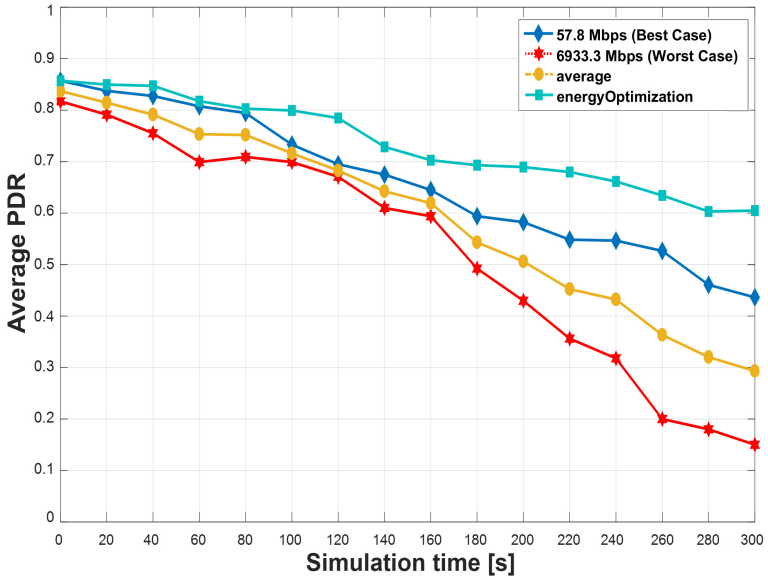

FIGURE 5.25: Packet Delivery Ratio comparison.

algorithm proposed in [199] has been implemented using *massiveMIMOURPA* module and setting the number of elements to 90; therefore, also the simulation time was doubled.

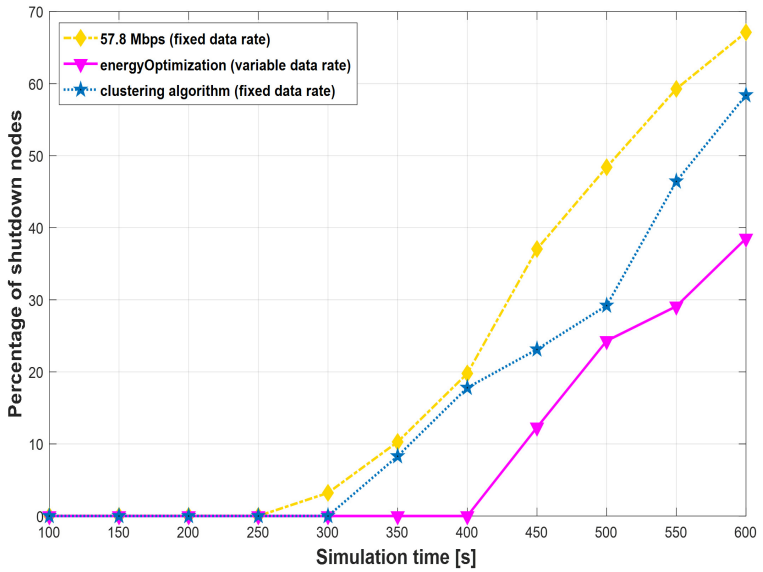

FIGURE 5.26: Energy consumption of nodes comparison.

Fig. 5.26 depicts percentage values of nodes that fully depleted their energy in function of the simulation time; the best fixed data rate case with cluster algorithm and the proposed algorithm have been compared. Observe how *energyOptimization* is very similar to cluster algorithm until 300 s. However, after 300 s, our solution tends to linearly outperform cluster algorithm. Indeed, the final percentage of nodes that completely exhausted their battery when our algorithm is used is 38,51 % against 58,4 % provided by clustering algorithm; this improvement is probably

attributable to two factors: primarily, the best SNR management in the system provided by variable data rate with respect to other considered cases; secondly, clustering algorithm provides that nodes use only directional beams; this translates into a large amount of wasted energy due to the use of high gain beams for a long time; nevertheless, the use of directional beams in sensing channel phase implies an high percentage of control packets exchanged by nodes for synchronizing themselves; this latest aspect also contributes to increase the overall energy consumption.

Chapter 6

Conclusion

In this thesis main concepts about directional antenna communications in Mobile ad Hoc Networks environments have been presented. The present work has the objective to illustrate main common issues related to directional protocols in MANET with special focus to physical and MAC layers; however, the main purpose has to present main advances accomplished by author of this thesis in order to limit or overcome some of the problems encountered in the present work. The overall work has been structured into five chapters each of them exposing a particular topic related to directional communications in MANET. The chapter 1 has been the goal to provide a background about directional communications compared with the omnidirectional case. In the chapter 2 theoretical basics about SAS and Massive MIMO have been presented; in particular, about SAS, the concept of beamforming has been deeply discussed and main adaptive beamforming algorithms have been presented; because the most of the existing beamforming algorithms provide a slow convergence, as personal research contribution it has been designed the VMA algorithm presenting a variable metric estimation mechanism; among other things, it has been shown that VMA is able to overcome the slow convergence problem by reducing the overall number of computations implied by the use of MSE. However, in the chapter 3, it has been highlighted that the current state of art relating to network simulators supporting directional and asymmetrical communications is quite poor; in view of this it has been shown how, by considering a well known simulator that is the Omnet++ network simulator, it is possible to implement modules emulating operations of SAS and Massive MIMO systems and extending Omnet++ features to enable a support of directional communications. In the chapter 4, it has been addressed one of the most common issue relating to directional MAC context that is the deafness problem. Because the use of the virtual carrier sensing it has been shown to be not sufficient to limit effectively deafness especially when using high complex antenna technology as SAS, it has been designed a directional MAC approach based on Round-Robin scheduling (RR-MAC). RR-MAC is able to reduce the large number of collisions involved by the use of classical directional antennas in mobile nodes; as a result, the Packet Delivery Ratio is improved as well as the fairness of the systems. About fairness, a new metric index that is the $(DRTS/DCTS)_{ratio}$ it has been created. Furthermore, the static nature of Round Robin could brake the

benefits of reducing beamforming time through the use of sectorized antenna; for this reason, a Weighted Round Robin approach (WRR-MAC) it has been designed in order to improve capabilities of Round Robin. WRR-MAC provides for a dynamic weights assignment to sectors based on the activity degree of nodes in each sector and on the level of misalignment between transmitter and receiver. In this way performance in terms of reduction of frame collisions and fairness results improved with respect to RR-MAC. In the chapter 5, mobility and energy consumption issues have been investigated. Relating the first aspect, the RR-MAC approach presented in chapter 4 has been enhanced in order to support a mechanism able to reduce effects of handoff implied by mobility of nodes. In this regard, the designed Enhanced RR-MAC presents an in-frame priority mechanism exploiting an Enhanced Triangle and Circle (ETRAC) predictive location model that allows to mitigate effects of node mobility. About energy consumption instead, an Adaptive Beamforming Time RR-MAC has been designed, with the goal to improve energy consumption allocation among sectors provided by Round-Robin approach. In particular, in this case the mean beamforming time and then the sector times are updated periodically in order that for each sector is assigned a quantum of time that is proportional to the size of the queue of that sector multiplied by the mean beamforming time (averaged by all sectors); in this way, sector times can be different and unbalanced, and the major fraction of time is assigned to the sector having the biggest queue size. Finally, in this chapter, it has been shown that, when very high-directivity antenna systems such as the massive MIMO are employed, it is possible, by means of an efficient mechanism adapting the data rate at the transmitter to avoid the significant waste of energy due to the employment of very high gain in communications.

Chapter 7

List of Publications

- V. Inzillo, F. De Rango, A Directional MAC Approach Extending Omnet++ Simulator, Summer Computer Simulation Conference 2016 (SCSC), Canada.
- V. Inzillo, F. De Rango, A. Quintana, A new Switched Beam Smart Antenna Model for extending Inet Omnet++ framework, International Conference on Simulation and Modeling Methodologies, Technologies and Applications, SIMULTECH 2017, Madrid, Spain.
- V. Inzillo, F. De Rango, A.Quintana, A new Variable Error Metric Adaptive Beamforming Algorithm for Smart Antenna Systems, International Wireless Communications and Mobile Computing Conference, IEEE IWCMC 2017, Valencia, Spain and INW 2017, Falcade (BL), Italy.
- V. Inzillo, F. De Rango, A. Santamaria, A. Quintana, A new Switched Beam Smart Antenna Model for Supporting Asymmetrical Communications Extending Inet Omnet++ framework, International Symposium on Performance Evaluation of Computer and Telecommunication Systems 2017 (SPECTS 2017), Seattle, United States.
- V. Inzillo, A. Santamaria, A. Quintana, Integration of Omnet++ Simulator with Matlab for realizing an Adaptive Beamforming System, International Symposium on Distributed Simulation and Real Time Applications (DS-RT) 2017, Rome, Italy.
- V. Inzillo, F. De Rango, A. Quintana, A Low Energy Consumption Smart Antenna Adaptive Array System for Mobile Ad Hoc Networks, International Journal of Computing (IJC), Vol. 16, Issue 3.
- V. Inzillo, F. De Rango, A. Quintana, A Sectorized Directional MAC Proposal for Mitigating Deafness and Energy Consumption in Mobile Ad Hoc Networks , IEEE CCNC 2018, Las Vegas, Nevada, United States.
- V. Inzillo, F. De Rango, A. Quintana, Supporting 5G Wireless Networks Through IEEE802.11ac Standard With New Massive MIMO Antenna System Module Design in Omnet++ Simulator, SIMULTECH 2018, Porto, Portugal.

- V. Inzillo, F. De Rango, A. Quintana, A Round-Robin MAC Approach for Limiting Deafness in Mobile Ad Hoc Network Beamforming Environments, IEEE WD 2018, Dubai, EAU.
- V. Inzillo, F. De Rango, A. Quintana, Mobility Beamforming Prediction and a Round Robin Scheduling in a Directional MAC for MANET, WMNC 2018, Prague, Czech Rep.
- V. Inzillo, F. De Rango, A. Quintana, L. Zampogna, Design and Implementation of New Planar Massive MIMO Systems for 5G Wireless Networks Extending Omnet++ Simulator, DS-RT 2018, Madrid, Spain.
- A. Quintana, V. Inzillo, Chapter: Inetmanet Framework, Recent Advances in Network Simulation, Springer, 2019.
- V. Inzillo, L. Zampogna, F. De Rango, A. Quintana, Chapter: Smart Antenna Systems model simulation design for 5G Wireless Network Systems. Array Pattern Optimization; Intech, 2018.
- V. Inzillo, F. De Rango, A. Quintana, F. Santamaria, An Adaptive Beamforming Time with Round-Robin MAC Algorithm for Reducing Energy Consumption in MANET, Journal of Sensor and Actuator Networks (JSAN), Vol. 7, Issue 4, 2018.
- V. Inzillo, F. De Rango, A. Quintana, Packet Error Rate and Channel Performance Evaluation in 5G Wireless Networks with Massive MIMO Module Extending Omnet++, IEEE CCNC 2019, Workshop 5G Simulators and Testbeds (5GSIM), Las Vegas, Nevada, United States.
- F. De Rango, V. Inzillo, A. Quintana, Exploiting Frame Aggregation and Weighted Round Robin with Beamforming Smart Antennas for Directional MAC in MANET Environments, Ad Hoc Networks, Vol. 89, pp. 186–203, Elsevier, 2019.
- V. Inzillo, F. De Rango, A. Quintana, A Novel Algorithm For Limiting Energy Consumption in 5G Wireless Environments Using Massive MIMO Systems, IEEE 89th Vehicular Technology Conference (VTC Spring), 2019.
- V. Inzillo, F. De Rango, A. Quintana, A Novel Self Clocked Fair Queueing MAC approach for reducing deafness problem in directional MANET environments, IFIP Wireless Days 2019.
- V Inzillo, A Serianni, A. Quintana, A secure adaptive beamforming mechanism exploiting deafness in directional beamforming MANET, Signal Processing, Sensor/Information Fusion, and Target Recognition XXVIII Conference, (SPIE) 2019.

Bibliography

[1] J. Li, C. Blake, D. S. De Couto, H. I. Lee, and R. Morris, "Capacity of ad hoc wireless networks", in *Proceedings of the 7th annual international conference on Mobile computing and networking*, ACM, 2001, pp. 61–69.

[2] P. Gupta and P. R. Kumar, "The capacity of wireless networks", *IEEE Transactions on information theory*, vol. 46, no. 2, pp. 388–404, 2000.

[3] M. Franceschetti, M. D. Migliore, and P. Minero, "The capacity of wireless networks: Information-theoretic and physical limits", *IEEE Transactions on Information Theory*, vol. 55, no. 8, pp. 3413–3424, 2009.

[4] W. L. Stutzman and G. A. Thiele, *Antenna theory and design*. John Wiley & Sons, 2013.

[5] L. Josefsson and P. Persson, *Conformal array antenna theory and design*. John wiley & sons, 2006, vol. 29.

[6] Y.-J. Wu, B.-H. Sun, J.-F. Li, and Q.-Z. Liu, "Triple-band omni-directional antenna for wlan application", *Progress In Electromagnetics Research*, vol. 76, pp. 477–484, 2007.

[7] C.-C. Lin, L.-C. Kuo, and H.-R. Chuang, "A horizontally polarized omnidirectional printed antenna for wlan applications", *IEEE Transactions on Antennas and Propagation*, vol. 54, no. 11, pp. 3551–3556, 2006.

[8] V. Chandrasekhar and J. G. Andrews, "Uplink capacity and interference avoidance for two-tier cellular networks", in *Global Telecommunications Conference, 2007. GLOBECOM'07. IEEE*, IEEE, 2007, pp. 3322–3326.

[9] M. Gustafsson, C. Sohl, and G. Kristensson, "Physical limitations on antennas of arbitrary shape", in *Proceedings of the Royal Society of London A: Mathematical, Physical and Engineering Sciences*, The Royal Society, vol. 463, 2007, pp. 2589–2607.

[10] X.-W. Dai, Z.-Y. Wang, C.-H. Liang, X. Chen, and L.-T. Wang, "Multiband and dual-polarized omnidirectional antenna for 2g/3g/lte application", *IEEE Antennas and Wireless Propagation Letters*, vol. 12, pp. 1492–1495, 2013.

[11] H.-N. Dai, K.-W. Ng, R.-W. Wong, and M.-Y. Wu, "On the capacity of multichannel wireless networks using directional antennas", in *INFOCOM 2008. The 27th Conference on Computer Communications. IEEE*, IEEE, 2008, pp. 628–636.

[12] J. J. Wang, "A critique and new concept on gain bandwidth limitation of omnidirectional antennas", in *Progress in Electromagnetics Research Symposium (PIERS)*, 2005.

[13] X. M. Zhang, Y. Zhang, F. Yan, and A. V. Vasilakos, "Interference-based topology control algorithm for delay-constrained mobile ad hoc networks", *IEEE Transactions on Mobile Computing*, vol. 14, no. 4, pp. 742–754, 2015.

[14] X. Zhang, Q. Liu, D. Shi, Y. Liu, and X. Yu, "An average link interference-aware routing protocol for mobile ad hoc networks", in *Wireless and Mobile Communications, 2007. ICWMC'07. Third International Conference on*, IEEE, 2007, pp. 10–10.

[15] J. Loo, J. L. Mauri, and J. H. Ortiz, *Mobile ad hoc networks: current status and future trends*. CRC Press, 2016.

[16] S. Taneja and A. Kush, "A survey of routing protocols in mobile ad hoc networks", *International Journal of innovation, Management and technology*, vol. 1, no. 3, p. 279, 2010.

[17] M. A. Marsan, L. Chiaraviglio, D. Ciullo, and M. Meo, "Optimal energy savings in cellular access networks", in *Communications Workshops, 2009. ICC Workshops 2009. IEEE International Conference on*, IEEE, 2009, pp. 1–5.

[18] D. Jiang, Z. Xu, and Z. Lv, "A multicast delivery approach with minimum energy consumption for wireless multi-hop networks", *Telecommunication systems*, vol. 62, no. 4, pp. 771–782, 2016.

[19] I. Caragiannis, C. Kaklamanis, E. Kranakis, D. Krizanc, and A. Wiese, "Communication in wireless networks with directional antennas", in *Proceedings of the twentieth annual symposium on Parallelism in algorithms and architectures*, ACM, 2008, pp. 344–351.

[20] H.-N. Dai, K.-W. Ng, M. Li, and M.-Y. Wu, "An overview of using directional antennas in wireless networks", *International Journal of Communication Systems*, vol. 26, no. 4, pp. 413–448, 2013.

[21] Z. Yu, J. Teng, X. Bai, D. Xuan, and W. Jia, "Connected coverage in wireless networks with directional antennas", *ACM Transactions on Sensor Networks (TOSN)*, vol. 10, no. 3, p. 51, 2014.

[22] A. P. Subramanian and S. R. Das, "Addressing deafness and hidden terminal problem in directional antenna based wireless multi-hop networks", *Wireless networks*, vol. 16, no. 6, pp. 1557–1567, 2010.

[23] H. Gossain, C. Cordeiro, and D. P. Agrawal, "Minimizing the effect of deafness and hidden terminal problem in wireless ad hoc networks using directional antennas", *Wireless Communications and Mobile Computing*, vol. 6, no. 7, pp. 917–931, 2006.

[24] K. Kosek-Szott, "A survey of mac layer solutions to the hidden node problem in ad-hoc networks", *Ad Hoc Networks*, vol. 10, no. 3, pp. 635–660, 2012.

[25] K. Zhu, D. Niyato, P. Wang, E. Hossain, and D. In Kim, "Mobility and handoff management in vehicular networks: A survey", *Wireless communications and mobile computing*, vol. 11, no. 4, pp. 459–476, 2011.

[26] C. Yu, B. Lee, and H. Yong Youn, "Energy efficient routing protocols for mobile ad hoc networks", *Wireless communications and mobile computing*, vol. 3, no. 8, pp. 959–973, 2003.

[27] S Gopinath, N Sureshkumar, G Vijayalakshmi, N. Natraj, T Senthil, and P Prabu, "Energy efficient routing protocol for manet", *International Journal of Computer Science Issues (IJCSI)*, vol. 9, no. 2, p. 292, 2012.

[28] G. V. Kumar, Y. V. Reddyr, and D. M. Nagendra, "Current research work on routing protocols for manet: A literature survey", *international Journal on computer Science and Engineering*, vol. 2, no. 03, pp. 706–713, 2010.

[29] C. Huang, C.-T. Lea, and A. K.-S. Wong, "A joint solution for the hidden and exposed terminal problems in csma/ca wireless networks", *Computer networks*, vol. 56, no. 14, pp. 3261–3273, 2012.

[30] Z. Huang and C.-C. Shen, "A comparison study of omnidirectional and directional mac protocols for ad hoc networks", in *Global Telecommunications Conference, 2002. GLOBECOM'02. IEEE*, IEEE, vol. 1, 2002, pp. 57–61.

[31] R. R. Choudhury, X. Yang, R. Ramanathan, and N. H. Vaidya, "Using directional antennas for medium access control in ad hoc networks", in *Proceedings of the 8th annual international conference on Mobile computing and networking*, ACM, 2002, pp. 59–70.

[32] G. Jakllari, I. Broustis, T. Korakis, S. V. Krishnamurthy, and L. Tassiulas, "Handling asymmetry in gain in directional antenna equipped ad hoc networks.", in *PIMRC*, Citeseer, 2005, pp. 1284–1288.

[33] V. Kolar, S. Tilak, and N. B. Abu-Ghazaleh, "Avoiding head of line blocking in directional antenna [mac protocol]", in *Local Computer Networks, 2004. 29th Annual IEEE International Conference on*, IEEE, 2004, pp. 385–392.

[34] X. Lu, D. Towsley, P. Lio, and Z. Xiong, "An adaptive directional mac protocol for ad hoc networks using directional antennas", *Science China Information Sciences*, vol. 55, no. 6, pp. 1360–1371, 2012.

[35] K. Adere and G. R. Murthy, "Solving the hidden and exposed terminal problems using directional-antenna based mac protocol for wireless sensor networks", in *Wireless And Optical Communications Networks (WOCN), 2010 Seventh International Conference On*, IEEE, 2010, pp. 1–5.

[36] Y.-B. Ko, V. Shankarkumar, and N. H. Vaidya, "Medium access control protocols using directional antennas in ad hoc networks", in *INFOCOM 2000. Nineteenth Annual Joint Conference of the IEEE Computer and Communications Societies. Proceedings. IEEE*, IEEE, vol. 1, 2000, pp. 13–21.

[37] A. Nasipuri, S. Ye, J You, and R. E. Hiromoto, "A mac protocol for mobile ad hoc networks using directional antennas", in *Wireless Communications and Networking Confernce, 2000. WCNC. 2000 IEEE*, IEEE, vol. 3, 2000, pp. 1214–1219.

[38] Y. Wang, H. Zhu, and J. Zhang, "Using directional antenna to realize multi-relay mac for wireless ad hoc networks", in *Wireless Communication Systems, 2007. ISWCS 2007. 4th International Symposium on*, IEEE, 2007, pp. 257–261.

[39] R. R. Choudhury and N. H. Vaidya, "Deafness: A mac problem in ad hoc networks when using directional antennas", in *Network protocols, 2004. ICNP 2004. Proceedings of the 12th IEEE international conference on*, IEEE, 2004, pp. 283–292.

[40] M. Takai, J. Martin, R. Bagrodia, and A. Ren, "Directional virtual carrier sensing for directional antennas in mobile ad hoc networks", in *Proceedings of the 3rd ACM international symposium on Mobile ad hoc networking & computing*, ACM, 2002, pp. 183–193.

[41] T. Korakis, G. Jakllari, and L. Tassiulas, "Cdr-mac: A protocol for full exploitation of directional antennas in ad hoc wireless networks", *IEEE Transactions on Mobile Computing*, vol. 7, no. 2, pp. 145–155, 2008.

[42] A. Nasipuri, J. Mandava, H. Manchala, and R. E. Hiromoto, "On-demand routing using directional antennas in mobile ad hoc networks", in *Computer Communications and Networks, 2000. Proceedings. Ninth International Conference on*, IEEE, 2000, pp. 535–541.

[43] S. Bandyopadhyay, K. Hasuike, S Horisawa, and S Tawara, "An adaptive mac and idirectional routing protocol for ad hoc wireless network using espar antenna", in *Proceedings of the 2nd ACM international symposium on Mobile ad hoc networking & computing*, ACM, 2001, pp. 243–246.

[44] K. Gyoda and T. Ohira, "Design of electronically steerable passive array radiator (espar) antennas", in *Antennas and Propagation Society International Symposium, 2000. IEEE*, IEEE, vol. 2, 2000, pp. 922–925.

[45] C. Perkins, E. Belding-Royer, and S. Das, "Ad hoc on-demand distance vector (aodv) routing", Tech. Rep., 2003.

[46] D. B. Johnson and D. A. Maltz, "Dynamic source routing in ad hoc wireless networks", in *Mobile computing*, Springer, 1996, pp. 153–181.

[47] B. Hu and H. Gharavi, "Dsr-based directional routing protocol for ad hoc networks", in *Global Telecommunications Conference, 2007. GLOBECOM'07. IEEE*, IEEE, 2007, pp. 4936–4940.

[48] R. R. Choudhury and N. H. Vaidya, "Impact of directional antennas on ad hoc routing", in *IFIP international conference on personal wireless communications*, Springer, 2003, pp. 590–600.

[49] A. N. Le, D.-W. Kum, S.-H. Lee, Y.-Z. Cho, and I.-S. Lee, "Directional aodv routing protocol for wireless mesh networks", in *Personal, Indoor and Mobile Radio Communications, 2007. PIMRC 2007. IEEE 18th International Symposium on*, IEEE, 2007, pp. 1–5.

[50] G. Okamoto, *Smart antenna systems and wireless LANs*. Springer Science & Business Media, 2006, vol. 474.

[51] S. Bellofiore, C. A. Balanis, J. Foutz, and A. S. Spanias, "Smart-antenna systems for mobile communication networks. part 1. overview and antenna design", *IEEE Antennas and Propagation Magazine*, vol. 44, no. 3, pp. 145–154, 2002.

[52] J. H. Winters, "Smart antenna techniques and their application to wireless ad hoc networks", *IEEE wireless communications*, vol. 13, no. 4, pp. 77–83, 2006.

[53] K. Sengar, N. Rani, A. Singhal, D. Sharma, S. Verma, and T. Singh, "Study and capacity evaluation of siso, miso and mimo rf wireless communication systems", *arXiv preprint arXiv:1403.7774*, 2014.

[54] Z. Ding, C. Zhong, D. W. K. Ng, M. Peng, H. A. Suraweera, R. Schober, and H. V. Poor, "Application of smart antenna technologies in simultaneous wireless information and power transfer", *IEEE Communications Magazine*, vol. 53, no. 4, pp. 86–93, 2015.

[55] M.-J. Ho, G. L. Stuber, and M. D. Austin, "Performance of switched-beam smart antennas for cellular radio systems", *IEEE Transactions on vehicular technology*, vol. 47, no. 1, pp. 10–19, 1998.

[56] J. G. Andrews, S. Buzzi, W. Choi, S. V. Hanly, A. Lozano, A. C. Soong, and J. C. Zhang, "What will 5g be?", *IEEE Journal on selected areas in communications*, vol. 32, no. 6, pp. 1065–1082, 2014.

[57] E. G. Larsson, O. Edfors, F. Tufvesson, and T. L. Marzetta, "Massive mimo for next generation wireless systems", *IEEE communications magazine*, vol. 52, no. 2, pp. 186–195, 2014.

[58] E. Björnson, J. Hoydis, M. Kountouris, and M. Debbah, "Massive mimo systems with non-ideal hardware: Energy efficiency, estimation, and capacity limits", *IEEE Transactions on Information Theory*, vol. 60, no. 11, pp. 7112–7139, 2014.

[59] J. Hoydis, S. Ten Brink, and M. Debbah, "Massive mimo in the ul/dl of cellular networks: How many antennas do we need?", *IEEE Journal on selected Areas in Communications*, vol. 31, no. 2, pp. 160–171, 2013.

[60] R. J. Mailloux, *Phased array antenna handbook*. Artech house, 2017.

[61] M. T. Ma, *Theory and application of antenna arrays*. John Wiley & Sons, 1974.

[62] C. Dohmen, J. W. Odendaal, and J. Joubert, "Synthesis of conformal arrays with optimized polarization", *IEEE Transactions on Antennas and Propagation*, vol. 55, no. 10, pp. 2922–2925, 2007.

[63] C. A. Balanis, "Antenna theory: A review", *Proceedings of the IEEE*, vol. 80, no. 1, pp. 7–23, 1992.

[64] R. C. Hansen, *Phased array antennas*. John Wiley & Sons, 2009, vol. 213.

[65] N. Fourikis, *Phased array-based systems and applications*. Wiley, 1997.

[66] S. Chandran, *Adaptive antenna arrays: trends and applications*. Springer Science & Business Media, 2013.

[67] K. Kim, T. K. Sarkar, and M. S. Palma, "Adaptive antenna arrays", *Wiley Encyclopedia of Telecommunications*, 2003.

[68] C.-H. Tseng, C.-J. Chen, and T.-H. Chu, "A low-cost 60-ghz switched-beam patch antenna array with butler matrix network", *IEEE Antennas and Wireless Propagation Letters*, vol. 7, pp. 432–435, 2008.

[69] R. Athan, "Antenna beamforming and power control for ad hoc networks", *Mobile ad hoc networking*, vol. 139, 2004.

[70] V. Venkateswaran and A.-J. van der Veen, "Analog beamforming in mimo communications with phase shift networks and online channel estimation", *IEEE Transactions on Signal Processing*, vol. 58, no. 8, pp. 4131–4143, 2010.

[71] H. Steyskal, "Digital beamforming antennas", *Microwave journal*, vol. 30, no. 1, pp. 107–124, 1987.

[72] M. Chryssomallis, "Smart antennas", *IEEE Antennas and Propagation magazine*, vol. 42, no. 3, pp. 129–136, 2000.

[73] L. Zhou and C. Wen, "Smart antenna system", in *Optical Transmission, Switching, and Subsystems VI*, International Society for Optics and Photonics, vol. 7136, 2008, p. 713 643.

[74] P. Kułakowski, J. Vales-Alonso, E. Egea-López, W. Ludwin, and J. García-Haro, "Angle-of-arrival localization based on antenna arrays for wireless sensor networks", *Computers & Electrical Engineering*, vol. 36, no. 6, pp. 1181–1186, 2010.

[75] M. Rezk, W. Kim, Z. Yun, and M. F. Iskander, "Performance comparison of a novel hybrid smart antenna system versus the fully adaptive and switched beam antenna arrays", *IEEE Antennas and Wireless Propagation Letters*, vol. 4, no. 1, pp. 285–288, 2005.

[76] M. Kuwahara and N. Doi, *Radio communication system using adaptive array antenna*, US Patent 7,082,321, 2006.

[77] I. Stevanovic, A. Skrivervik, and J. R. Mosig, "Smart antenna systems for mobile communications", Tech. Rep., 2003.

[78] S. Das, "Smart antenna design for wireless communication using adaptive beam-forming approach", in *TENCON 2008-2008 IEEE Region 10 Conference*, IEEE, 2008, pp. 1–5.

[79] S.-S. Jeon, Y. Wang, Y. Qian, and T. Itoh, "A novel planar array smart antenna system with hybrid analog-digital beamforming", in *Microwave Symposium Digest, 2001 IEEE MTT-S International*, IEEE, vol. 1, 2001, pp. 121–124.

[80] C. Sun, *Handbook on advancements in smart antenna technologies for wireless networks*. IGI Global, 2008.

[81] K. Yao, R. E. Hudson, C. W. Reed, D. Chen, and F. Lorenzelli, "Blind beamforming on a randomly distributed sensor array system", *IEEE Journal on Selected Areas in Communications*, vol. 16, no. 8, pp. 1555–1567, 1998.

[82] S. F. Shaukat, M. Hassan, R Farooq, H. Saeed, and Z Saleem, "Sequential studies of beamforming algorithms for smart antenna systems", *World Applied Sciences Journal*, vol. 6, no. 6, pp. 754–758, 2009.

[83] S. Hossain, M. T. Islam, and S. Serikawa, "Adaptive beamforming algorithms for smart antenna systems", in *Control, Automation and Systems, 2008. ICCAS 2008. International Conference on*, IEEE, 2008, pp. 412–416.

[84] S. W. Varade and K. D. Kulat, "Robust algorithms for doa estimation and adaptive beamforming for smart antenna application", in *2009 Second International Conference on Emerging Trends in Engineering & Technology*, IEEE, 2009, pp. 1195–1200.

[85] S. Haykin and B. Widrow, *Least-mean-square adaptive filters*. John Wiley and Sons, 2003, vol. 31.

[86] B. Widrow, J. McCool, and M. Ball, "The complex lms algorithm", *Proceedings of the IEEE*, vol. 63, no. 4, pp. 719–720, 1975.

[87] B. Widrow, P. Mantey, L. Griffiths, and B. Goode, "Adaptive antenna systems", *Proceedings of the IEEE*, vol. 55, no. 12, pp. 2143–2159, 1967.

[88] K. N. Oh and Y. O. Chin, "Modified constant modulus algorithm: Blind equalization and carrier phase recovery algorithm", in *Communications, 1995. ICC'95 Seattle,'Gateway to Globalization', 1995 IEEE International Conference on*, IEEE, vol. 1, 1995, pp. 498–502.

[89] M Larimore and J Treichler, "Convergence behavior of the constant modulus algorithm", in *Acoustics, Speech, and Signal Processing, IEEE International Conference on ICASSP'83.*, IEEE, vol. 8, 1983, pp. 13–16.

[90] S. O. Haykin, *Adaptive filter theory*. Pearson Higher Ed, 2013.

[91] M. R. Bai, J. Jeng, and C. Chen, "Adaptive order tracking technique using recursive least-square algorithm", *Journal of vibration and acoustics*, vol. 124, no. 4, pp. 502–511, 2002.

[92] J.-I. Nagumo and A. Noda, "A learning method for system identification", *IEEE Transactions on Automatic Control*, vol. 12, no. 3, pp. 282–287, 1967.

[93] N. G. Reddy and K Ramadevi, "Smart antennas adaptive beamforming through statistical signal processing techniques", *IJRCCT*, vol. 2, no. 7, pp. 400–404, 2013.

[94] K. Siddappaji, "Sudha "a new time-varying lms adaptive filtering algorithm in noise cancellation system,"" *Journal of Basic and Applied Engineering Research (JBAER) ISSN*, pp. 2350–0255,

[95] Y.-S. Lau, Z. Hussain, and R. Harris, "A time-varying convergence parameter for the lms algorithm in the presence of white gaussian noise", in *Submitted to the Australian Telecommunications, Networks and Applications Conference (ATNAC), Melbourne*, 2003.

[96] K. C. Blom, M. D. van de Burgwal, K. C. Rovers, A. B. Kokkeler, and G. J. Smit, "Angular cma: A modified constant modulus algorithm providing steering angle updates", in *Seventh International Conference on Wireless and Mobile Communications, ICWMC*, 2011, pp. 42–47.

[97] Z. Shengkui, M. Zhihong, and K. Suiyang, "Modified lms and nlms algorithms with a new variable step size", in *Control, Automation, Robotics and Vision, 2006. ICARCV'06. 9th International Conference on*, IEEE, 2006, pp. 1–6.

[98] Q. Yan-Bin, M. Fan-Gang, and G. Lei, "A new variable step size lms adaptive filtering algorithm", in *Industrial Electronics, 2007. ISIE 2007. IEEE International Symposium on*, IEEE, 2007, pp. 1601–1605.

[99] P. Fazio, M. Tropea, F. Veltri, and S. Marano, "A novel rate adaptation scheme for dynamic bandwidth management in wireless networks", in *Vehicular Technology Conference (VTC Spring), 2012 IEEE 75th*, IEEE, 2012, pp. 1–5.

[100] P. Fazio, F. De Rango, C. Sottile, P. Manzoni, and C. Calafate, "A distance vector routing protocol for vanet environment with dynamic frequency assignment", in *Wireless Communications and Networking Conference (WCNC), 2011 IEEE*, IEEE, 2011, pp. 1016–1020.

[101] P. Fazio, F. De Rango, and C. Sottile, "A new interference aware on demand routing protocol for vehicular networks", in *Performance Evaluation of Computer & Telecommunication Systems (SPECTS), 2011 International Symposium on*, IEEE, 2011, pp. 98–103.

[102] V. Inzillo, F. De Rango, and A. A. Quintana, "A new variable error metric adaptive beamforming algorithm for smart antenna systems", in *Wireless Communications and Mobile Computing Conference (IWCMC), 2017 13th International*, IEEE, 2017, pp. 1195–1200.

[103] R. J. Hyndman *et al.*, "Another look at forecast-accuracy metrics for intermittent demand", *Foresight: The International Journal of Applied Forecasting*, vol. 4, no. 4, pp. 43–46, 2006.

[104] Q. Zhang, S. Jin, K.-K. Wong, H. Zhu, and M. Matthaiou, "Power scaling of uplink massive mimo systems with arbitrary-rank channel means", *IEEE Journal of Selected Topics in Signal Processing*, vol. 8, no. 5, pp. 966–981, 2014.

[105] A. L. Swindlehurst, E. Ayanoglu, P. Heydari, and F. Capolino, "Millimeter-wave massive mimo: The next wireless revolution?", *IEEE Communications Magazine*, vol. 52, no. 9, pp. 56–62, 2014.

[106] K. Zheng, S. Ou, and X. Yin, "Massive mimo channel models: A survey", *International Journal of Antennas and Propagation*, vol. 2014, 2014.

[107] J. H. Kotecha and J. C. Mundarath, *Reference signaling scheme using compressed feedforward codebooks for multi-user, multiple input, multiple output (mu-mimo) systems*, US Patent 7,961,807, 2011.

[108] R. C. de Lamare, "Massive mimo systems: Signal processing challenges and future trends", *URSI Radio Science Bulletin*, vol. 86, no. 4, pp. 8–20, 2013.

[109] J. Choi, D. J. Love, and P. Bidigare, "Downlink training techniques for fdd massive mimo systems: Open-loop and closed-loop training with memory", *IEEE Journal of Selected Topics in Signal Processing*, vol. 8, no. 5, pp. 802–814, 2014.

[110] V. Jungnickel, K. Manolakis, W. Zirwas, B. Panzner, V. Braun, M. Lossow, M. Sternad, R. Apelfrojd, and T. Svensson, "The role of small cells, coordinated multipoint, and massive mimo in 5g", *IEEE Communications Magazine*, vol. 52, no. 5, pp. 44–51, 2014.

[111] E. Bjornson, M. Kountouris, and M. Debbah, "Massive mimo and small cells: Improving energy efficiency by optimal soft-cell coordination", in *Telecommunications (ICT), 2013 20th International Conference on*, IEEE, 2013, pp. 1–5.

[112] D. Ha, K. Lee, and J. Kang, "Energy efficiency analysis with circuit power consumption in massive mimo systems", in *Personal Indoor and Mobile Radio Communications (PIMRC), 2013 IEEE 24th International Symposium on*, IEEE, 2013, pp. 938–942.

[113] L. Fan, S. Jin, C.-K. Wen, and H. Zhang, "Uplink achievable rate for massive mimo systems with low-resolution adc", *IEEE Communications Letters*, vol. 19, no. 12, pp. 2186–2189, 2015.

[114] S. Jin, X. Wang, Z. Li, K.-K. Wong, Y. Huang, and X. Tang, "On massive mimo zero-forcing transceiver using time-shifted pilots", *IEEE Transactions on Vehicular Technology*, vol. 65, no. 1, pp. 59–74, 2016.

[115] E. Björnson, L. Sanguinetti, J. Hoydis, and M. Debbah, "Designing multi-user mimo for energy efficiency: When is massive mimo the answer?", in *Wireless Communications and Networking Conference (WCNC), 2014 IEEE*, IEEE, 2014, pp. 242–247.

[116] Y. Mehmood, W. Afzal, F. Ahmad, U. Younas, I. Rashid, and I Mehmood, "Large scaled multi-user mimo system so called massive mimo systems for future wireless communication networks", in *Automation and Computing (ICAC), 2013 19th International Conference on*, IEEE, 2013, pp. 1–4.

[117] P. Ioannides and C. A. Balanis, "Uniform circular and rectangular arrays for adaptive beamforming applications", *IEEE Antennas and Wireless Propagation Letters*, vol. 4, no. 1, pp. 351–354, 2005.

[118] Z. Pi, J. Choi, and R. Heath, "Millimeter-wave gigabit broadband evolution toward 5g: Fixed access and backhaul", *IEEE Communications Magazine*, vol. 54, no. 4, pp. 138–144, 2016.

[119] H. Xie, F. Gao, and S. Jin, "An overview of low-rank channel estimation for massive mimo systems", *IEEE Access*, vol. 4, pp. 7313–7321, 2016.

[120] E. Weingartner, H. Vom Lehn, and K. Wehrle, "A performance comparison of recent network simulators", in *Communications, 2009. ICC'09. IEEE International Conference on*, IEEE, 2009, pp. 1–5.

[121] J. Lessmann, P. Janacik, L. Lachev, and D. Orfanus, "Comparative study of wireless network simulators", in *Networking, 2008. ICN 2008. Seventh International Conference on*, IEEE, 2008, pp. 517–523.

[122] A. Varga, "Omnet++ simulator", *Omnet++ simulator available at http://www.omnetpp. org*, vol. 138, 2007.

[123] A. Varga and R. Hornig, "An overview of the omnet++ simulation environment", in *Proceedings of the 1st international conference on Simulation tools and techniques for communications, networks and systems & workshops*, ICST (Institute for Computer Sciences, Social-Informatics and Telecommunications Engineering), 2008, p. 60.

[124] T. Issariyakul and E. Hossain, "Introduction to network simulator 2 (ns2)", in *Introduction to Network Simulator NS2*, Springer, 2012, pp. 21–40.

[125] G. Carneiro, "Ns-3: Network simulator 3", in *UTM Lab Meeting April*, vol. 20, 2010.

[126] X. Chang, "Network simulations with opnet", in *Proceedings of the 31st conference on Winter simulation: Simulation—a bridge to the future-Volume 1*, ACM, 1999, pp. 307–314.

[127] A Quintana, *Inetmanet framework for omnet*, 2010.

[128] L. Chunjian, "Efficient antenna patterns for three-sector wcdma systems", *Master of Science Thesis, Chalmers University of Technology, Göteborg, Sweden*, 2003.

[129] V. Inzillo, F. De Rango, A. F. Santamaria, and A. A. Quintana, "A new switched beam smart antenna model for supporting asymmetrical communications extending inet omnet++ framework", in *Performance Evaluation of Computer and Telecommunication Systems (SPECTS), 2017 International Symposium on*, IEEE, 2017, pp. 1–7.

[130] V. Inzillo, A. F. Santamaria, and A. A. Quintana, "Integration of omnet++ simulator with matlab for realizing an adaptive beamforming system", in *Distributed Simulation and Real Time Applications (DS-RT), 2017 IEEE/ACM 21st International Symposium on*, IEEE, 2017, pp. 1–2.

[131] V. Inzillo, F. De Rango, and A. A. Quintana, "Supporting 5g wireless networks through ieee802.11ac standard with new massive mimo antenna system module design in omnet++ simulator", in *SIMULTECH*, 2018.

[132] W. Tan, S. D. Assimonis, M. Matthaiou, Y. Han, X. Li, and S. Jin, "Analysis of different planar antenna arrays for mmwave massive mimo systems", in *Vehicular Technology Conference (VTC Spring), 2017 IEEE 85th*, IEEE, 2017, pp. 1–5.

[133] V. Jain, A. Gupta, D. Lal, and D. P. Agrawal, "A cross layer mac with explicit synchronization through intelligent feedback for multiple beam antennas", in *Global Telecommunications Conference, 2005. GLOBECOM'05. IEEE*, IEEE, vol. 6, 2005, pp. 3196–3200.

[134] A. I. Alshbatat and L. Dong, "Adaptive mac protocol for uav communication networks using directional antennas", in *Networking, Sensing and Control (ICNSC), 2010 International Conference on*, IEEE, 2010, pp. 598–603.

[135] S. Majumder, S Haque, and F. N. Nur, "Directional mac protocols in ad-hoc networks", *International Journal Of Computer Applications*, vol. 100, 2014.

[136] O. Bazan and M. Jaseemuddin, "Performance analysis of directional csma/ca in the presence of deafness", *IET communications*, vol. 4, no. 18, pp. 2252–2261, 2010.

[137] V. Pourgolzari and S. A. Ghorashi, "A cdma based mac protocol for ad hoc networks with directional antennas", in *Computer Networks and Distributed Systems (CNDS), 2011 International Symposium on*, IEEE, 2011, pp. 73–77.

[138] M. N. Alam, M. A. Hussain, and K. S. Kwak, "Neighbor initiated approach for avoiding deaf and hidden node problems in directional mac protocol for ad-hoc networks", *Wireless networks*, vol. 19, no. 5, pp. 933–943, 2013.

[139] M. Takata, M. Bandai, and T. Watanabe, "A mac protocol with directional antennas for deafness avoidance in ad hoc networks", in *Global Telecommunications Conference, 2007. GLOBECOM'07. IEEE*, IEEE, 2007, pp. 620–625.

[140] Y. Li and A. M. Safwat, "Dmac-daca: Enabling efficient medium access for wireless ad hoc networks with directional antennas", in *Wireless Pervasive Computing, 2006 1st International Symposium on*, IEEE, 2006, 5–pp.

[141] M. Takata, M. Bandai, and T. Watanabe, "Ri-dmac: A receiver-initiated directional mac protocol for deafness problem", *International Journal of Sensor Networks*, vol. 5, no. 2, pp. 79–89, 2009.

[142] H. Gossain, C. Cordeiro, and D. P. Agrawal, "Mda: An efficient directional mac scheme for wireless ad hoc networks", in *Global Telecommunications Conference, 2005. GLOBECOM'05. IEEE*, IEEE, vol. 6, 2005, 5–pp.

[143] S.-B. Ko and J.-W. Jwa, "A dual-tone dmac protocol for mobile ad hoc networks", *IEICE transactions on communications*, vol. 90, no. 2, pp. 354–357, 2007.

[144] H. Gossain, C. Cordeiro, D. Cavalcanti, and D. P. Agrawal, "The deafness problems and solutions in wireless ad hoc networks using directional antennas", in *Global Telecommunications Conference Workshops, 2004. GlobeCom Workshops 2004. IEEE*, IEEE, 2004, pp. 108–113.

[145] M. Takata, M. Bandai, and T. Watanabe, "A directional mac protocol with deafness avoidance in ad hoc networks", *IEICE transactions on communications*, vol. 90, no. 4, pp. 866–875, 2007.

[146] W. K. Lai, K.-S. Tseng, and J.-C. Chen, "Mars: A multiple access scheme with sender driven and reception first for smart antenna in ad hoc networks", *Wireless Communications and Mobile Computing*, vol. 9, no. 2, pp. 197–208, 2009.

[147] J. Feng, P. Ren, and S. Yan, "A deafness free mac protocol for ad hoc networks using directional antennas", in *Industrial Electronics and Applications, 2009. ICIEA 2009. 4th IEEE Conference on*, IEEE, 2009, pp. 449–454.

[148] N. Kaushik, K. Choudhary, and N. S. Yadav, "New deafness-aware mac protocol for directional antennas in wanet's", *International Journal of Computer Applications*, vol. 127, no. 12, pp. 28–35, 2015.

[149] A. A. Abdullah, L. Cai, and F. Gebali, "Dsdmac: Dual sensing directional mac protocol for ad hoc networks with directional antennas", *IEEE Transactions on Vehicular Technology*, vol. 61, no. 3, pp. 1266–1275, 2012.

[150] C.-Y. Chang, H.-C. Sun, and C.-C. Hsieh, "Mcda: An efficient multi-channel mac protocol for 802.11 wireless lan with directional antenna", in *Advanced Information Networking and Applications, 2005. AINA 2005. 19th International Conference on*, IEEE, vol. 2, 2005, pp. 64–67.

[151] W. Na, L. Park, and S. Cho, "Deafness-aware mac protocol for directional antennas in wireless ad hoc networks", *Ad Hoc Networks*, vol. 24, pp. 121–134, 2015.

[152] A. Capone, F. Martignon, and L. Fratta, "Directional mac and routing schemes for power controlled wireless mesh networks with adaptive antennas", *Ad Hoc Networks*, vol. 6, no. 6, pp. 936–952, 2008.

[153] Y. Liao, K. Bian, L. Song, and Z. Han, "Full-duplex mac protocol design and analysis", *IEEE Communications Letters*, vol. 19, no. 7, pp. 1185–1188, 2015.

[154] Q. Chen, J. Tang, D. T. C. Wong, X. Peng, and Y. Zhang, "Directional cooperative mac protocol design and performance analysis for ieee 802.11 ad wlans", *IEEE Transactions on Vehicular Technology*, vol. 62, no. 6, pp. 2667–2677, 2013.

[155] J. Wang, H. Zhai, P. Li, Y. Fang, and D. Wu, "Directional medium access control for ad hoc networks", *Wireless Networks*, vol. 15, no. 8, pp. 1059–1073, 2009.

[156] V. Inzillo, F. De Rango, A. F. Santamaria, and A. A. Quintana, "A round-robin mac approach for limiting deafness in mobile ad hoc network beamforming environments", in *Wireless Days (WD), 2018*, IEEE, 2018, pp. 98–100.

[157] V. Inzillo and F. De Rango, "A directional mac approach extending omnet++ simulator", in *Proceedings of the Summer Computer Simulation Conference*, Society for Computer Simulation International, 2016, p. 48.

[158] Y. Wei-na, "Study of waiting queue problem in commercial bank based on monte carlo simulation [j]", *Technoeconomics & Management Research*, vol. 1, p. 007, 2009.

[159] K. Silvester, R. Lendon, H. Bevan, R. Steyn, and P. Walley, "Reducing waiting times in the nhs: Is lack of capacity the problem?", *Clinician in Management*, vol. 12, no. 3, 2004.

[160] B. Ginzburg and A. Kesselman, "Performance analysis of a-mpdu and a-msdu aggregation in ieee 802.11 n", in *Sarnoff symposium, 2007 IEEE*, IEEE, 2007, pp. 1–5.

[161] F. De Rango, V. Inzillo, and A. A. Quintana, "Exploiting frame aggregation and weighted round robin with beamforming smart antennas for directional mac in manet environments", *Ad Hoc Networks*, vol. 89, pp. 186–203, 2019.

[162] V. Inzillo, F. De Rango, and A. A. Quintana, "A sectorized directional mac proposal for mitigating deafness and energy consumption in mobile ad hoc networks", in *Consumer Communications & Networking Conference (CCNC), 2018 15th IEEE Annual*, IEEE, 2018, pp. 1–2.

[163] R. Jain, A. Durresi, and G. Babic, "Throughput fairness index: An explanation", 1999.

[164] D. Taht, J. Gettys, T Hoeiland-Joergensen, T. Hoeiland-Joergensen, E. Dumazet, J Gettys, P. McKenney, E Dumazet, and P McKenney, "The flow queue codel packet scheduler and active queue management algorithm", 2018.

[165] O. Usmani, *Packet scheduling using a programmable weighted fair queuing scheduler that employs deficit round robin*, US Patent 8,943,236, 2015.

[166] D. A. Mahmood and G. Horváth, "A simple approximation for the response times in the two-class weighted fair queueing system", in *International Conference on Analytical and Stochastic Modeling Techniques and Applications*, Springer, 2017, pp. 125–137.

[167] G. Liu and Q. Li, "Research article packet scheduling in high-speed networks using improved weighted round robin", 2014.

[168] W. Su, S.-J. Lee, and M. Gerla, "Mobility prediction and routing in ad hoc wireless networks", *International Journal of Network Management*, vol. 11, no. 1, pp. 3–30, 2001.

[169] X. Li, N. Mitton, and D. Simplot-Ryl, "Mobility prediction based neighborhood discovery in mobile ad hoc networks", in *International Conference on Research in Networking*, Springer, 2011, pp. 241–253.

[170] B. Divecha, A. Abraham, C. Grosan, and S. Sanyal, "Impact of node mobility on manet routing protocols models", *JDIM*, vol. 5, no. 1, pp. 19–23, 2007.

[171] F. Bai and A. Helmy, "A survey of mobility models", *Wireless Adhoc Networks. University of Southern California, USA*, vol. 206, p. 147, 2004.

[172] G. Vijayavani and G Prema, "Performance comparison of manet routing protocols with mobility model derived based on realistic mobility pattern of mobile nodes", in *Advanced Communication Control and Computing Technologies (ICACCCT), 2012 IEEE International Conference on*, IEEE, 2012, pp. 32–36.

[173] R. M. Nosofsky and T. J. Palmeri, "An exemplar-based random walk model of speeded classification.", *Psychological review*, vol. 104, no. 2, p. 266, 1997.

[174] J. Ariyakhajorn, P. Wannawilai, and C. Sathitwiriyawong, "A comparative study of random waypoint and gauss-markov mobility models in the performance evaluation of manet", in *Communications and Information Technologies, 2006. ISCIT'06. International Symposium on*, IEEE, 2006, pp. 894–899.

[175] M. S. Murty and M. V. Das, "Performance evaluation of manet routing protocols using reference point group mobility and random waypoint models", *International Journal of Ad hoc, Sensor & Ubiquitous Computing (IJASUC)*, vol. 2, no. 1, pp. 33–43, 2011.

[176] G. Carofiglio, C.-F. Chiasserini, M. Garetto, and E. Leonardi, "Route stability in manets under the random direction mobility model", *IEEE Transactions on Mobile Computing*, vol. 8, no. 9, pp. 1167–1179, 2009.

[177] S. M. Mousavi, H. R. Rabiee, M Moshref, and A Dabirmoghaddam, "Mobisim: A framework for simulation of mobility models in mobile ad-hoc networks", in *Wireless and Mobile Computing, Networking and Communications, 2007. WiMOB 2007. Third IEEE International Conference on*, IEEE, 2007, pp. 82–82.

[178] G. Jayakumar and G. Ganapathi, "Reference point group mobility and random waypoint models in performance evaluation of manet routing protocols", *Journal of Computer Systems, Networks, and Communications*, vol. 2008, p. 13, 2008.

[179] G. Jayakumar and G Gopinath, "Performance comparison of manet protocols based on manhattan grid mobility model", *Journal of Mobile communication*, vol. 2, no. 1, pp. 18–26, 2008.

[180] K.-T. Feng, "Lma: Location-and mobility-aware medium-access control protocols for vehicular ad hoc networks using directional antennas", *IEEE Transactions on Vehicular Technology*, vol. 56, no. 6, pp. 3324–3336, 2007.

[181] S. Roy, S. Chatterjee, S. Bandyopadhyay, T. Ueda, H. Iwai, and S. Obana, "Neighborhood tracking and location estimation of nodes in ad hoc networks using directional antenna: A testbed implementation", in *IEEE Proc of the Int Conf on Wireless Networks, Communications and Mobile Computing*, 2005, pp. 1–6.

[182] H. H. Dumanli, "Beamswitch: System solution for energy-efficient directional communication on mobile devices", PhD thesis, Rice University, 2010.

[183] X. Lu, P. Lio, P. Hui, and H. Jin, "A location prediction algorithm for mobile communications using directional antennas", *International Journal of Distributed Sensor Networks*, vol. 9, no. 11, p. 418 606, 2013.

[184] V. Inzillo, F. De Rango, and A. A. Quintana, "Mobility beamforming prediction and a round robin scheduling in a directional mac for manet", in *2018 11th IFIP Wireless and Mobile Networking Conference (WMNC)*, IEEE, 2018, pp. 1–7.

[185] J.-C. Cano and P. Manzoni, "A performance comparison of energy consumption for mobile ad hoc network routing protocols", in *Modeling, Analysis and Simulation of Computer and Telecommunication Systems, 2000. Proceedings. 8th International Symposium on*, IEEE, 2000, pp. 57–64.

[186] L. M. Feeney and M. Nilsson, "Investigating the energy consumption of a wireless network interface in an ad hoc networking environment", in *INFOCOM 2001. Twentieth Annual Joint Conference of the IEEE Computer and Communications Societies. Proceedings. IEEE*, IEEE, vol. 3, 2001, pp. 1548–1557.

[187] G. Allard, P. Minet, D.-Q. Nguyen, and N. Shrestha, "Evaluation of the energy consumption in manet", in *International Conference on Ad-Hoc Networks and Wireless*, Springer, 2006, pp. 170–183.

[188] G Jayanthi, V. Golla, H. Suresh, and S. Shivashankar, "Designing energy routing protocol with power consumption optimization in manet", *IEEE Transactions on Emerging topics in Computing*, no. 1, p. 1, 2013.

[189] E. Lochin, A. Fladenmuller, J.-Y. Moulin, S. Fdida, and A Manet, "Energy consumption models for ad-hoc mobile terminals", in *In Med-Hoc Net*, Citeseer, 2003.

[190] M. Handy, M. Haase, and D. Timmermann, "Low energy adaptive clustering hierarchy with deterministic cluster-head selection", in *Mobile and Wireless Communications Network, 2002. 4th International Workshop on*, IEEE, 2002, pp. 368–372.

[191] S. Y. Han and D. Lee, "An adaptive hello messaging scheme for neighbor discovery in on-demand manet routing protocols", *IEEE communications letters*, vol. 17, no. 5, pp. 1040–1043, 2013.

[192] A. Spyropoulos and C. S. Raghavendra, "Energy efficient communications in ad hoc networks using directional antennas", in *INFOCOM 2002. Twenty-First Annual Joint Conference of the IEEE Computer and Communications Societies. Proceedings. IEEE*, IEEE, vol. 1, 2002, pp. 220–228.

[193] Z. Ren, Q. Li, Q. Chen, and Y. Huang, "Energy-efficient routing based on directional antennas for wireless sensor networks", in *Broadband Network and Multimedia Technology (IC-BNMT), 2010 3rd IEEE International Conference on*, IEEE, 2010, pp. 579–583.

[194] B. Chen, K. Jamieson, H. Balakrishnan, and R. Morris, "Span: An energy-efficient coordination algorithm for topology maintenance in ad hoc wireless networks", *Wireless networks*, vol. 8, no. 5, pp. 481–494, 2002.

[195] M. Hanaoui, H. Bouassam, M. Rifi, and H. Terchoune, "Improvement of energy efficiency by using smart antenna system of bts application", *International Journal of Computer Science and Information Security*, vol. 13, no. 11, p. 47, 2015.

[196] A. Kumar and S. Joshi, "Improvement of power efficiency using smart antenna system in manets", *International Journal of Electronics Communication and Computer Engineering*, vol. 5, no. 6, p. 1255, 2014.

[197] H. B. Kassa, Y. Astatke, F. Moazzami, T. Y. Chernet, E. Yohannes, and D. H. Woldegebreal, "Energy efficient smart antenna system using recursive least square algorithm and kaiser side lobe cancellation technique", in *Information Sciences and Systems (CISS), 2017 51st Annual Conference on*, IEEE, 2017, pp. 1–5.

[198] F. E. Salem, A. Tall, Z. Altman, and A. Gati, "Energy consumption optimization in 5g networks using multilevel beamforming and large scale antenna systems", in *Wireless Communications and Networking Conference (WCNC), 2016 IEEE*, IEEE, 2016, pp. 1–6.

[199] M. J. Sivasankari and B Sridevi, "Enhancing energy efficiency using massive mimo technique applicable for next generation networks", *Journal of Engineering Trends and Technology (IJETT)*, 2017.

[200] V. P. Koppisetti and N. R. Surya, "Massive mimo for 5g wireless networks: An energy efficiency perspective", PhD thesis, University of British Columbia, 2015.

[201] V. Inzillo, F. De Rango, A. A. Quintana, and A. F. Santamaria, "An adaptive beamforming time with round robin mac algorithm for reducing energy consumption in manet", *Journal of Sensor and Actuator Networks (JSAN)*, vol. 7, no. 4, 2018.

[202] V. Inzillo, F. De Rango, and A. A. Quintana, "A novel algorithm for limiting energy consumption in 5g wireless environments using massive mimo systems", in *Vehicular Technology Conference (VTC Spring), 2019*, IEEE, 2019, p. xx.

[203] G. Pei and T. R. Henderson, "Validation of ofdm error rate model in ns-3", *Boeing Research Technology*, pp. 1–15, 2010.

[204] V. Inzillo, F. De Rango, and A. A. Quintana, "Supporting 5g wireless networks through ieee802.11ac standard with new massive mimo antenna system module design in omnet++ simulator", in *8th International Conference on Simulation and Modeling Methodologies, Technologies and Applications (SIMULTECH)*, INSTICC, 2018.

[205] K. S. V. Prasad, E. Hossain, and V. K. Bhargava, "Energy efficiency in massive mimo-based 5g networks: Opportunities and challenges", *IEEE Wireless Communications*, vol. 24, no. 3, pp. 86–94, 2017.